FACULTY OF HEALTH SCIENCES
AARHUS UNIVERSITY

Strontium in the Bone-Implant Interface

PhD dissertation

Marianne Toft Vestermark

Faculty of Health Sciences
Aarhus University
2010

Strontium in the Bone-Implant Interface

PhD dissertation

Marianne Toft Vestermark

Faculty of Health Sciences
Aarhus University
Department of Orthopaedic Surgery
Aarhus University Hospital

Supervisors

Prof. Kjeld Søballe, MD, DMSc
Department of Orthopaedic Surgery
Aarhus University Hospital, Denmark

Assis. Prof. Jørgen Baas, MD, PhD
Department of Orthopaedic Surgery
Aarhus University Hospital, Denmark

Assoc. Prof. Ellen-Margrethe Hauge, MD, PhD
Research Unit for Rheumatology and Bone Biology
Aarhus University Hospital, Denmark

Evaluation committee

Prof. Carina B. Johansson, PhD
c/o Oral Surgery
Örebro University Hospital
SE 70185 Örebro
Sweden

Prof. Kim Brixen, MD, PhD
Department of Endocrinology
Odense University Hospital
Sdr. Boulevard 29
DK-5000 Odense C
Denmark

Assoc. Prof. Michel Dalstra, PhD
Department of Orthodontics
School of Dentistry
Vennelyst Boulevard 9
Building 1613, Room. 060
DK-8000 Aarhus C
Denmark

Preface

The three studies of this PhD dissertation were conducted at the Orthopedic Research Laboratory, Department of Orthopedics, Aarhus University Hospital, Denmark and at the Orthopedic Biomechanics Laboratory, Excelen Center for Bone and Joint Research and Education, Minneapolis Medical Research Foundation, Minneapolis, MN, USA.

The Danish Rheumatism Association, P. Carl Petersens Foundation, and Aarhus University financed my research fellowship.

The experimental surgeries and animal care were carried out at the Orthopedic Biomechanics Laboratory, Minneapolis. Specimens were then shipped to the Orthopedic Research Lab at Aarhus University, where all analyses were performed.

Prof. Kjeld Søballe introduced me to research in year 2000, where I conducted a Pre-graduate research diploma on studies initiated by him. I am very thankful to Prof. Kjeld Søballe for all the support and possibilities he has afforded me. He also introduced me to the late Prof. Flemming Melsen, who taught me bone biology, and Assoc. Prof. Joan E. Bechtold. Assoc. Prof. Joan E. Bechtold has been very valuable to me as both a collaborator and friend and has made it possible for us to perform the experimental surgeries in Minneapolis. I am in great debt to my co-supervisors, Ellen-Margrethe Hauge and Jørgen Baas, who have willingly held endless discussions with me on various academic subjects but also in matters of my career and general life. Thank you; you are true mentors. Delia S Brauer has been very helpful and it has been a great joy to work alongside her. Also great thanks to the laboratory Technicians, "the aunties", for keeping the lab running with a good atmosphere. And special thanks to Jane Pauli, for help on any histological matter. I thank my colleagues, for all the advice and for making our coffee breaks so joyful. Secretary Tina Stenumgaard, thank you for making things happen and being helpful throughout. Many thanks to Prof. Jens Randel Nyengaard and Assoc. Prof. Jesper Skovhus Thomsen for stereological advice and discussions. A special thanks to my mom, Dora Toft, who has helped me with the shipping and customs of different goods, and translating papers into French and German.

But more than anyone I thank my supportive and patient husband Tommy and our sons Rune and Falke for bringing me joy and happiness and for being so dear to me.

Marianne T. Vestermark
October 2010

Acknowledgements

These studies were supported financially by the following non-commercial institutions and funds:

- Danish Rheumatism Association
- P. Carl Petersens Fond
- Aarhus University, Denmark
- NIH AR42051
- The A.P. Moeller Foundation for Advancement of Medical Science

The studies have benefitted from an institutional research grant from Bioceramic Therapeutics Ltd, which holds a patent for the bioactive glass coating.

The following companies supported the studies with materials:

- Osteologix Aps: SrHA and HA powder, study I and II.
- Medicoat AG: VPS coating of SrHA and HA, study I.
- Bioceramic Therapeutics Ltd: Bioactive glass coating and HA coating, study III.
- DePuy Inc: Porous coating, study II.

During the course of this PhD study I have been involved in research, which has received institutional support from the following companies with commercial interest in orthopedics:

DePuy Inc.

The dissertation is based on the following papers:

I. Strontium Substituted Hydroxyapatite Coating did not Improve Implant Fixation and Osseointegration. Vestermark MT, Hauge EM, Bechtold JE, Jakobsen T, Gruner H, Soballe K, Baas J. In preparation.

II. Strontium Doping of Bone Graft Extender: Effect on Fixation of Allografted Experimental Implants. Vestermark MT, Hauge EM, Soballe K, Bechtold JE, Jakobsen T, Baas J. Submitted.

III. Grit-blasting of Titanium Implants Affects Structure and in vivo Performance of Strontium-substituted Bioactive Glass Coating. Vestermark MT, Brauer DS, Soballe K, Jakobsen T, Hauge EM, Bechtold JE, and Baas J. In preparation.

Correspondence

Marianne Toft Vestermark, MD
Orthopaedic Research Laboratory
Aarhus University Hospital
Norrebrogade 44, Build. 1A
DK-8000 Aarhus C
Web: www.orthoresearch.dk

Email: marianne.t@vestermark.dk

Contents

Abbreviations

Ca	Calcium
BGE	Bone Graft Extender
HA	Hydroxyapatite
HA BGE	Hydroxyapatite Bone Graft Extender
P	Phosphorus
RAP	Regional Acceleratory Phenomenon
SEM	Scanning Electron Microscope
Sr	Strontium
SrHA	Strontium hydroxyapatite
SrHA BGE	Strontium hydroxyapatite Bone Graft Extender
Ti	Titanium
VPS	Vacuum plasma spray
VUR	Vertical Uniform Random

1. English summary

Total hip replacement surgery is being performed on an increasingly large part of the population and at increasingly younger age. Because we live and stay physically active longer, and since hip replacement surgery has become quite successful, the treatment is being offered to progressively more patients.

Unfortunately, about 17% of hip replacement surgeries currently involve revisions. Consequently, the longevity of both the primary and revision implant is an issue and warrants further investigation.

Implants undergoing early instability or even subsidence correlate with an increased risk of aseptic loosening, subsequently requiring revision. Thus, the goal is early fixation by osseointegration of the implant. For revision implants, this is an even greater challenge since an allograft is often needed during surgery to obtain immediate stability of the implant. Bone grafts are rapidly resorbed. Thus, instability of the prosthesis may develop before new bone formation is well established and can mechanically secure the prosthesis.

Strontium is a dual action drug; being both bone anabolic and anti-catabolic. In the form of strontiumranelate, it is used in the treatment of osteoporosis. Strontium may potentially improve the early osseointegration and fixation of implants.

This dissertation consists of three studies investigating the effect of strontium at the bone-implant interface. The questions were first, what is the optimal delivery method for strontium to the interface, and second, can strontium exercise its dual action at the interface? The studies were performed in a cementless, experimental gap model in canine. The effects of strontium were evaluated by histomorphometrical analysis of the osseointegration and mechanical push-out test of implant fixation. Different stereological methods were used for the histomorphometrical analysis of each study. The methods used were reviewed critically and found valid.

Study I compared a 5% strontium-substituted hydroxyapatite (HA) coating with an HA coating after 4 weeks and 12 weeks observation time. We examined whether fixation of the implant was improved by the strontium substitution. It was found that fixation of the implant was not improved by the strontium substituted HA coating at any of the two time points.

Study II compared a 5% strontium-doped HA bone graft extender with a HA bone graft extender. The bone graft extender was mixed with allograft and impacted around a titanium implant. The objective of this study was to determine whether strontium doping of the bone graft extender could protect the allograft from fast resorption and increase gap healing, leading to the improved fixation of the implant. We found that the strontium doping increased gap healing and protected the allograft, however, results of the mechanical test were inconclusive. The reason might have been that the increased gap healing had not yet reached the implant during the 4 weeks observation time, so ongrowth onto the implant was not improved.

Study III investigated the effects of bioactive glass coating with a 0%, 10% or 50% strontium-substitution versus HA coating of grit-blasted titanium alloy implants. The goal was to determine whether fixation of the implant would be improved by the bioactive glass coating, and then further improved by the strontium-substitution of the coating in a dose-dependent manner. Unfortunately, the bioactive glass coating failed, presumably due to aluminum contamination originating from the grit-blasting powder. The HA coated implants were superior in all parameters of osseointegration and the mechanical fixation of the implants.

These studies show the importance of performing further experimental investigation. Even when investigating a known agent for use in a new application. Strontium delivered as doping of a HA bone graft extender showed potential as a dual acting agent in the interface. However, delivery methods of strontium to the bone-implant interface clearly need further investigation.

2. Danish Summary

Hofteproteser isættes i en stigende andel af den vestlige befolkning. Behandlingen med en kunstig hofte er succesfuld og tilbydes derfor ved et stigende antal hoftelidelser og ved tiltagende yngre alder. Disse faktorer er medvirkende til at andelen af hofteproteser, der fejler og må skiftes forsat er høj. Hele 17% af alle hofteprotese operationer i dag er hel eller delvis udskiftning af protesen. Den hyppigste enkeltstående årsag til udskiftning er, at protesen er gået løs uden tilstedeværelse af infektion, og knoglevæv er gået tabt omkring protesen. Disse aseptisk løsnede hofteproteser er meget smertefulde og invaliderer ofte patienten. Under udskiftning af protesen er det ofte nødvendigt at stabilisere den nye protese ved at pakke donor knoglevæv omkring. Hofteproteser der initialt var stabiliseret med donor knoglevæv går oftere og tidligere løs, fordi donor vævet ofte nedbrydes hurtigere end ny knoglevæv kan nå at dannes til forankring af protesen. De efterfølgende hofteproteser holder i gennemsnit kortere tid inden de igen skal udskiftes. For både patienternes og samfund-ets skyld er der behov for at forbedre levetiden af både den første og de efterfølgende hofteproteser.

Strontium, som strontiumranelat, kendes fra behandlingen af osteoporose, hvor det øger mængden af knoglevæv og derved reducerer risikoen for osteoporosebetingede knoglebrud. Strontium har dobbelt virkningsmekanisme, da både knoglenydannelsen øges samtidigt med at knoglenedbrydningen bremses. Derved er det muligt at strontium tilsat i overganen mellem protesen og knoglen vil øge forankringen af både førstegangs og de efterfølgende proteser. Derved kan overlevelsen af hofteproteser forlænges. I denne afhandling bliver to spørgsmål belyst: først hvordan skal strontium leveres til overgangen og dernæst kan strontiums dobbelte virkning demonstreres og gavne i overgangen mellem implantatet og knoglen?

I hunde blev tre eksperimentelle studier udført, hvor strontium blev tilsat på tre forskellige måder i overgangen mellem knoglen og et test implantatet. Efterfølge blev forankringen af implantaterne evalueret histologisk med hensyn til mængden og fordelingen af knoglevæv samt mekanisk. De valgt metoder blev gennemgået kritisk og fundet anvendelige til formålet.

Studie I: Implantater belagt med hydroxyapatite. HA, uden eller med erstatning af 5% calcium med strontium blev undersøgt efter 4 og 12 uger. Hverken den histologiske eller mekaniske forankring var forbedret efter 4 eller 12 uger ved strontium erstatning af HA belægningen.

Studie II: Donor knoglevæv blandet med HA uden eller med erstatning af 5% calcium med strontium blev pakket omkring et implantat og undersøgt efter 4 uger. Ved strontium erstatning var mere donor væv bevaret og mere ny knogle var dannet omkring implantatet men ikke på implantatets overflade. Formentligt derfor var den mekaniske forankring heller ikke forbedret.

Studie III: Sandblæste implantater var belagt med HA, eller bioaktivt glas med 0%, 10%, eller 50% erstatning af calcium med strontium. Ingen af implantaterne belagt med bioaktivt glas var forankret hverken histologisk eller mekanisk efter 4 uger. Det er muligt at glas belægningen var blevet forurenet med aluminium fra sandblæsnings pulveret, hvilket ændrede glassets kemiske egenskaber, bland andet var glasset mod forventning ikke blevet opløst.

Det konkluderes, at eksperimentelle studier er nødvendige, når et godkendt lægemiddels indikations området forsøges udvidet. På baggrund af studierne i denne PhD afhandling ses der en tendens til, at strontiums dobbelte virkning kan demonstreres og gavne i knogle-implantat overgangen. Samtidigt har studierne i afhandlingen vist at levering af strontium til knogle-implantat overgangen er en store udfordring, som endnu ikke er klarlagt.

3. Background

Total hip replacements surgery is performed on an increasingly large part of the population. The reasons are that firstly, the treatment of hip conditions with a hip replacement is overall very successful. As a result of the success, hip replacement is offered to patient with a wide range of hip conditions and at increasingly younger age. Secondly, we live longer and stay physically active at increasingly higher ages. According to the Annual Report 2008 from the Danish Arthroplasty Register, 136 per 100,000 citizens received primary hip replacement surgeries and the number will increase [1]. Unfortunately, the revision rate is unacceptably high, especially if the patient is less than 50 years old at the time of primary surgery, because 20% of these surgeries are revised within 14 years. The high revision rate of prostheses in young patients is related to their high level of physical activity. The survival rate of cemented and cementless implants is the same for patients under 50 years and maybe in favor of the cementless implant in patients 50-60 years of age. Cementless implants seem more easily revised, and the loss of bone around the implant tends to be smaller. Cementless implants are the focus of this dissertation. For the younger patients, the main indication for revision surgery is aseptic loosening of the implant. An aseptically loosened implant is a painful and disabling condition. Clearly, patients with an aseptically loosened implant have a reduced quality of life. Revised implants have an even higher failure rate, which increases with increasing number of re-revisions [2]. Therefore the issue of aseptically loosened implants also constitutes a financial burden for the society in terms of repeated operations, the daily care of the disabled patients, and the disabled patients' inability to work. So, the longevity of both primary and revision implants clearly needs further investigation.

Aseptic loosening

The causes and optimal treatment of aseptically loosened implants seem complex and not fully understood.

Instability of the implant is known to induce aseptic loosening. Under experimental settings, micromotions of implants as small as 150 μm inhibit osseointegration of the implant. Instead, a fibrous membrane encapsulates the implant and motion is continuous motion takes place [3]. Clinically, Kärrholm et al. observed that subsidence of the prosthesis is correlated with an increased risk of the prosthesis becoming aseptically loosened [4].

Inflammation is another well-known aspect of aseptic loosening [5]. Particles of wear debris from the implant materials can induce the inflammation. Subsequently, osteoclasts are differentiated and activated [6]. The consequence of inflammation is bone resorption and loss of bone around the prosthesis [7]. Hereby, instability of the implant is further increased.

Early osseointegration will both stabilize the implant and prevent the wear debris from reaching the bone-implant interface [8].

Osseointegration

During experiments on blood flow in bone, Brånemark found that the titanium oculars placed into bone could not be removed after healing. Brånemark then conducted extensive research into insertion of screw-shaped dental implants. In 1977, Brånemark stated in his doctoral dissertation: "The re- and new-formed bone tissue enclosed the implant with perfect congruency to the implant form and surface irregularities, thus establishing a true osseointegration of the implant without any interpositioned connective tissue" [11]. His co-worker Albrektsson defined in 1981 the osseointegration as direct contact between living bone and implant at the light-microscopic level (Table 1) [9]. But histological analysis of the interface could not be performed in vivo.

Osseointegration
1981, definition by Albrektsson [9]: • Direct contact between living bone and implant at light microscopic level 1990, Zarb and Albrektsson added a functional definition [10]: • A process whereby clinically asymptomatic, rigid fixation of alloplastic materials in bone during functional loading is achieved and maintained for 80% over 10 years

Table 1: Definitions of osseointegration.

Therefore, a functional or biomechanical definition was added [10]: "A process whereby clinically asymptomatic, rigid fixation of alloplastic materials in bone during functional loading is achieved and maintained for 80% for ten years." Roentgen stereophotogrammetric analysis can evaluate the functional osseointegration. Thus, simply speaking, osseointegration is a direct structural and functional connection between host bone and the surface of an implant.

The biological process leading to osseointegration can be split into gap healing, when a initial gap between host bone and the implant is present, and ongrowth [12]. The reason for splitting up the process is because the surface of the implant can have or release an agent with bioinert, osteoconductive, osteoproductive, or osteoinductive properties (Table 2).

Whether the aspects of osseointegration of dental implants can be applied to major arthroplasties in orthopedics has been questioned [14]. Albrektsson objections are firstly that orthopedic implants are less biocompatible, secondly heat during surgery can damaged the host bone, and thirdly immediate postoperative loading of the implants does not favor bone formation. On the other hand, hip arthroplasty is a quite successful because in 2008 92% of all hip prosthesis had survived for 10 years [15]. Based on roentgen stereophotogrammetric analysis, Kärrholm concluded that painful prostheses are correlated with subsidence of the implants [16]. This finding is in according with the definition of functional osseointegration. So it seems that the rules of osseointegration can be applied to arthroplasties. Furthermore, as Albrektsson states, the bone density in the interface must resemble the density of the surrounding bone. Arthroplasties are inserted into cancellous bone, so arthroplasty implants are not to be fully covered by bone. Moreover, great efforts to improve biocompatibility and otherwise promote osseointegration of the arthroplasty implants have been and still are being made [17, 18]. Also, the studies of this dissertation are efforts to improve the osseointegration of arthroplasty implants.

Nearly Bioinert	Formation of a non-adherent fibrous capsule of variable thickness; e.g. Alumina, Zirconia, and Polyethylene.
Osteoconductive	Bone grows on the surface; e.g. HA.
Osteoproductive (osteostimulative)	Biologically active hydroxyl carbonate apatite layer on the glass surface is formed chemically and is colonized with osteogenic cells; e.g. Bioactive Glasses.
Osteoinduction	Osteogenesis is induced i. e. immature cells are differentiated into preosteoblasts; e.g. Bone Morphogenic Protein 2.

Table 2: Definitions of bioactive properties [13, 14].

The osseointegration of implants can be influence by several local factors that can be divided into: 1) implant stability in respect of implant design, implantation technology, surgical technique, and patient variables, such as bone quality and possible bone defects; 2) distance between the host bone and the implant, despite the cavity at surgery being carefully prepared for a tight implant fit; 3) bioactivity of the implant surface and any material in the gap between host bone and implant [19].

Early osseointegration must be established during fracture healing and then maintained during modeling, and remodeling.

Fracture healing

Fracture healing of long bones is defined as primary and secondary healing [20]. Primary healing can take place in aligned fragments of bone cortex. The fracture is healed by directly coupled removal of and replacement with

lamellar bone when the cutting cone moves from one fragment to the opposite fragment across the fracture. Primary healing of the cortex demands stability of the fracture site, so that the fragments stay aligned. Secondary healing is characterized by callus formation, which is replaced by lamellar bone. Secondary healing shows the closest resemblance to the process seen around an inserted implant, because woven bone is abundant and the implantation site is in the cancellous bone.

Secondary fracture healing runs through four overlapping phases: an inflammatory, a resorptive, a formative, and a modeling/re-modeling phase [20, 21].

Inflammatory phase: a hema-toma with platelets and inflammatory cell forms immediately at the fracture site. Cytokines and growth factors, including TNFα, IL-1, PDGF, GDF and BMP, with chemotaxic and osteoinductive functions are released from the site [22, 23]. Then mesenchymal stem cells, preosteoclasts, and preosteoblasts are mobilized to the site from the neighboring living tissues and the blood stream. The cells are stimulated to proliferation, differentiation, and activation. Strong signals of resorption and formation are initiated. During the inflammation phase, the hematoma is invaded and replaced by callus. A callus consists of fibrovascular tissue in which abundant amounts of collagen fibers and woven bone matrix is laid down. The callus is anchored to living bone fragments by newly formed bone.

Resorptive phase: Within a week resorption of both necrotic and misplaced bone fragments begins [20]. The necrotic bone fragments can serve as scaffolds for new bone formation and contribute to implant stabilization [24]. In the initial 4 weeks, the effect of high resorption activity and pending effect of new bone formation is seen as a reduction in bone density surrounding implants [25]. Low bone densities have also been correlated with inferior implant fixation [26].

Formative phase: If the implant or fracture site is stable, then after about a week HA is beginning to be precipitated in the collagen [20, 27]. In successful fracture healing, the gap between bone fragments or to the implant surface is entirely bridged by woven bone, which stabilizes the site. Successful fracture healing at the implant site, i.e. osseointegration, can take place if a porous-coated implant is subject to a micromotion of 28 μm. [3]. Then if the micromotions are increased to 150 μm, the implant is not osseointegrated but becomes encapsulated into a fibrous membrane. The volume of the newly formed, woven bone is excessive and needs to be reduced by modeling.

Modeling/remodeling: Over 1-4 years, the last phase of fracture healing occurs. Any excessive or misplace bone tissue is removed, and trabelulae of lamella bone are formed in an architectural pattern that matches the mechanical strain on the bone [28, 29].

Fracture healing of cancellous bone is a little different from healing of cortex because only an internal callus is formed. The cancellous bone is very well vascularized, so only a relative small amount of bone becomes necrotic. A large area of bony contact at the fracture site ensures that a union is rapidly formed between fragments in direct contact via the endosteal callus. The union of fragments will subsequently spread across the fracture site, unless the distance between fragments is too great [30].

Successful fracture healing results when fractured bone ends are connected without interpositioned connective tissue. Fracture healing can fail if, for instance, the fracture site is infected or subjected to motion. Then connective tissue is positioned between the bone fragments even at a late time point. Failed healing around an implant is characterized by a fibrous encapsulation of the implant. These aspects of fracture healing clearly show similarities to aspects of implant osseointegration. The similarities between osseointegration and fracture healing are perhaps more clear, if a bioactive implant material or implant surface is used because new bone formation proceeds unidirec-tionally, like in fractures, from host bone and from the surface of the bioactive material [12].

Bioactive substances

A bioactive material is defined as: "A bioactive material is one that elicits a specific biological response at the interface of the material, which results in the formation of a bond between the tissue and the material" (Table 3) [13]. Several materials, e.g. HA and bioactive glasses, elicit different but yet bioactive responses in bone, and the only common characteristic feature of these bioactive implant materials is that "a layer of biologically active hydroxyl carbonate apatite forms on the implant surface"[13]. The effect of the bioactive substance can be classified as *osteoconductive or osteoproductive* [14, 31].

An *osteoconductive* substance releases calcium and phosphate, mainly by ion exchange, which forms a biocompatible surface of a biologically active hydroxyl carbonate apatite for bone formation to migrate [14, 32]. HA is an osteoconductive substance, which can be added to the bone-implant interface as a coating or bone graft substitute. HA coatings bond to bone with a shear strength that is comparable with the shear strength of bone [33]. An osteoconductive substance only elicits en extracellular response, so that osteoblasts will have to be present for bone to be formed [13].

The *osteoproductive* property is only connected with bioactive glass which elicits both an extracellular and intracellular response [13]. The osteoproductive property is defined as the biologically active hydroxyl carbonate apatite layer on the glass surface being colonized with osteogenic cells [34]. The osteogenic cells are recruited from the surgical site. Bioactive glass substance are both osteoconductive and osteoproductive [13].

- Bioactive materials elicit a specific biological response at the interface of the material and tissue, which results in the formation of a bond between the tissue and the material

Table 3: Definition of bioactivity [13].

HA

The extracellular part of bone consists of organic and inorganic materials. The organic material is collagen, mainly type 1 and non-collagenous proteins entrapped in the collagen. The inorganic material consists of crystalline apatite compounds, which are precipitated in the collagen. Apatites are a group of calcium phosphate minerals with OH^-, F^-, and Cl^- ions bound in a hexagonal dipyrimal lattice structure. These apatites are referred to as hydroxyapatite, fluorapatite, and chlorapatite. Ideally, the apatite of bone is hydroxyapatite, HA. The apatite is a carbonate hydroxyapatite with the formula $(Ca, Mg, Na)_{10}(PO_4HPO_4CO_3)_6(OH)_2$ [32]. It is also possible to substitute some of the calcium with, for instance, strontium and magnesium, strontium hydroxyapatite, and magnesium hydroxyapatite [35]. With substitution of the calcium with magnesium in the HA, the apatite structure is less chemically stabile; in consequence the substituted HA can more easily convert to ß-tricalcium phosphate when heated [36]. ß-tricalcium phosphate is more readily dissolved and subsequently more bioactive especially at low pH, such as during fracture healing [21, 37]. Strictly speaking, ß-tricalcium phosphate is not an apatite.

Apatites are widely formed in nature but can also be synthesized for commercial medical use. HA is usually synthesized by precipitation and subsequently sintering at 1000°-1300° Celsius. HA granules are used as bone graft substitutes, and HA vacuum plasma-spray coatings are used for many types of joint prostheses. Under stable conditions the HA is mainly removed by cell-mediated resorption and dissolution, but under unstable conditions then also by mechanical erosion [37, 38].

HA bone graft substitutes

HA granules are commercially available, like Calcibon®, for use as a bone graft substitute for filling critical bone defects.

When HA is used as bone grafts substitute, several morphological and mechanical aspects influence the bioactive property and clinical application of the material. A certain morphological profile for the HA material is recommended, e.g. porosity of 50-60% for optimizing the bioactivity of the material (Table 4).

Recommended morphological profile
• 50-60% porosity • Minimal interconnection channel diameter size of 50-100 µm • Minimum 20% strut porosity

Table 4: Recommendations for the morphology of the bone graft substitute material.

However, the mechanical strength of the material, unfortunately, decreased with increasing porosity [39]. Verdonschot showed that the high total deformation of the HA/TCP (80:20) with 50% porosity is the most important factor for the decreased mechanical property of the bone graft substitute material compared with allografts. The difference in mechanical properties between the synthetic and biological material is especially the lack of viscoelastic properties of the HA. The aspect of low mechanical strength limits the clinical use of bone graft substitutes. The grafted bone site will then have to be mechanically supported by internal or external fixation. Additionally, HA bone graft substitutes are less bioactive than allograft, and an osteoinductive agent often needs to be added to obtain successful healing of the bone defect [40, 41].

HA coating

Plasma-sprayed HA coating was introduced in the 1980s and is still the most common calcium phosphate coating used clinically [33, 42]. Today, the HA plasma spray coating is performed under vacuum (vps), which gives a denser HA coating with a higher adhesive strength to the underlying metal substrate, a higher crystallinity and purity of HA [43]. The ratio of crystallinity versus amorphous structure of the calcium phosphate is greatly influenced by temperature during plasma spraying, because HA can be transform by heat to ß-tricalcium phosphate (ß-TCP). When the plasma spraying is performed under vacuum, then the temperature can be lower while the HA is still viscous. Any amorphous calcium phosphate of the coating is more readily dissolved than HA [44]. A crystalline HA-coated Ti implant surface provides a long-term bioactive surface [45]. Whereas an amorphous calcium phosphate or ß-TCP coated Ti surface will only be bioactive for a short term until the coating has dissolved, which will leave the implant with a raw Ti surface. The performance of the HA coating is greatly influenced by purity, crystallinity, Ca/P ratio, porosity, and mechanical strength [45]. Hence it is advisable to determine and control these factors. The vps HA coating is strongly bonded to a porous Ti surface and delamination rarely happens [46, 47]. In 2003, Rössler et al. published work on HA coating of implants by electrochemically assisted deposition of the HA at 36° Celsius [48].

Clinically, HA-coated implants show less subsidence on roentgen stereophotogrammetric analysis, which subsequently may reduce the risk of developing aseptic loosening of the implant [49]. Initially in the history of HA-coated implants, the survival rate of hip prostheses was as high as 99% and 100% after 6 years [50]. But in a recent study, the superior survival rate of HA-coated implants was not found after 3.5 years [51]. The decline in prognosis is perhaps because the HA-coated implants are chosen for patients with a poor prognosis for the implant survival, like young and physically active patients. Experimentally, osseointegration is enhanced by HA coating [52, 53]. Experimentally, no difference in osseointegration was found between a vps HA coating and a coating of electrochemically assisted HA deposition [54].

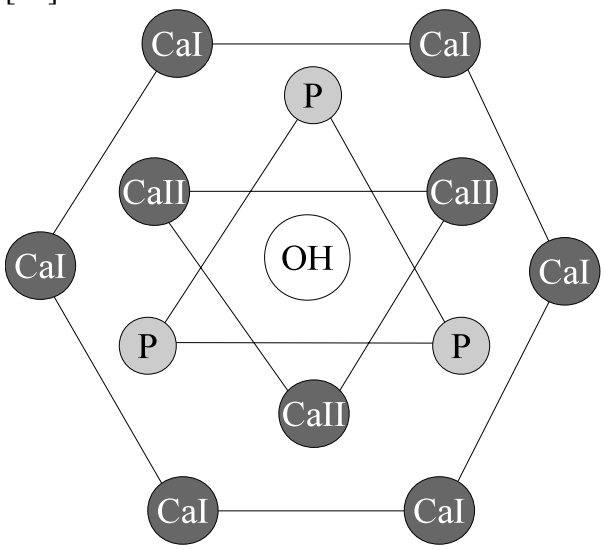

Figure 1: A sketch of the chemical structure of hydroxyapatite. Strontium is preferably incorporated at the CaII position, and this expands the apatite structure and cause destabilization [57].

Elements like magnesium, strontium, and sodium can substitute calcium in the apatite lattice. Substitution of calcium in HA can influence the bioactivity of the bone graft substitute and the HA coatings two-fold [55]. Firstly, substitution of elements can cause lattice defect or destabilization, so the modified HA dissolves more readily (Fig. 1) [56, 57]. Secondly, the element substituted into the HA can thus be released into the surroundings by dissolution, ion exchange of the ions at the HA surface, or by cellular biodegradation [58]. The substituted HA then has an additional effect, besides the osteoconductive property, caused by the elements (ions) released [32]. The studies of this dissertation investigate the effects of strontium-doped or -substituted HA and thereby the effect of strontium in the bone-implant interface.

Bioactive glass

Bioactive glass was invented during the Vietnam War. An American orthopedic surgeon challenged Larry L. Hench, Florida, USA to invent a biomaterial to help regenerate bone defects. Hench invented 45S5 BioGlass®, and many variants of bioactive glass have since been made. Glass is characterized as an amorphous material during its solid state and transforms from solid state to liquid state via a soften state. Degradation of the bioactive glass is essential for the glass to be bioactive and osteoproductive. Ions, especially of Si^{4+}, are released by degradation. The released ions are then exchanged with the ions in the surrounding milieu, and a biologically active hydroxyl carbonate calcium phosphate layer is formed. The layer is at first amorphous and later becomes a crystalline HA layer. The glass-bone interface is strongly bonded by predominantly Si-O-Si bonds [59-63]. Furthermore, at the optimum concentration of ions released, DNA synthesis will be activated and turnover of both osteoclasts and osteoblasts will be regulated [64]. The sum of the intracellular and extracellular responses leads to rapid bone formation at the same rate as the glass is degradated [60, 65].

To date, commercially available bioactive glass particles, such as Biogran® (FBFC International, Dessel, Belgium and Orthovita, Malvern, PA, USA), have been widely used in dentistry as bone grafts extenders or bone grafts substitutes. Under these clinical conditions involving critical bone defects, the bioactive glass performs well, because it induces rapid new bone formation [66, 67]. Orthopedic implants coated with bioactive glass, on the other hand, are not yet commercially available. The reason for this is two-fold. Firstly, implants coated by enameling technique are dipped into a glass suspension and sintered in a furnace at 730°C in order for the glass to become a homogenous adhesive glass coating. When the implants are heated, the materials expand, as characterized by the thermal expansion coefficient (TEC), which is specific for a given material. If there is a mismatch between the TEC of the metal core (e.g. Ti) of the implant and the glass coating material, then delamination of the glass coating take place, especially during the cool down phase. The TEC of the glass is determined by the chemical composition, so by changing the composition, the TEC of the glass can be matched to the TEC of the metal core of the implant. Secondly, chemical composition greatly influences the degradability of the glass and therefore the osteoproductive property of the glass. Summing up, the challenge of bioactive glass-coated implants is to match the TEC of the metal implant core and the bioactive glass coating and at the same time maintain the osteoproductive property of the glass. These chemical properties of the glass have been reported to oppose one another [68] if the glass is not designed correctly [69].

For maintaining the osteoproductive property of the glass, attention must be paid to the sintering window of the glass. The sintering window is the temperature range between glass softening and the onset of crystallization. The glass must also show a large sintering window to prevent crystallization during the firing process. The sintering window of the glass can be increased by increasing the number of components in the glass, which increases the

enthalpy of mixing, stabilizes the disordered glass state, and increases the barrier for crystallization. Ideally, the glass should also show viscous flow sintering behavior in order to obtain a cohesive glass coating [69].

It was decided to study the influence of strontium (Sr) substitution for calcium (Ca), because Sr has shown to increase the degradability and apatite formation of bioactive glasses. While CaO and SrO are both network modifiers, the Sr^{2+} cation is slightly larger than the Ca^{2+} cation (1.16 nm for Sr^{2+} and 0.94 nm for Ca^{2+}), resulting in expansion of the glass network. For this reason, the molar substitution of Ca by Sr in bioactive glasses increases the rate of degradation of bioactive glasses and thereby increases their bioactivity [70, 71]. This means the osteoproductive properties of the glass would also be expected to increase [13, 60, 72, 73].

The issues of bioactive glass coating of Ti implants is investigated in vivo in study I. Bioactive glass-coated implants with strontium substitution of the glass are evaluated by analysis of osseointegration and mechanical fixation.

Allograft

In 1975, bone grafts were used for the first time for restoring the bone stock in connection with total hip replacement surgery [74]. There are three types of grafts: autografts, where donor and recipient are the same individual; allograft, where donor and recipient are of the same species; and xenograft, where donor and recipient are of different species. Autografts are regarded the gold standard for achieving osseointegration, but the disadvantages in connection with harvesting of the graft are considerable [75]. Therefore an autograft is often not the first choice clinically. Second best are allografts, but fresh allografts can induce an immunological host-versus-graft response leading to non-union by intervening fibrous tissue. Additionally, fresh allografts can transfer infectious diseases [76]. Freezing at minus 80° C, freeze drying, or irradiation can considerably reduce these disadvantageous effects of fresh allografts [31, 77]. These procedures also preserve the allografts for later use. The graft material can be of structural or morselized cortical or corticocancellous bone, or morselized cancellous bone. The different materials possess different properties in regard to mechanical strength during the replacement by viable bone and the extent to which it is replaced. Today, morselized corticocancellous allografts are often used during revision hip replacement surgery in which a great loss of bone stock has occurred [2]. The allograft is impacted hard around the prosthesis to immediately stabilize the implant at surgery and to restore the bone stock in the long-term [78]. The long-term stability is then obtained by osseointegration of the implant. In that process any intervening graft material gets partially or fully replaced by new living bone [77, 79]. Allografts are an osteoconductive substance. If the site of impacted necrotic allografts becomes vascularized, then bone resorption is intensively stimulated, and, to a less extent, the coupled bone formation is also stimulated [75]. But the quick resorption of the allograft may exceed the slower replacement of new bone [79]. Then the implant may become instable and at risk of becoming aseptically loosened. By regulating the mismatch between fast resorption of the biologic graft and slower new bone formation, the outcome of grafted revision arthroplasty can perhaps be improved. An investigation of the inhibition of the fast resorption of the allograft by bisphosphonates alone and in combination with BMP-2 has been conducted [80, 81]. Both bisphosphonates and BMP-2 are very potent and strong acting agents. In these studies of soaking the allograft with the agents, implant fixation and osseointegration were impaired. The authors concluded that the therapeutic window of the agents is narrow and further studies of the agents at different dosage are needed.

Study II of this dissertation also addresses the issue of the fast resorption of the allograft and slow new bone formation. A strontium-doped HA bone graft extender is mixed with allograft, because strontium is both an anabolic and anti-catabolic agent in bone [82].

Strontium

Strontium is element number 38 of the periodic system. Placed in the second group of earth alkaline metals together with calcium, strontium and calcium have a quite similar kinetic profile in the body [83]. Strontium was found in 1790 in a mine near the Scottish village Strontian. Strontium does not exists freely in nature because it oxides quickly. Strontium can be made radioactive: Sr85, Sr89, and Sr90. Radioactive strontium is used for tracing sites of high bone formation in vivo, studying kinetics of strontium, and treatment of the pain of bone metastases [83, 84]. In nature, strontium is found in the mineral compounds celestite (SrSO4) and strontianite (SrCO3), which are present in soil and drinking water. In a normal diet, strontium is present in vegetables and cereals at 2-4 mg/day. In 2004 strontium, as strontiumranelate, was introduced to the European market for the treatment of osteoporosis.

Pharmacokinetics of strontium

In humans, the gastrointestinal tract is the main route of entrance for strontium into the body [85]. The absorption efficiency of strontium is age-dependent and in competition with calcium. Almost all the absorbed strontium (99.1%) is deposited in bone and mainly in newly formed bone [86]. The blood is the second most important location for strontium in the body. A serum strontium concentration of 10,560 ng/ml, after taking 2 g/day strontiumranelate orally, has proven effective in reducing fracture risk in postmenopausal osteoporosis [87]. The single most important excretion route is by the kidneys, and a secondary excretion route is by the intestines [85, 88]. The renal clearance of strontium is about three times higher than that of calcium [83]. The interspecies differences of pharmacokinetics are difficult to clarify, but caution must be made when extrapolating results between species. The majority of animal studies of strontium are made on rodents. Rodents have a high bone formation rate and do not reach a steady-state of remodeling [19]. Therefore results from studies of bone formation and bone resorption performed in rodents must be interpreted with great care and perhaps only be considered preliminary [89]. In a study by Raffalt et al. the content of strontium in bone was increased to 9 mg/g bone, when 3000 mg/kg/day strontium malonate was administrated orally [90]. The calcium content was constant despite strontium administration. In a study in monkeys, Boivin et al. found the average Sr/Ca ratio in bone can be as high as 1:10 after oral strontium ranelate administration for 13 weeks [86]. Boivin et al. also found that strontium is quickly cleared from the bone after treatment.

In the studies of this dissertation, the strontium is applied locally and not orally. Therefore the pharmacokinetic aspects of greatest interest are the therapeutic range of strontium concentration in bone, deposition of strontium in the body, and the elimination of strontium.

Mechanism of action at the molecular and cellular levels

As yet, strontium's mechanisms of action on osteoblasts are not fully understood. Strontium is believed to have more than one mechanism of action. Several studies have proved that strontium can stimulate the calcium-sensing receptor, CaSR, situated in the membrane of osteoblasts and osteoclasts [91-93]. Stimulation of the CaSR situated in the osteoblast cell line triggers mitogenic signals leading to proliferation, differentiation, and activation of the osteoblasts [94, 95]. When the CaSR situated in osteoclast cell line is stimulated, the cells retract and bone resorption is inhibited [95]. Via the CaSR, strontium can also suppress the RANKL production by osteoblasts, which leads to diminished proliferation, differentiation, and survival of the osteoclasts [94, 96]. Hurtel-Lemaire has shown that strontium can induce apoptosis of osteoclasts via the CaSR but in a different manner than that which calcium stimulates the CaSR [97]. In short, strontium simulates, together with the normal level of calcium in the bone marrow, a homeostatic hypercalcemia. A statement was made in the 1960s, that strontium is not under homeostatic control of

either the total amount in the body or the concentration in blood [83]. As yet, no studies have disproved the statement. Even in mice with the knocked-out CaSR gene, strontium has an effect on osteoblasts. Other proposed mechanisms of action have been suggested, e.g. release of an autocrine growth factor leading to osteoblast replication or activations of Akt pro-survival pathway in osteoblasts, which leads to a higher increase in bone formation than resorption, so the total effect is an increase in bone mass [93] [92].

The effects of strontium on the cellular level are to increase the pool of active osteoblasts and decrease the number of less active osteoclasts (Fig. 2) [98-101].

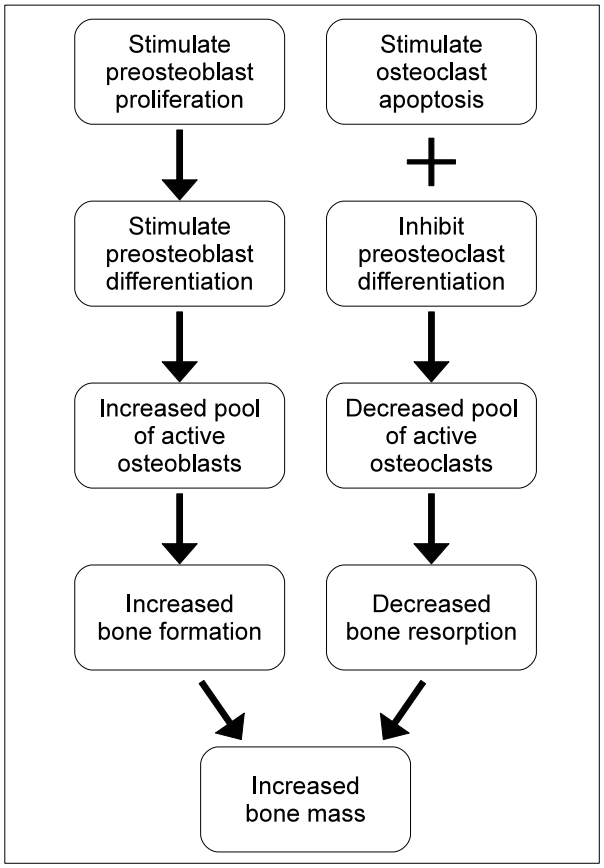

Figure 2: The effects of strontium at the cellular and tissue levels.

Effect on bone tissue

When administrated orally as strontium ranelate, the strontium is found incorporated into hydroxyapatite in place of calcium at a maximum Sr/Ca ratio of 1:10 [86, 102]. In old bone, strontium is incorporated by ion exchange on the bone surface and during bone formation by ion substitution. This does not have a deleterious effect on bone mineralization as long as calcium intake is adequate [103-105]. Hypomineralization caused by strontium has been shown in rats by Grynpas et al. [104]. Grynpas et al. have also described how high bone formation, which rats have, can cause hypomineralization of bone, especially if the formation is increase, e.g. by strontium [56]. In another study by Grynpas et al. the rats were feed a normal calcium-containing diet [106]. Then the bone formation was increased by a relative low strontium dosage without causing hypomineralization.

Several studies on humans, monkeys, and dogs show an increase in parameters of bone formation, such as osteoblast surface, mineral apposition rate, and S-alkaline phosphatase [90, 105]. *In vitro*, strontium increased bone formation in rat calvaria cultures, but 72 hours after removal of the strontium, the effect was no longer detectable [100]. As yet, the anti-catabolic effect of strontium *in vivo* in large animals has only been shown in one study of monkeys [99].

Ammann et al. have studied the mechanical effects of strontium on bone in rats [107]. A strontium dose-dependent increase in mechanical properties was found, which was associated with the increase in bone volume and improved micro-architecture in terms of trabeculae number and thickness (Fig. 2).

Clinically, in the treatment of osteoporosis, strontium ranelate has been found to reduce the risk of especially non-vertebral fracture but also vertebral fractures [108-111].

Studies of strontium in connection with cementless arthroplasty are limited and still at the experimental stage. Results are promising but based on studies of rodents [112-114].

Likewise studies of strontium containing bone graft substitutes are promising, but so far only in studies performed on rats [55, 115, 116].

4. Aims of the studies

In a larger perspective, the aim of these studies is to contribute to a general assessment of whether strontium addition to the bone-implant interface is advisable. To begin with, what is the best method of strontium delivery to the interface; and then, can strontium exercise its dual effects in the bone-implant interface?

Before an agent like strontium can be advised for addition to the bone-implant interface, beneficial effects must be evident. At the same time, evidence of no or minimal deleterious effects of strontium must be clarified and estimated.

The aim of the studies in this PhD dissertation was to investigate whether strontium added to the bone-implant interface under various conditions would improve implant fixation.

Hypotheses for the studies

Study I

SrHA, strontiumhydroxyapatite, coating on Ti implants will enhance implant fixation both at 4 weeks and 12 weeks.

Theory rationale: Strontium increases bone formation, and SrHA is more bioactive than HA.

Study II

Strontium-doped HA as a bone graft extender mixed with allograft will enhance implant fixation.

Theory rationale: Strontium increases bone formation, SrHA granules are more bioactive, and the anti-catabolic effect of strontium may slow down resorption of the allograft.

Study III

1) Bioactive glass coating of Ti implants will enhance implant fixation compared to HA coating.

Theory rationale: Bioactive glass is osteoproductive, while HA is only osteoconductive.

2) Strontium-substitution of the bioactive glass coating on Ti implants will further enhance implant fixation compared to bioactive glass coating without strontium.

Theory behind: Strontium increases bone formation.

Sub-hypotheses for the studies

Implant fixation was to be investigated histologically and mechanically. Therefore histomorphometrical analysis was chosen for evaluating implant osseointegration, gap healing and ongrowth, at the microscopic level [14]. Mechanical implant fixation was evaluated by biomechanical push-out test to failure.

Several sub-hypotheses, based on several variables, were setup and tested to elucidate the issue of implant fixation in details:

- Gap healing (as volume of new bone in the gap) will be improved by addition of strontium to the interface.
- Ongrowth onto the implant (as surface area of new bone on the implant) will be increased by strontium addition to the interface.
- Ongrowth onto the bone graft extender will be increased by strontium doping of the bone graft extender.
- The allograft will be preserved for longer when the bone graft extender is strontium-doped.
- Peri-implantary fibrous tissue will be reduced by strontium addition to the interface.
- Apparent shear stiffness will be improved by strontium addition to the interface.
- Ultimate shear strength will be improved by strontium addition to the interface.
- Total energy absorption will be improved by strontium addition to the interface.

All three studies were conducted with a paired study design and with non-loaded implants. The implants were inserted into the metaphysis of the humerus and surrounded by a concentric gap of variable size between studies. All analyses were performed blinded.

5. Methodological consideration

The majority of health research is aimed at gaining knowledge concerning the diagnosis and treatment of human disease. These investigations usually start with *in vitro* observations, proceed to *in vivo* tests in animals of increasing size before being applied to humans. In order to apply results from one level to the next, the model and method used must resemble the conditions of the end goal of the diagnosis or treatment as closely as possible [117]. Discrepancies between the experimental study and the clinical endpoint in humans must be clarified and estimated when possible.

Design

All studies are paired, block-randomized intervention studies. The paired study designs eliminated various foreseen and unforeseen variables of inter-individual biological and conditional character. Thus, the statistical power of the studies was strengthened and a lower number of animals could be included.

In the three studies, the implants were positioned in the proximal humerus, and the locations were alternated systematically with random start between right and left limb, and between proximal and distal hole in the same limb in study III. The positioning was alternated in order to rule out bias due to systematic differences between the implantation sites with regards to bone quality or loading pattern [26].

In the two four-arm studies (I and III), the interventions were strontium-substituted coatings. The strontium-substituted coatings were expected to be readily soluble and strontium would be released into the surrounding marrow space. The strontium would then become present in the surroundings of the neighboring implant. To eliminate any risk of strontium contamination of a strontium-free neighboring implant, the implants with strontium-substituted coatings were placed in the same humerus. In study I, the intervention of SrHA coating was investigated at 4 weeks and 12 weeks (Fig. 3).

As a consequence, each humerus was operated twice, 8 weeks apart. One potential disadvantage here could be the influence of regional acceleratory phenomenon (RAP) inflicted upon the host bone both at time zero and at time 8 weeks (Fig. 4). For assessment of the effect by RAP, the following questions should be considered:

1. How far from the fracture/drill hole does RAP increase remodeling activity and at which time points?

   In a previous study RAP was not observed in a zone 2-5 mm from the implant after 8 weeks [118]. It is possible that the RAP had already passed at the distance of 2-5 mm so where the RAP effect would be after 8 weeks is uncertain.
2. Does RAP cause improved fracture healing of the neighboring bone?

   I have not found literature on the subject; but if fracture healing of the implants at 4 weeks observation time was improved by a RAP stimulus from the surgery 8 weeks earlier of the neighboring implant, then due to the paired study design the fracture healing of both treatment arms would be equally improved. Additionally the increase in bone turnover activity by RAP must be less than the increase in bone turnover caused by the fracture healing. The reason is that the stimulus of fracture healing gives rise to the RAP and the induced increase in bone turnover spreads out over time like concentric waves forming with fading intensity when a stone falls into water (Fig. 4).

The effect of RAP on neighboring fracture healing has been found to be minimal and of no relevance in previous studies [22, 119].

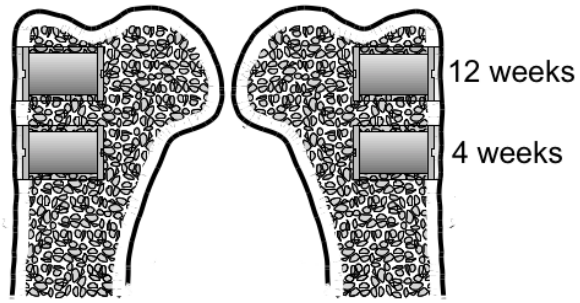

Figure 3: Positioning of the implants in studies I and III. In study II only one implant was inserted at the proximal implantation site, bilaterally.

Sample size

For economical and ethical reasons, the number of dogs needed to be included in the studies were estimated as follows [120]:

Equation 1

$$N = (C_{2\alpha} + C_{\beta})^2 \cdot CV_{diff}^2/\Delta^2$$

- $C_{2\alpha} = 2.26$ (p=0.05)
- $C_{\beta} = 0.883$ (p=0.2)
- $CV_{diff} = 30\%$
- $\Delta = 30\%$

Equation 1 is designed for normal distributed data that fulfils the assumption of the paired t-test. The criteria were assumed fulfilled. The risk of accepting a false positive and false negative difference was set at 5%, $C_{2\alpha} = 2.26$ and 20%, $C_{\beta} = 0.883$, respectively. The minimum relative difference in means, Δ, to be detected between intervention and control was set at 30% for any variable in the studies. The estimated value of coefficient of variance was based on previous studies with the same model for the variables of the histomorphometrical analysis and the push-out test [24, 121, 122].

Equation 2

$$N = (2.26 + 0.884)^2 \cdot (50\%)^2/(50\%)^2$$

Equation 3

$$N = 9.88$$

Hence, 10 dogs were included in each study.

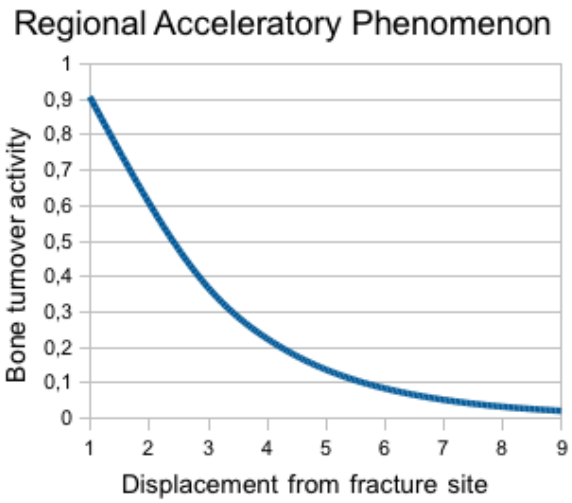

Figure 4: Regional acceleratory phenomenon is an increase in bone turnover activity, which originates from the fracture healing stimulus and fades out over distance from fracture site. The curve is a principal drawing ($Y = E^{(-0.1 \cdot X)}$) of spreading of a wave for illustrating the aspects of decreasing intensity with increasing displacement.

Experimental animal model

The studies in this dissertation were all conducted in skeletally mature American Foxhounds. The implants were inserted into cancellous bone of the metaphysis of the humerus bilaterally. The canine shows great resemblance to humans with regards to bone mineral density, biochemical composition, mechanical quality, and most importantly, bone growth reaches a steady state characterized by remodeling activity [19, 89, 123]. Alongside primates, the canine is regarded as the best experimental animal model for orthopedic research [123, 124]. However, the bone turnover time of the remodeling activity is complete on average of approximately 2.5 times as fast as in humans [125]. In opposition, rodents have a high bone formation rate and do not reach a steady-state of remodeling [19].

When studying bone biology in an animal model, it could be suggested to use rodents for studying conditions and fracture healing in humans between 0 years and 25 years of age; dogs for studying conditions and fracture healing between 25 and 60 years of age; and sheep for studying conditions and fracture healing in humans over 60 years of age.

Therefore, the results of the studies in this dissertation may be a little too positive and show a greater effect of strontium under certain conditions than would be expected clinically in elderly humans. On the contrary, a study by Shaw et al. has indicated equally good potential of implant ingrowth between younger dogs and postmenopausal monkeys [123]. Yet, this choice of animal model is acceptable for a first line of experimental studies since any positive effect will be magnified. Any future studies of strontium can be targeted toward its main field of effect.

Canines are also easy to handle and the large size of their bone makes it possible to conduct four-arm, paired studies in cancellous bone, which reduces the number of animals used for research. The implantation site is easily accessible so the implants were inserted with minimal cause of trauma.

The dogs included in the studies were bred for research purposes. Minneapolis Medical Research Foundation, and the Animal Care and Use Committee approved the protocol of the study. The surgeries were carried out at AAALAC-approved animal care facility and NIH guidelines for care and use of laboratory animals (NIH Publication #85-23 Rev. 1985) were observed.

Implant model

Direct versus indirect loading of the implant

In humans, remodeling of the bone from the waist down is balanced by the stimulus of weight loading which helps to maintain bone mass; as a consequence, prolonged bedrest will reduce bone mass [126]. Direct load on allografts has also been found to increase the area of active graft incorporation but not to increase the area of new bone [127]. Clinically the hip implant is directly loaded with body weight during gait. The direct load is then transferred from the implant to the host bone. If the femoral implant is large, the direct load is often not evenly distributed e.g. femoral implant will be inserted at press-fit at least in the distal area, which facilitates bone ingrowth and stress-shielding takes place more proximally [128]. In this case, the areas with high transferral of the direct load usually at the distal tip of the femoral implant, Gruen zone 3 and 5 (Fig. 5), bone formation is increased and osseointegration of the implant is achieved [129, 130]. At areas of low or no transferral of direct load, usually at the proximal part of the femural implant, Gruen zone 1 and 7, bone mass is lost and the implant is not osseointegrated. Subsequently, in a situation of pronounced stress-shielding the implant is not well anchored in bone and instability can develop ultimately resulting in aseptic loosening. The distribution of transferral of direct load is mainly dependent on the size, but also on the shape, material, and design of the implant, which is outside the scope of this dissertation. Therefore, the test implants were placed in the humerus of a fully loaded forelimb but were not subject to direct loading.

Clinically it is not possible to control conditions in this manner. Still it was relevant to control the conditions in these studies in order to investigate the isolated effect of strontium in the implant-bone interface.

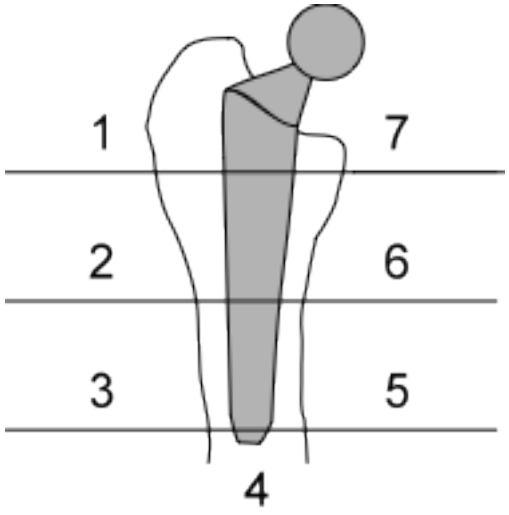

Figure 5: Gruen zones in relation to a femoral component.

	Observation time	
Implant model	4 weeks	12 weeks
Gap	**Anabolic** effect	**Anti-catabolic** effect on the modelling activity
Inserted by compaction technique	**Anti-catabolic** and **anabolic** effect	**Anti-catabolic** effect on the modelling activity
Allografted implant	**Anti-catabolic** and **anabolic** effect	**Anti-catabolic** effect on the modelling activity

Table 5: Anabolic and anti-catabolic effects of agents or coatings can be investigated with the implant model dependent on the implant type, insertion technique and observation time

Gap versus press-fit

During hip replacement surgery, a cavity in the host bone is carefully prepared to closely fit the implant. Even so, Geesink has described that the surface of the implant is separated from the bone by a series of small gaps. Therefore, it is important that the implant surface is bioactive to facilitate the healing of the intervening gap.

Hence, the anabolic effect of an implant surface or an agent added to the bone-implant interface is more clearly seen when a gap is introduced between the implant and the host bone [131, 132]. This gap magnifies the anabolic effect (Table 5).

Additionally, the gap model has an advantage during evaluation because on the relevant new bone is present in the interface and will influence the results of the mechanical test and, during histomorphometrical analysis, no mistakes can be made made concerning whether the mineralized tissue is newly formed or old, necrotic bone originating from insertion of the implant.

The anti-catabolic effect of an implant surface or agent added to the bone-implant interface is most clearly seen if the implant is inserted by the compaction technique or if an implant model with an allograft in the gap between the implant and the host bone is used [24, 121].

Study	Gap size
I, Strontium-substitutes HA coating	1.3 mm (± 0.1 mm)
II, Strontium-doped HA bone graft extender	2.8 mm (± 0.2 mm)
III, Strontium-substituted bioactive glass	1.1 mm (± 0.1 mm)

Table 6: The size of the gap varied between studies.

A gap model was used for all three studies of this dissertation, which allowed investigation of a possible anabolic effect of strontium (study I and III) (Table 6). A possible anti-catabolic effect of strontium was investigated in an allografted implant model (study II).

Observation time

Early implant fixation is essential for longevity of the implant (see section "Aseptic loosening"). Therefore, it must be ensured that any new intervention first secure early implant fixation. This is also the case when substances of a proposed long-term effect such as anti-catabolic interventions are investigated, where these interventions also must perform as well as the gold standard (control) in the field. Early implant fixation is established during the formative phase of fracture healing and the effect of anabolic interventions can become evident with an observation time at the end of the formative phase (Table 5). When early implant fixation is confirmed, investigations must then be extended to include the modeling and remodeling phase. To investigate the anti-catabolic effect of new interventions an observation time well into the modeling phase is also needed. Based on previous studies of this particular implant model, the formative phase of the fracture healing is usually well established after 4 weeks in dogs [133, 134]. Factors like size of the intervening gap at the bone-implant interface, motion at the fracture site, and general or local delayed bone biological activity influences the fracture healing time. These factors need to be taken

into account when determining the observation time for a study.

Modeling at the fracture site starts after the formative phase and takes one to four years in humans, slowing down with time [22]. In the proximal humerus of beagles, Kimmel determined the annual bone turnover rate to be between 156-220% faster than in humans [125]. A previous study using the same model as the studies in this dissertation showed that fracture healing is in the modeling phase 12 weeks after implantation [81].

For all three studies, our hypotheses that strontium substitution or doping of HA improves implant fixation when applied as a coating or bone graft extender were tested for early implant fixation at 4 weeks. In study I the hypothesis of improved late implant fixation by strontium substitution of the HA coating at 12 weeks was also tested.

Implant specifications

Core

The implants used in all three studies of this dissertation were made of a 10 mm high cylindrical Ti alloy (Ti6Al4V) core with a smooth surface to which a rough surface texture was applied. The mean final outer diameter of the implants were 5.7 mm (± 0.1 mm) in study I, 5.7 mm (± 0.2 mm) in study II, and 5.9 mm (± 0.1 mm) in study III. End-cap screws were then mounted on the implants creating a gap of various sizes; see section "Gap versus press-fit".

Surface texture and coatings

The surface of commercial orthopedic joint implants is fully or partly rough-textured. The rough texture can be grit-blasted, sintered beads, Ti vacuum plasma sprayed, etc. The idea behind the rough textured surface is that bone grows into the porosity, improving the anchorage of the implant [135]. It is a matter for debate which surface texture is most ideal for experimental research. Smooth textured implants perhaps give a clearer picture of the effect(s) of the intervention. Yet smooth surfaced implants may not be able to withstand even small loads of force during the push-out test, regardless of the amount of ongrowth. Additionally, experimental implants with a rough surface texture show greater resemblance to the clinically used orthopedic implants. But most importantly, since the metal surface of the implant is not the subject of these investigations, the key issue with the surface is that it is kept constant because it serves only as a substrate. In the studies of this dissertation three different rough surfaces were chosen: *Ti VPS surface with SrHA/HA coating, a sintered bead surface, and a grit-blasted surface with bioactive glass coating* (Table 6).

SrHA/HA coating: The studies in this dissertation were inspired by the use of strontiumranelate as a treatment for osteoporosis, due to strontium's incorporatation into the hydroxyapatite of bone. By mimicking the non-harmful products of the body, the first barrier of unfamiliarity of the substance is usually bypassed. We decided to use a 5% substitution of calcium, based on the limited literature at the time in the field of strontium's effect on bone metabolism, mainly investigated in rodents [99, 100, 103, 104, 106, 107, 136-138]. Prof. Marc Grynpas, Toronto, Canada, was also consulted on the issue.

A precipitate of the 5% strontium substituted hydroxyapatite and pure HA was produced and donated by Osteologix Aps, Denmark, to be used for the SrHA coating and as bone graft extender. The rest of the coating procedure was performed and generously donated by Medicoat AG, Mägenwill, Switzerland. The precipitate SrHA and HA were converted to powder suitable for vacuum plasma spraying. This powder was characterized by x-ray powder diffraction and inductively-coupled plasma mass spectrometry (Table 7).

HA and SrHA Study I	A innermost Ti-bond coating: • Vacuum plasma sprayed • 50µm thick In the middle a Ti-structured coating: • Vacuum plasma sprayed • 250-300µm thick • R_a < 25µm On top a HA or SrHA coating: • Vacuum plasma sprayed • 60-80 µm thick Specifications of the HA and SrHA spray powder: • HA or SrHA purity of 95% • Ca/P or CaSr/P: 1.667 ± 0.004 • 4.86% Sr atoms in SrHA • Particle size distribution: 75 (45-125) µm • Bulk density: 1.16 g/cm3
Ti Study II	• Sintered beads • 40-50% porosity • Average pore size of 250-300 µm
Bioactive Glass Study III	• Grit-blasted implant cores • 0%, 10% and 50% of calcium oxide were replaced by strontium oxide in the glass system: SiO_2-Na_2O-CaO-SrO-K_2O-MgO-ZnO-P_2O_5 (Table 8) • Glass powder produced by melt-quench route • Dispersion of polymethylmethacrylate, chloroform, and particle smaller than 38 µm. • Implant cores dipped four times in the glass- containing dispersion • Implants with dip coating were sintered at 750˚ • Glass particles in the dip coated layers melted into a cohesive glass layer and the PMMA depolymerized and the monomer evaporated

Table 7: Specifications of the coatings investigated or used in the studies.

The Sr-content was uniformly distributed and morphology of the particles was visualized by SEM (Fig. 6).

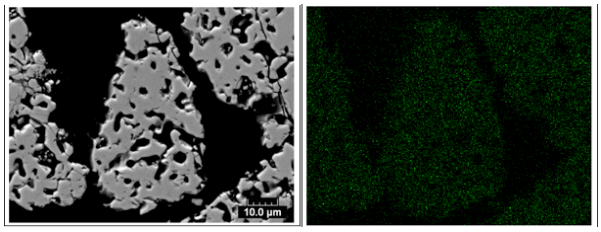

Figure 6: SEM image of the SrHA spray powder particles show morphology and Sr distribution.

A mechanical test of the tensile bond strength and shear stability was not performed. The spraying conditions and specifications of the powder were identical for SrHA and HA and furthermore identical with powder and conditions of the commercially available HA coatings of endoprosthesis for total hip replacement. For commercially available HA coatings, analyses have been made of both the HA spray powder and HA after VPS coating. The analyses confirmed that the specification of the HA powder listed above (Table 7) is similar to the specification of the HA coating. Similar analysis like XRD has not been done for the SrHA VPS coating, so whether the SrHA underwent any phase transformation during VPS is not known.

Implants with these HA and SrHA coatings were investigated in study I.

Mol. %			
Oxide	**Sr0**	**Sr10**	**Sr50**
SiO2	49,46	49,46	49,46
Na2O	3,30	3,30	3,30
CaO	32,62	29,36	16,31
SrO	0,00	3,26	16,31
K2O	3,30	3,30	3,30
MgO	7,25	7,25	7,25
ZnO	3,00	3,00	3,00
P2O5	1,07	1,07	1,07
Total	100,00	100,00	100,00

Table 8: Chemical composition of the bioactive glass with 0%, 10%, and 50% of calciumoxide substituted by strontiumoxide.

Sintered bead surface: The coating was donated by DePuy Inc, Warsaw, IN, USA. The surface of the test implant resembles the surface of commercially available orthopedic implants. Implants with the sintered beads were used in study II.

Grit-blasted: Plasma Biotal Ltd performed the grit-blasting of the implants for study III. The bioactive glass was expected to dissolve in vivo in approximately 3 weeks leaving a commercially available implant surface.

Bioactive glass coating: Production of the strontium-substituted powder and dip coating was performed by Bioceramic Therapeutics Ltd, London, UK (Table 7 and 8).

A VPS coating of the glass was also considered. The VPS coating method may minimize interactions between the grit-blasted Ti core implant and the bioactive glass yet still provide a good bond. The dip coating method was selected because this method allowed for the bioactive glass to be deposited at surfaces and spaces not accessible by the VPS method.

Bone Graft Extender

Solid, crystal precipitate of calciumhydroxyapatite (HA BGE) was studied as a control bone graft extender. In the intervention treatment arm, 4.93% of the calcium had been substituted by strontium (SrHA BGE). The synthetic HA BGE or SrHA BGE material only possess osteoconductive properties and an agent or material with osteoinductive signal needs to be added for gap healing to be successful [31]. Therefore the bone graft extender material was mixed with allograft at a 50:50 volume ratio. Additionally, it was hypothesized that the strontium-doped bone graft extender was ideal for mixing with allograft because of the proposed dual acting properties of released strontium which would regulate the mismatch of fast allograft resorption and slow new bone formation.

A HA bone graft extender was chosen over a TCP. HA is present in bone for longer than TCP [37], which is desirable in many clinical settings especially since the bone graft extender serves as a osteoconductive scaffold, promoting new bone formation. The disadvantage of HA compared to TCP is the lower osteoconductive activity. Therefore, the greatest challenge and interest was to improve the performance of HA as bone graft extender. Our hypothesis was that strontium doping of the HA bone graft extender would improve implant fixation.

The granules of the bone graft extender ranged between 0.6 to 2 mm in diameter (Fig. 7). The size of the granules was within the range recommended for well-graded particle-size, but it may have been beneficial for the size range to also have gone below 0.6 mm [139]. However, in this model, granules of 2 mm can fill out the bone-implant interface in the full height of the specimen block for the mechanical push-out test, which was noted during the test. If or when this happens, the mechanical properties of the interface can be compromised in a matter of no clinical relevance. This issue also might have caused an increase in variation of the data, as well, contributing to non-significant differences between the treatment arms.

The issue of porosity of the bone graft extender material was not included in this investigation.

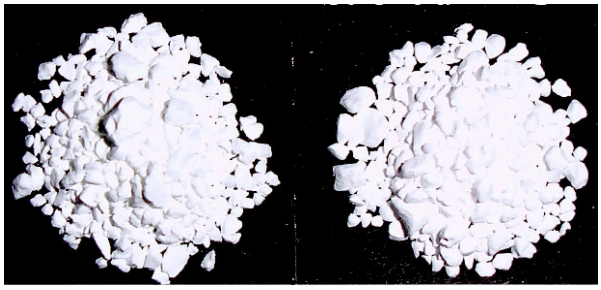

Figure 7: Bone graft extender material HA on the left and SrHA on the right.

Surgery

Surgery was performed under sterile conditions, and the dogs were fully anaesthetized during the procedure. A 7-cm long skin incision was made with cautery on the lateral proximal humerus. The deltoid muscle was bluntly dissected to expose the humerus. To match the clinical conditions of hip replacements, the test implants were inserted into cancellous bone. The surgical procedure is relatively small and well tolerated by the dogs with complications like infections and fractures rarely observed.

In study I, a 2.5-mm guide wire was inserted anterolaterally at the level of the greater tubercle and oriented perpendicularly to the surface. Another 1.5-mm guide wire was inserted 17 mm distally and parallel to the first. The distal guide wire was cut off approximately 2 mm above the bone surface. With a cannulated drill (∅ 8.0mm), a 12-mm cavity was drilled over the proximal guide wires at a maximum speed of two rotations per second. The edge of the hole was trimmed, and the cavity irrigated with 10 ml saline for removal of periosteum and loose bone chips. One implant was inserted into the cavity, and after securing hemostasis, the soft tissue was closed in layers. This procedure was repeated for the opposite humerus.

After 8 weeks, a second surgery was performed with the same surgical procedure as just described. At this second surgery, an implant with the same coating as in the proximal implant position was inserted at the position of the cut off 1.5 mm wire.

In study II, one surgery as described above was performed and implants were only inserted into the proximal implantation site, which was created with a cannulated drill (∅ 11.0mm). An implant with a mounted bottom screw was inserted into the cavity. A mixture of 1 mL allograft and 1mL SrHA or HA, was tightly packed around the implant, and the top screw was mounted. One surgeon impacted the graft mixture for all the implants.

In study III the surgery was performed as described above for study I. The only difference between the surgeries was that in this study all four implants were inserted during one surgery since observation was the same for all treatment arms (Fig. 8).

All dogs were given ceftriaxone (1 g, i.v) and buprenorphine hydrochloride (0.0075 mg/kg/day, i.m) administered immediately before surgery and 3 days postoperatively.

The dogs were given 30 mg/kg tetracycline i.m. day 18 and 20 mg/kg calcein i.v. day 25, for fluorochrome labeling of the mineralization front [140, 141]. After 28 days, the dogs were sedated and killed with an overdose of hyper-saturated barbiturate. Using these dogs, unrelated studies were conducted in the distal femur and proximal tibia. In the dogs of study II, a study of partial gold coating of implants was examined in the distal implant site of the humerus. Only studies with no systemic effects were carried out in the same series of animals.

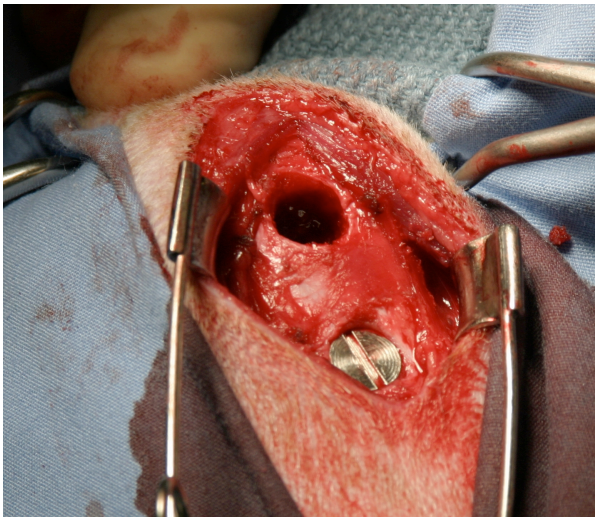

Figure 8: An implant with mounted end screw has been inserted in the distal implantation site while the proximal implantation site is ready for insertion of implant. The observation time for both implants is 4 weeks.

The studies within these dogs were of implant surface modifications, topical short-lived growth factors [142], and topical bisphosphonates, which have a high affinity for bone and therefore do not become systemically available [143].

Preparation of specimens

The bone cells in the specimens were not the main target of the analyses but it was advantageous to preserve them because they could become useful for morphologically determining the tissue type in the histomorphometrical analysis. On that account, formalin was the optimal fixation for these specimens. However, the lamellae of bone tissue are best preserved in ethanol.

Unfortunately, the specimens had to be transported from the USA to Denmark for further preparation and evaluation. Ethanol and formalin are classified a dangerous goods and are therefore not to be transported by airplane, so fixation in ethanol was found to be not feasible. Instead the specimens were retrieved *en bloc,* each containing two frozen implants which were kept frozen during transportation. This preserved the tissue until its fixation in ethanol in Denmark.

Freezing can cause cells to autolyse because the membrane becomes destabilized. Consequently, fewer cells will be available for morphological determination of the tissue type in the histomorphometrical analysis. Preservation by freezing, however, has been shown not to have adverse effect on the mechanical properties of cancellous bone [144, 145].

The *en bloc* proximal humeri specimens were cut to two approximately 2.5 x 2.5 x 2.5 cm cubes, each containing an implant and surrounding tissue. The implant specimens were randomly allocated a code number which was unknown to the observer for the treatment of the specimen during tests and analyses. The specimen with the 10 mm high implant was subsequently cut transversely using a water-cooled Accutom-50 wheel diamond saw (Struers A/S, Roedovre, Denmark) (Fig. 9). Each block was cut into two pieces: 1) a 3.0 mm high block for mechanical test closest to the surgical entry site, and 2) a 6 mm high block for histomorphometrical evaluation furthest away from the surgical entry site. The mechanical block was then refrozen while the histological block was submerged in ethanol, initiating fixation and dehydration.

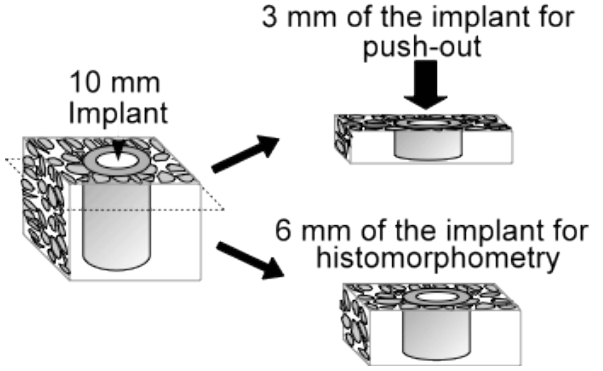

Figure 9: Specimen block cut in two for push-out test and histomorphometry.

In general, these methods of preparation and preservation of the specimens are gentle and do not adversely affect the parameters of later measurements and evaluations that were performed in these studies.

Biomechanical test

For all three studies, the primary goal was to improve mechanical and histological implant fixation. Preferably the test would closely resemble the nature of the mechanical force and load that a clinical implant is subject to. Clinical implants are subject to a simultaneous mixture of non-destructive compressive, shearing and bending forces in a hysteresis-like pattern. A test mimicking these forces is difficult to set up and carry out on a specimen block of 3 mm height and 2.5 x 2.5 cm base.

A destructive push-out test of the implant in the longitudinal axis was selected because the hip replacement prosthesis is subject greatly to axial load, especially during the gait cycle. The Ultimate Shear Strength of the interface found at a push-out test was expected to reflect the upper limit for the load of a given hysteresis-like loading pattern. During push-

out of the implant to failure, the inter-digitating interface of the porous implant material and ingrowth of bone is subject to a simultaneous mixture of tensile, shearing and compressive forces.

For the results to be comparable between specimens, the shape and size of the implant, together with the test procedure, had to be similar [146, 147]. Preparation of the specimens as well as the test itself was standardized and the test parameters were normalized in accordance with the surface area of the implant.

The push-out test was performed with a MTS Bionics Test Machine (Eden Prairie, MN, USA) with 5.0 mm diameter probe.

The specimens were thawed before testing and all were tested in one session. The flat surface of specimen block was placed on a flat support jig with a 7.4 mm diameter central opening [147]. The implant in the specimen block was placed centrally over the hole in the support jig, which assured a distance of 0.7 mm between the implant and the support jig [148]. The direction of loading was from the cortical surface inward. A custom made program kept the test standardized: A preload of 0.5 N was applied to standardize contact conditions before initiating loading. The displacement rate was 5 mm/min with a 500 N load cell. Data points for every 10 µm of displacement were entered into an excel spreadsheet and normalized in accordance with the surface area of the implant. The normalized force-displacement curve was then plotted (Fig. 10) and calculations of the mechanical parameters, *Apparent Shear Stiffness, Ultimate Shear Strength, and Total Energy Absorption [43, 147],* were auto-generated in the spreadsheet based on a PhD dissertation by Baas [146].

Apparent Shear Stiffness (MPa/m): The steepest slope on the force-displacement curve was calculated. The parameter characterizes the deformation property of the interface material and tissue. Note despite the parameter is named apparent *shear* stiffness then the interface is not only exposed to shear

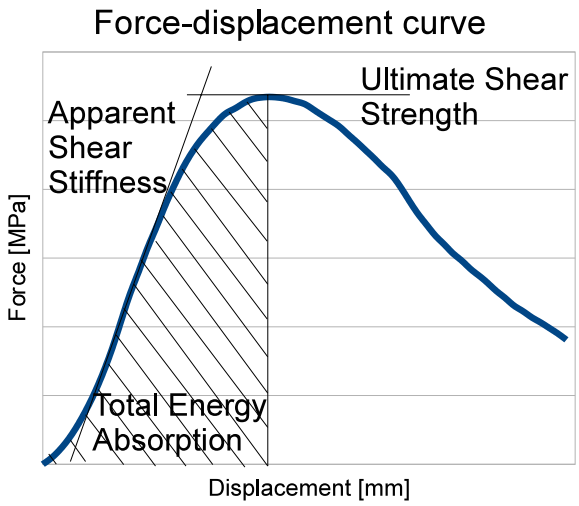

Figure 10: The force-displacement curve was normalized with respect to the surface area of the implant.

force. A high stiffness indicates bone anchorage of the implant because bone is rigid. A low stiffness indicates fibrous anchorage because fibrous tissue is more elastic than bone.

Ultimate Shear Strength (MPa): The first, highest point on the force-displacement curve defines the maximum force applied until failure. The largest shear strength of the interface is characterized by this parameter. The pushed out implant sections were inspected macroscopically; mineralized tissue was often observed on the HA coated implants. Thus, it was the shear strength of the tissue in the interface that was determined. Again note despite that the parameter is named ultimate *shear* strength, the interface is not subject to shear force alone. The strength of bone is usually higher for bone than fibrous tissue.

Total Energy Absorption (J/m): This is defined as the area under the force-displacement curve until failure. It characterizes the ability of the interface to absorb energy but this parameter is not characteristic for a given tissue type.

Together these parameters provide a picture of the mechanical implant fixation, which correlates well with desired osseointegration of the implant [43].

Histomorphometry

The osseointegration of the implants was evaluated at the microscopic level in accordance to Albrektsson's definition (Table 1, page 2) [9]. The aim was to obtain a quantitative, unbiased and representative estimation of the osseointegration. Histomorphometrical analysis provides a quantitative evaluation of the tissue in contact with and surrounding the implant. Various stereological designs exist and can provide unbiased estimates, but to adopt the method of a design in practice is not always possible and issues can arise.

Preparation

The 6 mm specimen block for histomorphometrical analysis was fixed and dehydrated in graded ethanol (70-99%). Specimens were then placed in 99% propanol before they were embedded in cold poly(methylmethacrylate), PMMA. Cold PMMA was chosen because the temperature up to 45° Celsius during hardening of ordinary PMMA polymer can damage cells and cause coagulation of tissue. Cold PMMA is equally good in regard to the quality of bone sections produced [149].

MMA embedding material is also a good choice for specimens to be surface stained because the polymer can be removed completely by H_2O_2, allowing the stain to bind to the tissue.

Sections were stained with toluidine blue at pH 7. Toluidine blue is a cation dye, which binds to negatively charged tissues and cells, and can be controlled by regulating the pH in the milieu. At pH 7, collagen, hyaluronic acid, DNA, and RNA are all negatively charged and get dyed in a purple-blue color. For histomorphometrical analysis, tissue classification was based on morphology (Fig. 11): new bone appears as a disorganized, dense substance with embedded cells colored relatively dark purple; while allograft is a dense substance with empty cell lacunae and clear cement lines colored relatively pale purple. Bone marrow is a cell rich conglomerate with intervening empty areas from dissolved fat and a few scattered thread-like structures. Fibrous tissue appears dense, with well-organized bundles of fibers with sparsely intervening small cells. BGE is identified as coarsely profiled shadows.

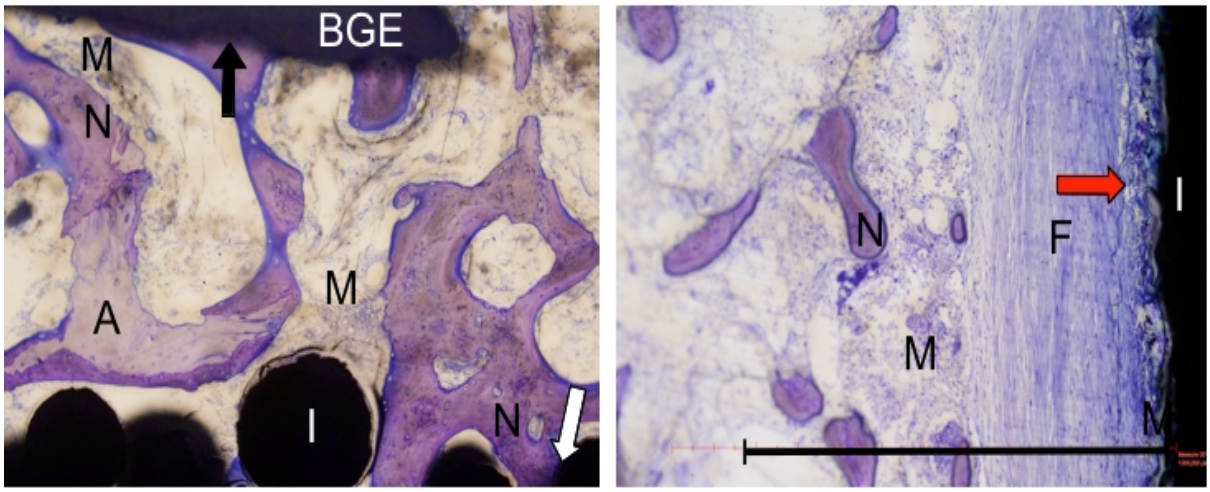

Figure 11: Morphology of the different tissue types: new bone (N), allograft (A), bone marrow (M), and fibrous tissue (F). Implant (I) and bone graft extender material (BGE) is also seen and the bar indicates the initial surrounding gap. Ongrowth onto the BGE (black arrow), ongrowth onto implant (white arrow) and fibrous tissue in contact with bioactive glass coating (red arrow) is also seen.

Toluidine blue does not fluoresce; hence the sections could simultaneously be evaluated by light microscopy and ultraviolet microscopy. This simultaneous evaluation was especially useful for the descriptive study in study III.

The dogs were given tetracycline and calcein for fluorechrome labeling of the mineralization front to alleviate any suspicion of a mineralization defect caused by strontium [141]. No suspicion of mineralization defect arose. Instead, in the bioactive glass coating study, the fluorechrome labels supported the theory that the bioactive glass coating had chemically induced the formation of HA and furthermore allowed us to estimate the time point of mineralization of the induced HA.

Surface staining is superior to infiltration staining of the whole specimen block. First, with a surface stain it is possible to strain almost any specific tissue type and cell of interest. Second, and of greater importance, evaluating the surface of the section is easier on the observer. In contrary to infiltration stains, bone situated deep inside the section is easily visualized due to the nature of light microscopy, which is based on trans-illumination of the section. If more than the tissue at the surface of the section is evaluated then the estimates of bone can be overestimated. With the specific toluidine blue surface staining used in the studies of this dissertation, the depth of staining was estimated to be a mean of 4.1 μm (± 0.56 μm s.d.).

Stereology

The fundamental idea behind stereology is to gain unbiased estimates of number, length, surface, and volume. The estimates are obtained in a two-dimensional material such as histological sections and anisotropy of the features must be considered and dealt with accordingly. The reason for isotropy is that the probability of interceptions between the test probe and the structure must be independent of the orientation of the structure and the probe. Only when the intercepts are isotropic and sampled at uniform random can the estimates be unbiased. Trabeculae of bone are anisotropicically orientated for cancelling the anisotropy of mechanical stress [28].

In the studies of this dissertation, stereological software (Visiopharm Integrator system, NewCast ver. 3.0.9.0 Visiopharm, Hoersholm, Denmark) superimposed the test probes onto a picture of the field of view from the microscope.

In general the number of dimensions for the probe plus the number of dimensions for the structure to estimate must add up to 3. For volume density estimates, the probe is a point: zero-dimensional and without orientation. Unbiased volume estimates are obtained by Cavalieri's principles described by Gundersen [150]. The method is easily carried out and used in all three studies of this dissertation. For surface area density estimates, the probe is a one-dimensional lineprobe, which therefore has an orientation and the issue of isotropy becomes relevant. For obtaining isotropic uniform random intercepts, either the lineprobe or the structure (the interface) must be isotropic. The issue of isotropy is ensured in stereological designs by keeping the lineprobe isotropic and in stereological models by assumptions defined in regard to the structure of interest, respectively.

The surface of the bone graft extender granules used in study II was isotropic (Fig. 7).

The Vertical Uniform Random, VUR, design was used in the study of bioactive glass coatings (III). A cylindrical model was used in studies of strontium-substituted HA coating and of strontium-doped bone graft extender (I and II, respectively). Unless stated otherwise, the sections the dissertation concerning stereology are based on the book by Howard and Reed [151].

Vertical uniform random

The VUR design is based on a combination of three sampling techniques but no assumptions are made: firstly, sections must be obtained

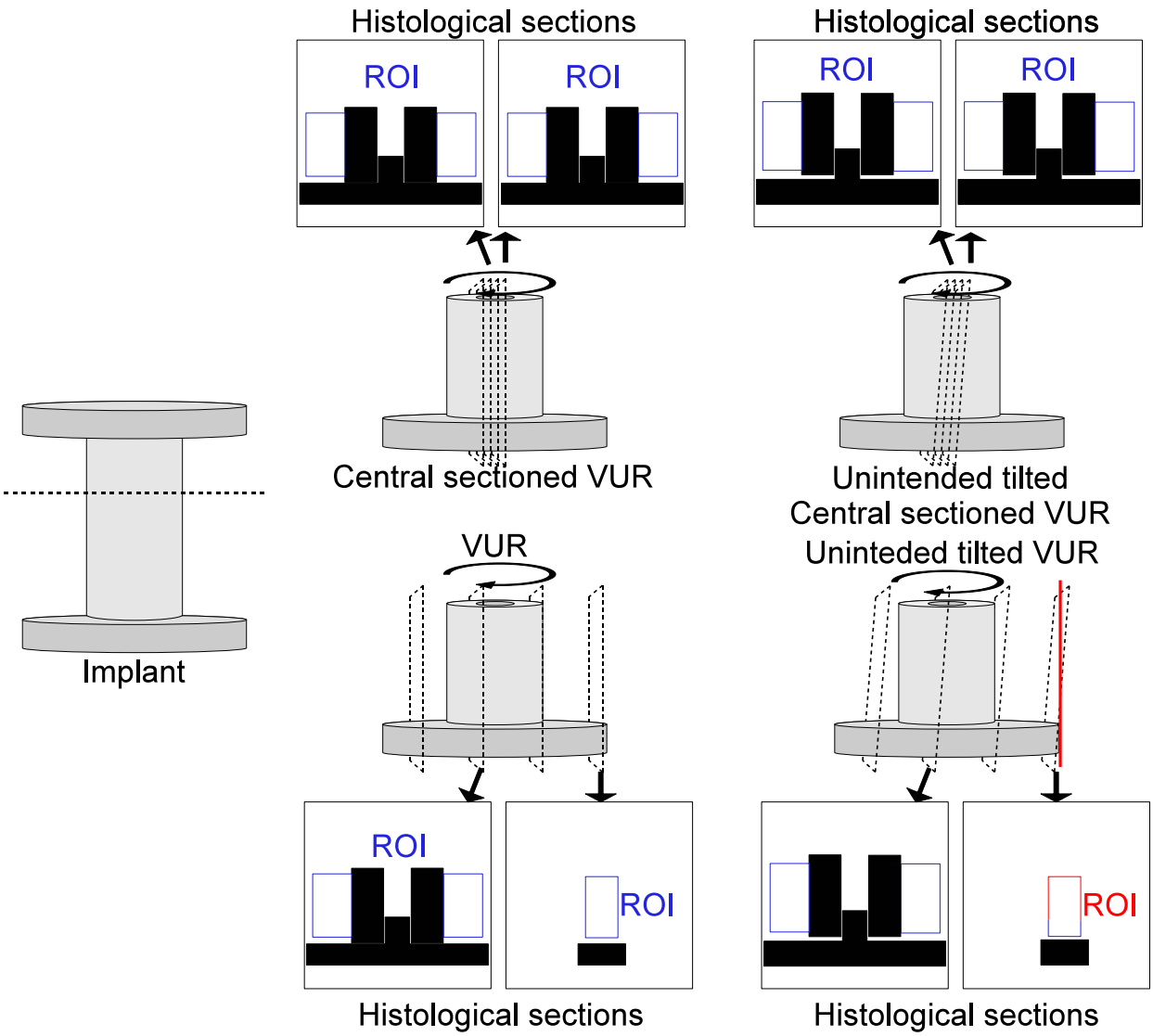

Figure 12: Sketch of the histology sections and the region of interest (ROI). Position and orientation of the sections influence the position of ROI drawn during histomorphometrical analysis. By the VUR technique there is a risk of wrongfully drawing the ROI outside the gap of implant model, indicated by ROI in red down right side corner.

The VUR design is based on a combination of three sampling techniques but no assumptions are made: firstly, sections must be obtained by uniform random sampling in the predefined vertical axis. In this case, naturally assigned to the longitudinal axis of the implant. Secondly, the defined vertical axis is recognized in the microscope and aligned prior to histomorphometrical sampling. Thirdly, the line-probes are sine-weighted.

This method is highly useful for analyzing biological structures that do not resemble a geometrical shape. In 2000 Overgaard applied this method to the gap implant model (also used in the studies of this dissertation) and optimized the sampling of the VUR design [152]. He found that the number of sections per implant could be reduced to every fourth, which in total were 3-4 sections of the 14 exhaustively cut serial sections. The reduction in sections could be done without compromising the quality of estimates of the surface area density and volume density by increased variance of the data. In the study by Overgaard, the exhaustive cutting of serial sections does not include the gap surrounding the implant at the beginning and end of the specimen block, which contains the Region

Of Interest (ROI) for the only volume estimates (Fig. 10). Even if these parts of the specimen block were cut, the ROI is difficult to determine because it is defined in relation to the implant. Usually, the end screw securing the gap at surgery will be present but only in one end because the superficial part of the implant has been cut off for the mechanical analysis. Despite careful efforts to cut parallel to the vertical axis of the implant the sections may be slightly tilted, which on the micron-scale can be considerable. Therefore, the ROI cannot be drawn solely on the presence of one end screw. As a result of these issues, the optimized VUR method was modified for practical purposes so four sections were cut at the central part of the implant (through the plane of the internal thread for the end screw) (Fig. 12). Consequently the rule for uniform sampling was not followed in regard to the volume estimates at the sectioning level. In 2008, Baas calculated that in worst case the bias inflicted upon the volume densities was up to 7.6% underestimation of the volume of new bone and fibrous tissue in the gap and up to 6.3% overestimation of the volume of allograft in the gap [146]. In practice the bias was estimated to 1% systematic over- and underestimation for all parameters. This bias is negligible. For the central sectioned VUR method another issue - how well the biology is represented - has to be considered. The issue of biological representation will be discussed below. An alternative and more biological representative stereological method was desired, especially for study II because the main focus in that study was the volume of tissue in the gap.

Central sectioned VUR

The longitudinal axis of the implant was defined as the vertical axis of the specimen. The specimen block was randomly rotated around the vertical axis before sampling of the sections was started (Fig. 12). The first section was placed one-third into the implant and subsequently four consecutive sections were sampled from the central part of the implant at the level of the inner tread for the end screws.

Evaluation of the implant osseointegration was divided between two criteria: *gap healing* and *ongrowth* and the two components were estimated in a ROI. The ROI was manually drawn from the implant surface and 750 µm into the initial surrounding gap. At the top and bottom of the implant, 300 µm were excluded due to artifacts from the cutting and disruptive effects caused by the screw at the end.

Gap healing was defined as the volume of new bone, so every grid point was counted as either new bone or non-mineralized tissue (Table 10).

Ongrowth was defined as new bone in contact with the implant surface. Intersections between the implant surface and sine-weighted gridlines were counted as either new bone or non-mineralized tissue (Table 9).

All parameters were estimated at ×250 magnification in randomly sampled fields of view in 100% of the ROI.

The described techniques and preparation of specimens, together with the stereological software, made it possible to obtain estimates with negligible bias as described above [146].

Stereological model for a cylinder

Stereological models for estimating surface area density are based on assumptions, which for a cylinder includes three assumptions: First, that the structure to be estimated is a geometric cylinder. Second, that the orientation of the uniform random sampling of the histological sections is horizontal in order to present the surface of the cylinder (the interface) as an isotropic circle in the two-dimensional material (Fig. 13).

Stereological models are mainly applicable to man-made, engineered structures because

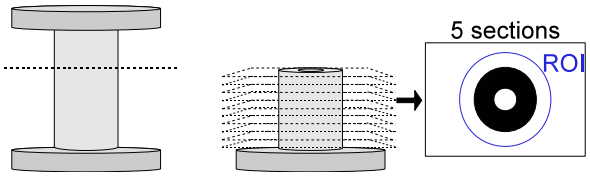

Figure 13: Horizontal sections and the ROI applied.

they often are a geometric shape. For geometric structures, equations for calculations of surface area are often known. For example, the equation for the surface area of a cylinder:

Equation 4

$$A = 2r\pi^2 \cdot h$$

-is the circumference of the horizontal circle multiplied by the height of the cylinder.

Therefore, the sampling orientation of the sections of the cylinder must be horizontal; which makes the two-dimensioned presentation of the implant a circle (Fig. 13). The circumference of the circle can be estimated based on Buffon's needle' relationship. In 7, he described that the probability of a needle intercepting a gridline is dependent on the length of the needle and the distance between the gridlines. Based on Buffon's needle relationship, the length of any arbitrary curve, a boundary, in two-dimensions can be estimated by a grid with isotropic direction, which is positioned over the object. T is the distance between gridlines, I is the number of intersections between the grid and the boundary:

Equation 5

$$B_{estimated} = \pi/2 \cdot T \cdot I$$

The distance between gridlines, T, represents a straight line but the equation is for estimating any arbitrary curve. $\pi/2$ is the average length correction factor between a straight and a curved line (Fig. 14):

Therefore, by multiplying the length of the straight lines by $\pi/2$ the distance between two gridlines, T, is corrected to be the average curved distance between two gridlines. By equation 5, the circumference is estimated as the addition of arches. Finally, the circumference of the circle, the two-dimensional representation of the implant, is multiplied by the height of the cylinder:

Equation 6

$$A = (\pi/2 \cdot T \cdot I) \cdot h$$

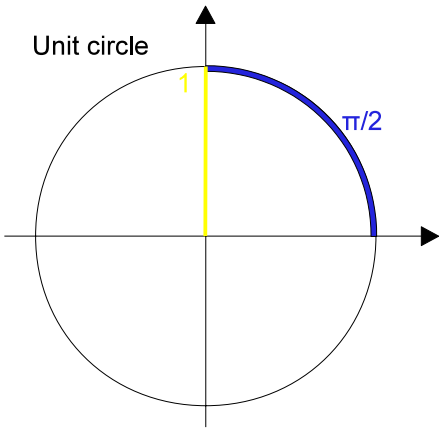

Figure 14: The unit circle shows the average correction factor between a straight and a curved line or arch.

The height of the cylinder is the distance between two consecutively cut sections.

Equation 6 calculates the absolute surface area density but in the studies of this dissertation only the relative surface area densities for specific tissue types of interest, because the total surface area of the implant (cylinder) can differ due to the preparation. Overall, when relative estimates for the surface area density are used, all the constants equal one which leaves the ratio between the specific tissue type divided by the total number of intercepts (the sum of intercepts for all tissue types estimated). For instance:

Equation 7

$$S_{new\ bone} = I_{new\ bone}/I_{total}$$

Average h was estimated by evaluating block advance, where consecutive cuts were made of decreasing depth into a specimen block which were not to be included in the studies. Secondly, sections were cut in the perpendicular plane to the first cuts (Fig. 15) and h was measured from the surface of one section to the surface of what would be the next section. Mean t was 493µm (± 45 µm).

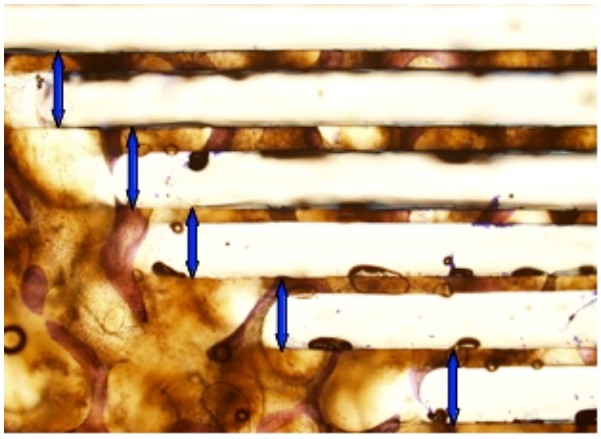

Figure 15: To estimate the bloc advance steps of cuts was made in a specimen bloc. Perpendicular to the first cuts, sections were made like the one on the picture. The distance from an upper surface of one section to the upper surface of the consecutive section was measured, blue arrows.

In general for the cylindrical model

Osseointegration, *gap healing* and *ongrowth*, was estimated as described for study III of the bioactive glass coatings.

The tissue types estimated in the study of strontium-substituted HA coatings (I) were: new bone, fibrous tissue, or bone marrow tissue (Table 9-10). In the study of strontium-doped bone graft extender (II), allograft and bone graft extender was also estimated (Table 9-10).

In the study of strontium-substituted HA coatings (I), the ROI was manually drawn from an applied grid of two centralized circles: an inner circle 2.9 mm in diameter to centralize the ROI with regard to the implant and an outer circle 7.5 mm in diameter to outline the ROI at a distance of 0.75 mm out into the surrounding gap of the implant (Fig. 13). In the strontium-doped bone graft extender study (II), the outer circle was 10.5 mm in diameter to outline the ROI at a distance of 2.45 mm out into the surrounding gap of the implant (Fig. 16).

The implant was also included in the ROI but the size in area and volume was roughly the same within the group and between groups of each study, which equalizes the effect.

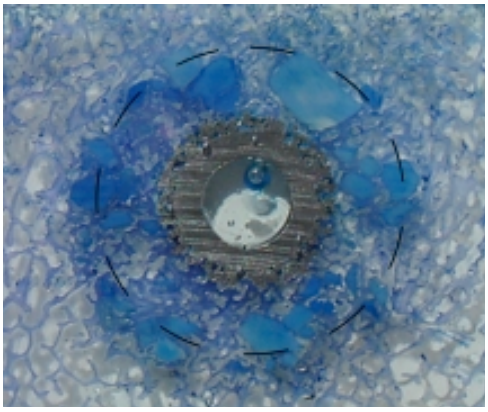

Figure 16: ROI manually drawn on the histology section.

Surface Area Density

Study	Number of intersections counted
I, Stronitum-substituted HA coating	443 (± 56)
II, Strontium –doped Bone Graft Extender	756 (± 54)
III, Strontium-substituted bioactive glass coatings	145 (± 24)

Table 9: The total number of intersections between gridline and implant surface counted for each specimen. Presented as mean (±sd).

Volume Density

Study	Number of grid points counted
I, Stronitum-substituted HA coating	946 (± 116)
II, Strontium –doped Bone Graft Extender	1539 (± 68)
III, Strontium-substituted bioactive glass coatings	314 (± 25)

Table 10: Total number of grid points counted for each specimen. Presented as mean (±sd).

The volume and surface area estimates were presented as relative differences in terms of the number of hits or intercepts for a given tissue type divided by the total number of hits or intercepts. The fraction was multiplied by 100 and presented as the percent of the

volume in gap occupied by the given tissue type and percent of the implant surface in contact with the given tissue type, respectively.

Overprojection

The issue of overprojection of the implant surface, such as the beads (250-300 µm in diameter) of the porous coating in study II, is considered negligible. Because in the worst cases of study II, 20 µm of the interface was in the shadow and could not be analyzed. To put this in perspective, an osteoclast measures 50-100 µm. Besides this, very thin layers of bone ongrowth onto the implant will not withstand a clinically relevant mechanical load.

Intra-observer variation

One observer performed the histo-morphometrical analysis. The observer was blinded to the treatment of the specimens except when the difference between treatment groups was visually clear, for example with glass coating versus HA coating. One randomly selected implant from each of the treatment groups was chosen for intra-observer variation analysis. The intra-observer variation was determined as coefficients of variation (CV) on double measurements of the selected implants.

Deviations from design and model

Any deviation from the stereological design or the assumptions of the model is likely to cause bias of the estimates.

Deviation from the design: In VUR, the sampling of the material must be uniform random after the vertical axis is assigned. In the central sectioned VUR method, sampling is systematic not uniform. This is an important issue when the material of the ROI is not homogenous in regard to the representation of the gap. The systematic non-uniform sampling of the gap caused the negligible bias of the volume density estimates [146].

Deviation from the cylindrical model: In the two studies where the stereological model of a cylinder was applied, the structure of the implant was assumed to be a perfect, smooth geometric cylinder. This was not completely the case, but the implant with rough textured coatings was considered a good approximation for the model because the surface of the implant still curved like a cylinder. Furthermore, the implant did not approach a shape that resembles any other geometrical shape. Hence, the discrepancy between the actual implant structure and a perfect cylinder is small. Any potential bias inflicted by this discrepancy is therefore considered small as well.

The second assumption was that the sections were sampled horizontally so that the implant could be represented as an isotropic circle on the sections. When the circle gird for drawing the ROI was applied it was clearly noticed that the implant was a circle and not an ellipsoid. Therefore the assumption of horizontal sampling orientation was considered valid.

Representation of the biology

As stated earlier, the histomorphometrical analysis should provide unbiased estimates. The estimates provided are only estimates of the actual values, which cannot be known. However, it is also important for the estimates to be of highest possible precision [153]. It is relevant to take into account the biological variation or heterogeneity within the tissue. If biological variation is not uniformly sampled for each specimen then the variation of data between specimen is likely to increase and subsequently lower the precision of the estimates.

This issue is dealt with by the stereological methods as long as the design method are followed and all assumptions are met. The issue arises when the stereological methods are modified, e.g. for practical reasons.

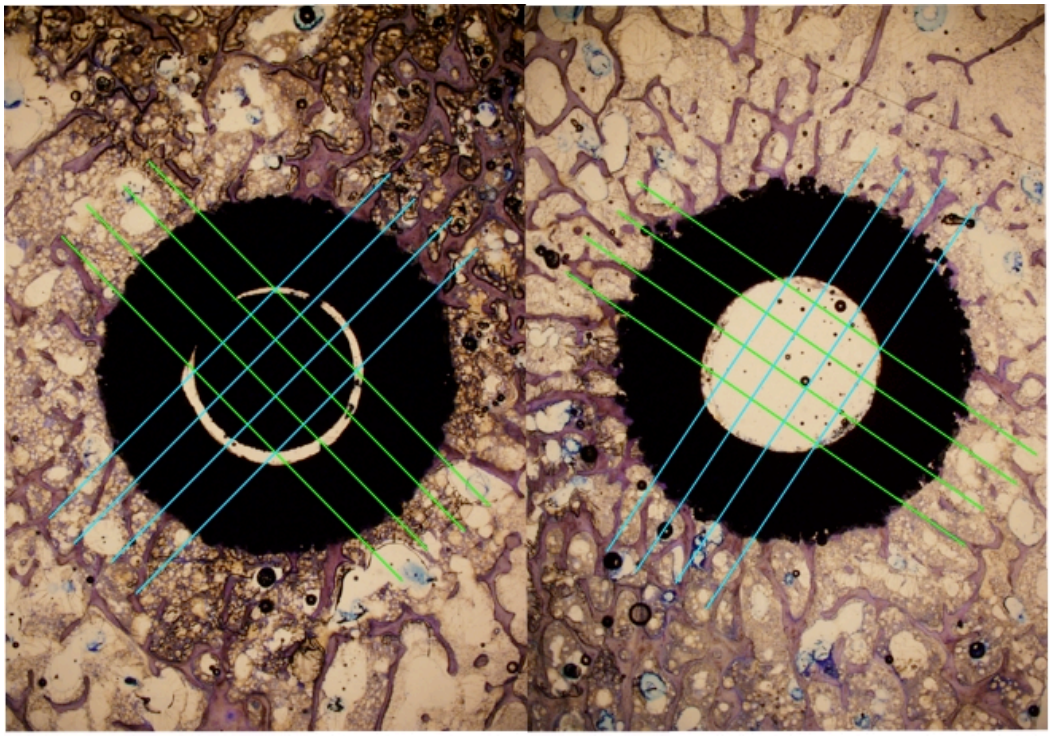

Figure 17: Inhomegeneity of the bone density can be seen in the ROI. If the sections of the central sectioned VUR method were place as the green lines then the estimates of the histomorphometrical analysis would be low compared to sections placed as the blue lines. The estimates would not be biased but the variation of the data would increase

For the implant model used for investigating strontium in the bone-implant interface, heterogeneity of the amount of new bone formed within the ROI of the specimen was observed. The density of newly formed bone seems to be influenced by the anisotropy of the trabeculae or location of the implant e.g. in relation to the cortex. For an implant placed in proximity to the cortex, the amount of new-formed bone was more abundant in the ROI nearest the cortex (Fig. 17). With this heterogeneity in mind, it seemed likely that the estimates of volume and surface area densities from the central sectioned VUR method would be influenced. Within the same treatment group, some specimens would be sampled form an area of high bone density, which would then give relatively high estimates of bone densities. Other specimens would be sampled from an area of low bone density, which would give relatively high estimates of bone densities. In consequence the density estimates would be increasingly imprecise because variation in the data would increase, making it more difficult to detect small differences between treatment arms of the study. The estimates were not biased because the increase in variation was not systematic for a given tissue type or position. The issue arose because the sections were not uniformly sampled within the ROI and heterogeneity was considerable around the circumference of the implant. When sampling was not uniformly distributed throughout the total ROI, the representation of the biological variation decreased. Estimating the representation of the full volume of the ROI can be difficult to grasp. Therefore, for standardizing the discussion and making the presentation more understandable, total ROI will be presented as the implant surface area.

Representation of the ROI can be estimated by calculating the total area of the implant surface that was subject to the uniform random sampling. Secondly, the surface length that was subject to analysis can be calculated to see if the analyzed length is comparable to that found as a minimum surface to be estimated by Overgaard when he optimized the sampling method [152].

In the cylindrical stereological model the area subject to uniform random sampling was the

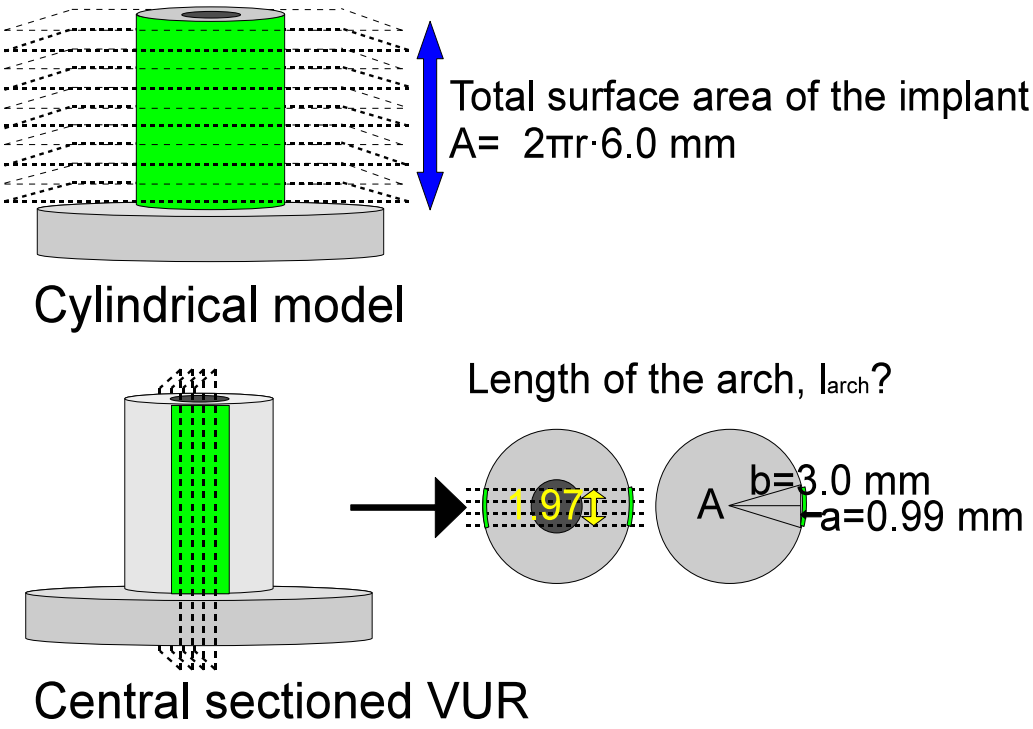

Figure 18: Size of the surface area, green, subject to sampling in the histomorphometrical analysis. For the central sectioned VUR technique, the length of the green arch must be calculated and then multiplied with the height of the cylinder.

whole 6 mm high implant with a standardized radius of 3 mm because the specimen block for histomorphometrical analysis was cut exhaustively throughout the implant height (Fig. 18). The surface area of a perfect cylinder is:

Equation 8

$$A = 2\pi rh$$

For each specimen the total area subject to sampling by the cylindrical model was **113mm^2**.

Secondly, 5 sections were subject to surface area density estimation, each with a length equal to the circumference of the circular implant:

Equation 9

$$\text{circumference} = 2\pi r$$

Equation 10

$$\text{circumference} = 19 \text{ mm}$$

The total implant surface length subject to estimation was in **94 mm**.

By using the central sectioned VUR the area subject to the uniform random sampling is more difficult to calculate because 4 sections were cut from the central part of the implant.

Based on the block advance evaluation, for each section cut 493µm is removed so in total the central 1972 µm of the implant was cut into 4 sections (Fig. 18). As a first step, the arch length on both sides of the cylindrical implant must be calculated and applied to equation 1, in order to calculate the surface area of the cylinder subject to the uniform random sampling.

Together with the radius of theimplant of 3 mm an isosceles triangle was made from which the angle A could be calculated (Fig. 18):

Equation 11

$$\sin A/a = \sin B/b$$

Equation 12

$$\sin A = (\sin 90° \cdot (1.972\text{mm}/2))/ 3\text{mm}$$

Equation 13

$$A = 19.2°$$

and since A is half of the total angle, then 38° is equivalent to the total length of the arch and entered into the equation for the length of the arch on one side. The length of the arch is:

Equation 14

$$l_{arch} = (\text{circumference} \cdot (38 \cdot \pi / 180°)) / 2\,\pi$$

where the circumference is 19 mm (equation 7), so the length of arch on one side is:

Equation 15

$$l_{arch} = 2.01 \text{ mm}$$

The arches on both sides were together 4.02 mm long, from which the 4 sections were cut. The total area subject to uniform random sampling was then 4.02 mm·6 mm = **24 mm^2** (according to equation 1).

The length of the implant surface subject to estimation is the height of the implant cylinder on both sides of the 4 sections:

Equation 16

When Overgaard optimized the stereological method, he found that 80 µm (the height of the implant 10 mm · 2 sides · 4 sections) implant surface length was enough for estimating densities for various tissue types [152]. Of course, the estimate of sufficient implant surface length subject to analysis is dependent on the extent of the given tissue type of interest. The tissue type of interest should be represented by approximately 200 counts per specimen [150]. Therefore, the estimates should be extrapolated between studies with care.

The ratio between the two methods of the area subject to sampling was 113 mm^2 / 24 mm^2 = 4.7. In conclusion, the implant surface was 4.7 times more represented by the stereological cylindrical model than by the central sectioned stereological design. The cylindrical model sampled a total length of implant surface of 94 mm, which should be sufficient compared to the length found by Overgaard of 80 mm for providing estimates with only limited variation of data due to sampling method. On the other hand, the 48 µm implant surface length subject to analysis by the central sectioned VUR method may be too low, which may have impaired the quality of the data by increasing variation. However, this possible increase in variation did not prevent large differences from being identified as statistically significant in the study of the strontium-substituted bioactive glass coatings (III).

Conclusions of the stereology

- The VUR is difficult to apply to this specific implant model.
- For the central sectioned VUR method, a negligible bias is introduced concerning the volume densities.
- By use of the cylindrical model based method, a small estimated bias was introduced.
- The representation of the biological variation is 4.7 times higher for the cylindrical model based method than the central sectioned VUR method.
- For the cylindrical model based method, the gain in biological representation seems much greater than the relatively small bias introduced.
- For the cylindrical model based method, the implant surface length subject to estimation is found comparable to the recommendation.
- Overall the applied stereological methods seem valid for use in these studies.

Statistical analysis

Statistical analysis was performed using Intercooled STATA 10.0 software (StataCorp LP, College Station, TX, USA).

Study I and II: In these paired studies, the histological and mechanical variable data were normally distributed. But the data of differences between treatment arms were not normally distributed for all variables. The histogram of the differences was skewed to the left and the effect measures show multiplicative behavior. Therefore, data were transformed by natural logarithm (ln) and found normally distributed on the natural logarithm scale. The differences between treatment arms were tested by student's t-test as the ratio of the paired data. Means and 95% CI of the t-test were transformed back by exponential function to medians and 95% CI, which are presented. Calculations of CV% for each variable was made via calculations of transformed mean and transformed standard deviation (sd) [154]:

Equation 17

$$\text{Mean} = \exp(\ln \text{mean} + (0.5 \cdot (\ln \text{sd})^2))$$

Equation 18

$$\text{sd} = \text{mean} \cdot (\sqrt{} (\exp(\ln \text{sd})^2 - 1)$$

Equation 19

$$CV\% = (\text{mean}/\text{sd}) \cdot 100\%$$

A *P* value less than 0.05 was considered statistically significant.

Study III: In this paired 4-arms study, histological and biomechanical data did not fulfil the assumptions for one-way repeated measurement ANOVA. Therefore, they were analyzed with a Friedman Repeated Measures Analyses of Variance on Ranks. When a statistically significant difference within the groups was detected, Wilcoxon signed rank test was used to identify the specific differences between two groups. The data were presented as medians with 75% and 25% interquartile ranges and p-values less than 0.05 were considered statistically significant.

The expected CV_{diff} % was set at 30 % and based on this expectation 10 animals were included in the studies. Unfortunately, in the strontium-doped bone graft extender study (II), the CV_{diff} % was often higher than 30%. Therefore, a true 30% improvement by strontium may not have been detected within the limitations of study II, a possible type 2 error.

6. Results

Study I

Hypothesis: SrHA, strontiumhydroxyapatite, coating on Ti implants will enhance implant fixation both at 4 weeks and 12 weeks.
Hypothesis disproved: Yes
Comments: The surface area density fraction of ongrowth of bone was as high as approximately 75% regardless of the strontium substitution of HA coatings. This fraction of ongrowth seemed even higher than observed in previous studies of HA coated implants in this model (Table 11 and Fig. 19). Scanning Electron Microscopy images of two pushed-out implants show bone on the HA coated implant but almost no bone on the SrHA coated implant.
In total, strontium substitution of the HA coating showed neither improvement nor impairment of any of the parameters for implant fixation or osseointegration.

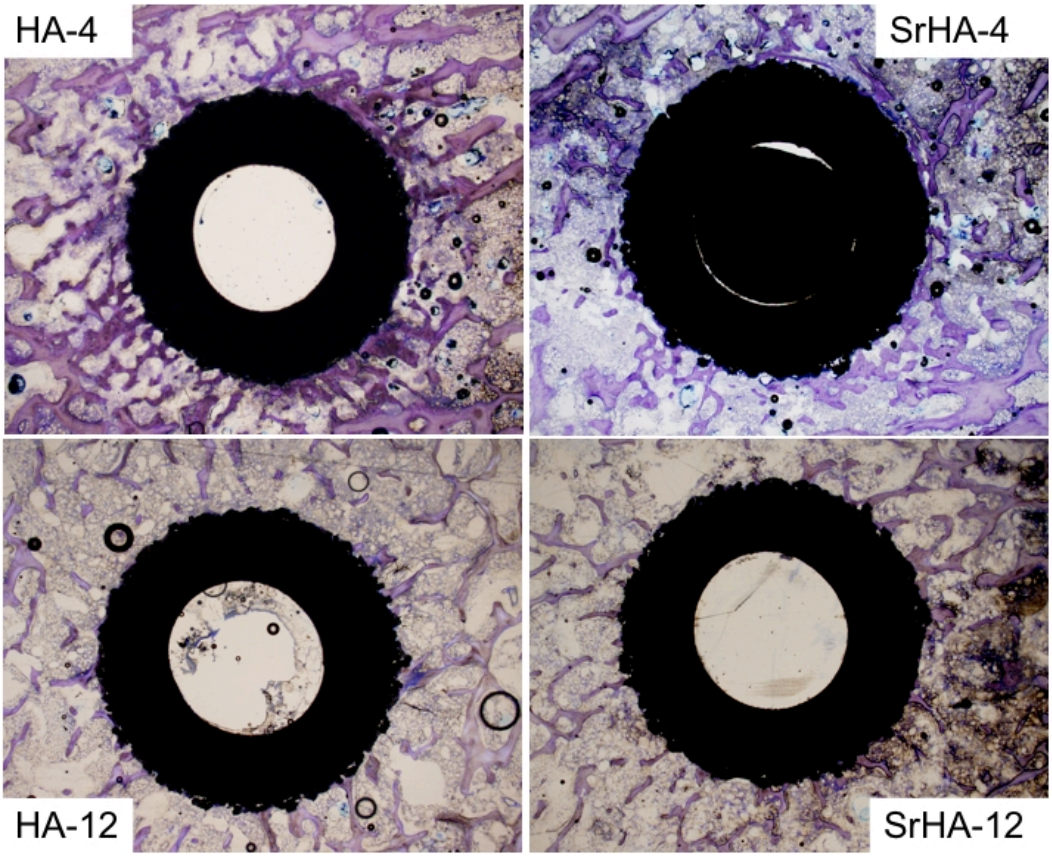

Figure 19: Gap healing and ongrowth of study I. These implants are representative of the medians for each group, but not from the same dog.

	Coating treatment groups			
	HA 4 weeks	SrHA 4 weeks	HA 12 weeks	SrHA 12 weeks
Gap healing	0	0	0	0
Ongrowth	0	0	0	0
Implant fixation	0	0	0	0

Table 11: Results of study I presented as relative change to control. "0" no change.

Study II

Hypotheses: Strontium-doped HA as a bone graft extender mixed with allograft will enhance implant fixation.
Hypothesis disproved: Yes
Comments: Strontium doping increased the volume of new bone formed by 21%, which increased gap healing (Fig. 20). Strontium doping of the bone graft extender also preserved 18% more allograft in the gap (Fig. 21). Additionally, 39% more new bone was in contact with the strontium-doped BGE. However, the increased new bone formation had not yet reached the surface of the implant so ongrowth onto the implant was not increased (Table 9). Perhaps the implant fixation was not improved due to the lack of improved ongrowth onto the implant.

	Bone graft extender treatment groups	
	HA	SrHA
Gap healing	0	+
Preserved allograft	0	+
Ongowth	0	0
Implant fixation	0	0

Table 12: Results are presented as change relative to control. "0" no change. "+" improvement.

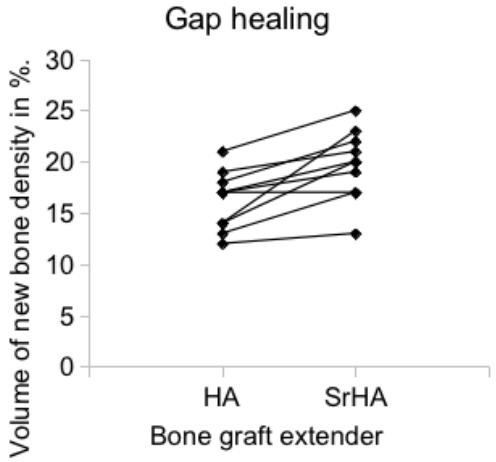

Figure 20: Fractions of new bone in gap of interconnected pairs.

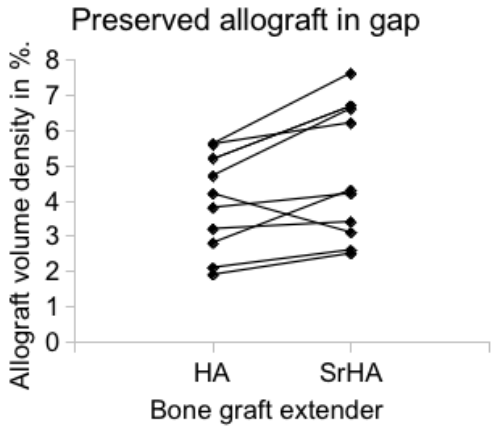

Figure 21: Fraction of allograft in the gap after 4 weeks of interconnected pairs.

Study III

Hypothesis 1: Bioactive glass coating of Ti implants will enhance implant fixation compared to HA coating.

Hypothesis 1 disproved: Yes

Hypothesis 2: Strontium-substitution of the bioactive glass coating on Ti implants will further enhance implant fixation compared to bioactive glass coating without strontium.

Hypothesis 2 disproved: Yes

Comments: The bioactive glass coating failed in achieving osseointegration and subsequent implant fixation (Table 13). Results of RAMAN spectroscopy suggest that the glass had become contaminated with aluminum. Therefore, the effects of strontium substitution of the glass on implant osseointegration and subsequent fixation could not be assessed.

However interesting observations were made in the gap surrounding the implant and a descriptive study of the findings were performed. A homogeneous substance was observed, which could be divided into three sub-groups and the third group of the substance was mineralizes (Fig. 22).

	Coating treatment groups			
	HA	Sr0	Sr10	Sr50
Gap healing	0	-	-	-
Ongrowth	0	-	-	-
Implant fixation	0	-	-	-

Table 13: Results of study III presented as change relative to control. "0" no change. "-" deterioration.

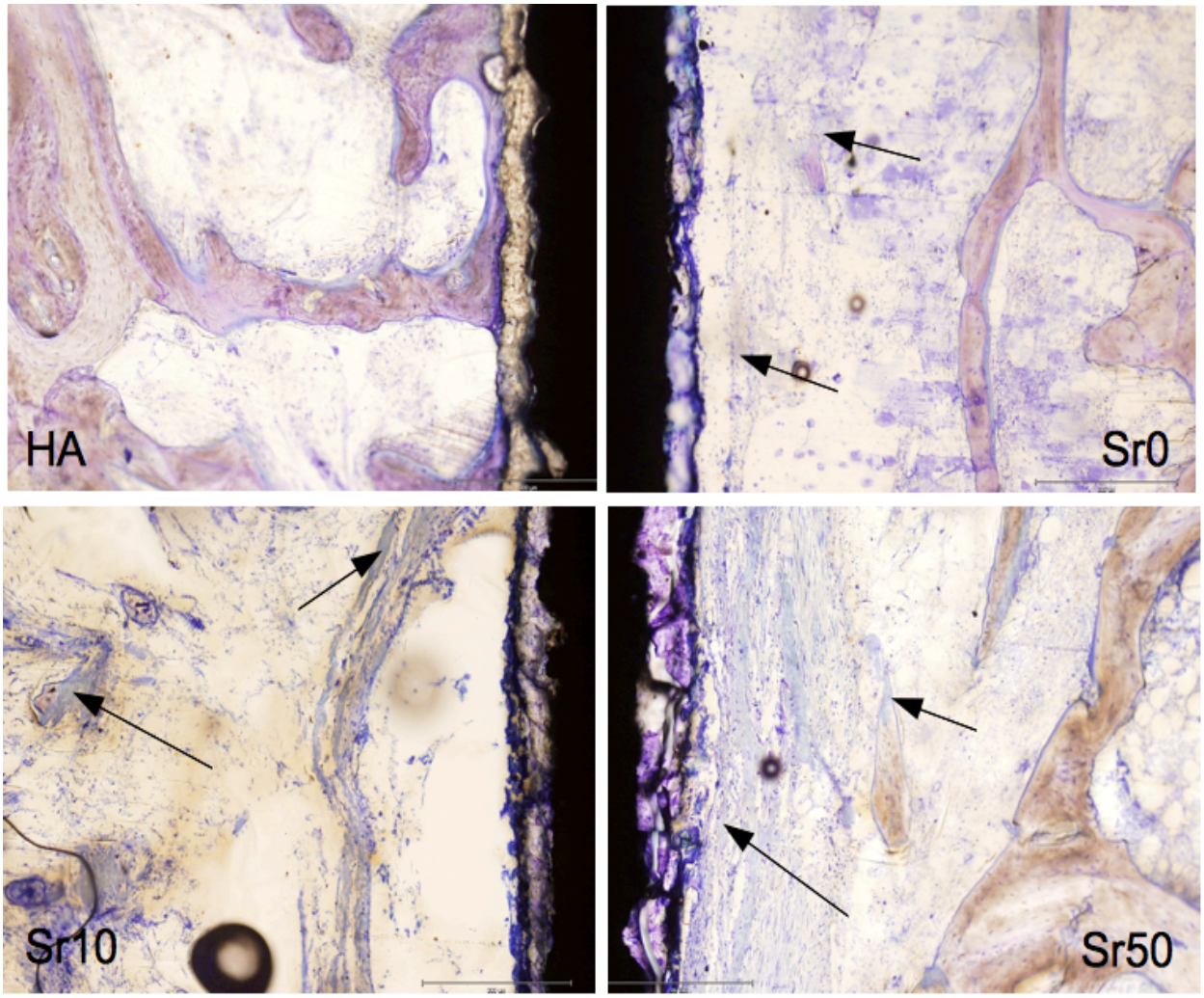

Figure 22: The HA coated implant was osseointegrated, but the implants with bioactive glass coatings were not (Sr0: bioactive glass without strontium; Sr10: 10% of the CaO_2 is substituted by SrO_2; and Sr50: 50% of the CaO_2 is substituted by SrO_2). In approximately half of the interfaces of each of the bioactive glass coated implants a homogeneous substance (arrows) was observed. The implants are representative of mean of each group but not from the same dog.

7. Discussion

The purpose of the three studies performed in this dissertation was to investigate to effect of strontium topically present at the bone-implant interface. The two main questions asked were: first, what is the optimal delivery method of strontium to the bone-implant interface? Second, can strontium exercise a dual action in the bone-implant interface?

To elucidate answers to these questions, three studies were conducted where strontium was delivered to the interface by three different methods. In these three studies, different model setups were used to investigate both a possible anabolic effect and anti-catabolic effect of strontium. The methods used in the three studies were overall found to be valid for testing the hypothesis stated for each study. Therefore, the results of these studies are valid for interpretation and subsequently the stated hypotheses can be verified or disproven.

Strontium delivered to the interface by doping a HA bone graft extender produced a histological anabolic and anti-catabolic effect. However, mechanical implant fixation was not improved. These histological findings involving strontium are in agreement with the literature [98-100, 137]. The strontium-doped HA bone graft extender was of high crystallinity and of high HA purity. Therefore, only a small fraction of the bone graft extender material could have been of ß-TCP or amorphous calcium strontium phosphate compounds, which can more easily dissolve and release strontium ions into the bone-implant interface [37, 44]. Strontium must have been released into the interface milieu because more allograft was preserved when mixed with the strontium-doped bone graft extender. The higher crystallinity and HA purity of the material the more osteoconductive it is [45]. Based on this, the non-doped HA bone graft extender was presumably a potent osteoconductive material Still, strontium doping of the HA increased the bone ongrowth onto the granules. The increased ongrowth onto the SrHA may indicate an increase in the osteoconductive property of the HA by strontium doping. The increase in osteoconductive property of the SrHA may explain the increase in gap healing (increased volume of new bone).

Yet, when strontium was delivered as 5% strontium substituted HA by vacuum plasma sprayed coating, neither an anabolic nor an anti-catabolic effect was detected after 4 and 12 weeks. This delivery method may not be optimal because the highly crystalline and HA pure coatings are not easily dissolved. Therfore, strontium would not have been delivered to the interface but would have stayed within the coating. Interestingly, the SrHA used as a bone graft extender did exhibit the anabolic effect and also should be expected to become evident in the study using the SrHA coatings. The difference between these two studies is that the SrHA as a bone graft extender had a much larger surface area so even small amounts of released strontium may have added up to a significant total amount. Based on the SEM images of the implants after push-out, however, (Appendics, paper 1, Fig. 4 and 5) almost no bone was seen on the SrHA coating but plenty was left on the HA coating. Therefore, I speculate that in the bone-implant interface of SrHA coated implants, a failure occured within the coating. For the HA coated implants, the failure happened in the surrounding bone. The tensile strength of the SrHA coating was not tested before implantation. The mechanical strength of the strontium-substituted coating could have been lower than the pure HA coating especially after 12 weeks *in vivo* because of a destabilized lattice structure [56, 57]. The destabilized strontium substituted HA more easily transformed into ß-TCP (ß-TCSrP) during the vacuum plasma spraying, was less crystalline and dissolved more easily [35, 58]. The possible tristrontiumcalciumphosphate or even amorphous strontium calcium phosphate compounds are likely to have formed a network of soluble material during the vacuum plasma spray coating. The soluble network would subsequently cause the coating to delaminate after 12 weeks *in vivo* when loaded during the push-out test. [155]. Li et al., enhanced the fixation of HA-coated

Ti screws in osteoporotic rats by administrating systemic strontium [156]. Accordingly, perhaps it would be more optimal to deliver the strontium to the bone-implant interface by systemic treatment in large animals and humans. However, in many respects a topical delivery is optimal, since the most frequently reported side effects of systemic strontium administration by mouth are nausea and diarrhea, which could be avoided by topical treatment.

The third strontium delivery method to the bone-implant interface failed so its effects at the interface could not be investigated. Presumeably, the strontium substituted bioactive glass coating had become contaminated with aluminum during grit-blasting of the implant cores. The unintentionally present aluminum presumably changed the chemical properties of the glass, resulting in reduced, unexpected degradability [157]. Boyd and Towler successfully composed bioactive glass particles containing various amounts of strontium, which performs well in health and osteoporotic rats [115, 116]. Unfortunately, Lopez-Sastre et al. also unexpectedly found inferior osseointegration and mechanical fixation of bioglass coated implants compared to Apatite-Wollastonite-glass ceramic and TCP coated implants. So, it may not be very difficult to manufacture strontium containing bioactive glass but it is a great challenge to coat metallic implants with bioactive glass. Perhaps this is due to the glass being very chemical reactive and therefore difficult to control during the sintering process.

There are many delivery methods of strontium. Based on thermodynamic calculations, it has been postulated that strontium phosphate compounds, like strontium hydroxyapatite, are very readily formed and virtually non-dissolvable. Based on this, perhaps strontium in the form of strontiumacetate is a better delivery method due to this compound's increased solubility.. A study by Gentleman et al. rejects the hypothesis that strontium phosphate compounds are virtually non-dissolvable since they found strontium ions released into a media with high phosphorus concentration [158]. Clearly, further investigation into the most optimal method of strontium delivery is needed.

8. Conclusion

Strontium showed potential to work as a dual acting agent in the bone-implant interface. The dual acting effect of strontium became evident in my study using a strontium-doped bone graft extender. Strontium doping of the bone graft extender increased the volume of new bone as well as the volume of the remaining allograft compared to the control without strontium doping. However, strontium doping did not improve mechanical implant fixation.

The dual acting effect of strontium did not become evident in the two studies using strontium-substituted coatings. Strontium substituted HA VPS coating neither showed improvement nor impairment of implant fixation. No difference between the strontium substituted coating and the control HA VPS coating was detected for any of the sub-hypotheses at any of the time points.

In the third study testing strontium-substituted bioactive glass coating, deterioration in implant fixation was observed for all glass coatings regardless of the doses of strontium substitution. It was presumed that the glass had been contaminated with aluminum during the coating procedure.

These studies show that strontium can work as a dual acting agent in the bone-implant interface yet the delivery of strontium to the interface is still a challenge.

9. Perspectives and future research

Despite the interesting results of these studies, there are still many uncertainties in regard to the effect of strontium in the bone-implant interface and the optimal method of strontium delivery to the interface. Since strontium showed both an anabolic and anti-catabolic effect in the interface of an allograft impacted implant, it is encouraging to pursuit the idea of adding strontium to the interface.

Clearly, further studies must be conducted to determine how strontium works in the interface to influence the osseointegration of the implant.

Most importantly, the delivery methods of strontium need study and attention. The mechanical strength of strontium-substituted HA VPS coatings must be determined before this delivery method can be considered for future *in vivo* investigations and at different strontium substitution doses. Moreover, SrHA may not be the optimal means of strontium delivery since SrHA does not dissolve very well, consequently, only sparse amounts of strontium would be delivered to the interface.

On the other hand, delivery of strontium to the interface by a strontium-substituted bioactive glass coating could still have potential for success, since the presumed aluminum contamination in our study likely led to the decrease in degradability and the osteoproductive property of the glass. Thus, future studies of this bioactive glass should: first, investigate the *in vitro* and *in vivo* effects of not grit blasting before coating, second, use silica or other aluminum-free particles rather than alumina for grit blasting, or third, clean the surface after grit blasting using hydrofluoric acid, for example, prior to glass coating of the implants.

Additionally, it should be tested whether strontium in the bone-implant interface only benefits a sub-group of all patients, such as osteoporotic patients receiving a joint replacement.

10. References

[1] Pedersen AB, Johnsen SP, Overgaard S, Soballe K, Sorensen HT, Lucht U. Total hip arthroplasty in Denmark: incidence of primary operations and revisions during 1996-2002 and estimated future demands. Acta Orthop 2005;76:182-9.

[2] Lie SA, Havelin LI, Furnes ON, Engesaeter LB, Vollset SE. Failure rates for 4762 revision total hip arthroplasties in the Norwegian Arthroplasty Register. JBone Joint SurgBr 2004;86:504-9.

[3] Pilliar RM, Lee JM, Maniatopoulos C. Observations on the effect of movement on bone ingrowth into porous-surfaced implants. ClinOrthopRelat Res 1986:108-13.

[4] Karrholm J, Borssen B, Lowenhielm G, Snorrason F. Does early micromotion of femoral stem prostheses matter? 4-7-year stereoradiographic follow-up of 84 cemented prostheses. JBone Joint SurgBr 1994;76:912-7.

[5] Bauer TW, Schils J. The pathology of total joint arthroplasty.II. Mechanisms of implant failure. Skeletal Radiol 1999;28:483-97.

[6] Murray DW, Rushton N. Macrophages stimulate bone resorption when they phagocytose particles. J Bone Joint Surg Br 1990;72:988-92.

[7] Cooper RA, McAllister CM, Borden LS, Bauer TW. Polyethylene debris-induced osteolysis and loosening in uncemented total hip arthroplasty. A cause of late failure. J Arthroplasty 1992;7:285-90.

[8] Rahbek O, Overgaard S, Lind M, Bendix K, Bunger C, Soballe K. Sealing effect of hydroxyapatite coating on peri-implant migration of particles. An experimental study in dogs. J Bone Joint Surg Br 2001;83:441-7.

[9] Albrektsson T, Branemark PI, Hansson HA, Lindstrom J. Osseointegrated titanium implants. Requirements for ensuring a long-lasting, direct bone-to-implant anchorage in man. Acta Orthop Scand 1981;52:155-70.

[10] Zarb GA, Alberktsson T. [Criteria for determining clinical success with osseointegrated dental implants]. Cah Prothese 1990:19-26.

[11] Branemark PI, Hansson BO, Adell R, Breine U, Lindstrom J, Hallen O, et al. Osseointegrated implants in the treatment of the edentulous jaw. Experience from a 10-year period. Scand J Plast Reconstr Surg Suppl 1977;16:1-132.

[12] Soballe K, Hansen ES, Brockstedt-Rasmussen H, Pedersen CM, Bunger C. Hydroxyapatite coating enhances fixation of porous coated implants. A comparison in dogs between press fit and noninterference fit. Acta OrthopScand 1990;61:299-306.

[13] Wanpeng C, Hench LL. 1996. p. 493-507.

[14] Albrektsson T, Johansson C. Osteoinduction, osteoconduction and osseointegration. EurSpine J 2001;10 Suppl 2:S96-101.

[15] Havelin LI, Fenstad AM, Salomonsson R, Mehnert F, Furnes O, Overgaard S, et al. The Nordic Arthroplasty Register Association: a unique collaboration between 3 national hip arthroplasty registries with 280,201 THRs. Acta Orthop 2009;80:393-401.

[16] Karrholm J, Snorrason F. Subsidence, tip, and hump micromovements of noncoated ribbed femoral prostheses. ClinOrthopRelat Res 1993:50-60.

[17] Baas J, Elmengaard B, Jakobsen T, Bechtold J, Soballe K. Crack Revision Improves Fixation of Uncemented HA-coated Implants Compared with Reaming: An Experiment in Dogs. ClinOrthopRelat Res 2009.

[18] Xie XH, Yu XW, Zeng SX, Du RL, Hu YH, Yuan Z, et al. Enhanced osteointegration of orthopaedic implant gradient coating composed of bioactive glass and nanohydroxyapatite. J Mater Sci Mater Med 2010.

[19] Kienapfel H, Sprey C, Wilke A, Griss P. Implant fixation by bone ingrowth. JArthroplasty 1999;14:355-68.

[20] McKibbin B. The biology of fracture healing in long bones. J Bone Joint Surg Br 1978;60-B:150-62.

[21] Cruess RL, Dumont J. Fracture healing. Can J Surg 1975;18:403-13.

[22] Frost HM. The biology of fracture healing. An overview for clinicians. Part II. Clin Orthop Relat Res 1989:294-309.

[23] Einhorn TA. The cell and molecular biology of fracture healing. Clin Orthop Relat Res 1998:S7-21.

[24] Jakobsen T, Baas J, Kold S, Bechtold JE, Elmengaard B, Soballe K. Local bisphosphonate treatment increases fixation of hydroxyapatite-coated implants inserted with bone compaction. J Orthop Res 2009;27:189-94.

[25] Dhert WJ, Thomsen P, Blomgren AK, Esposito M, Ericson LE, Verbout AJ. Integration of press-fit implants in cortical bone: a study on interface kinetics. J Biomed Mater Res 1998;41:574-83.

[26] Branemark R, Ohrnell LO, Nilsson P, Thomsen P. Biomechanical characterization of osseointegration during healing: an experimental in vivo study in the rat. Biomaterials 1997;18:969-78.

[27] Kold S, Rahbek O, Vestermark M, Overgaard S, Soballe K. Bone compaction enhances fixation of weightbearing titanium implants. ClinOrthopRelat Res 2005:138-44.

[28] Turner CH. On Wolff's law of trabecular architecture. J Biomech 1992;25:1-9.

[29] Frost HM. A 2003 update of bone physiology and Wolff's Law for clinicians. Angle Orthod 2004;74:3-15.

[30] Elkouri ER. Review of cancellous and cortical bone healing after fracture or osteotomy. J Am Podiatry Assoc 1982;72:464-6.

[31] Greenwald AS, Boden SD, Goldberg VM, Khan Y, Laurencin CT, Rosier RN. Bone-graft substitutes: facts, fictions, and applications. J Bone Joint Surg Am 2001;83-A Suppl 2 Pt 2:98-103.

[32] LeGeros RZ. Properties of osteoconductive biomaterials: calcium phosphates. ClinOrthopRelat Res 2002:81-98.

[33] de Groot K, Geesink R, Klein CP, Serekian P. Plasma sprayed coatings of hydroxylapatite. J Biomed Mater Res 1987;21:1375-81.

[34] Wilson J, Low SB. Bioactive ceramics for periodontal treatment: comparative studies in the Patus monkey. JApplBiomater 1992;3:123-9.

[35] Bigi AM, F; Ripamonti, A; Roveri, N;. Magnisium and Strontium Interaction with Carbonate-Containing Hydroxyapatite in Aqueous Medium. Journal of Inorganic Biochemistry 1981;15.

[36] Bertoni E, Bigi A, Cojazzi G, Gandolfi M, Panzavolta S, Roveri N. Nanocrystals of magnesium and fluoride substituted hydroxyapatite. J Inorg Biochem 1998;72:29-35.

[37] Overgaard S. Calcium phosphate coatings for fixation of bone implants: Evaluated mechanically and histologically by stereological methods. Acta Orthopaedica 2000;71:74.

[38] LeGeros RZ. Biodegradation and bioresorption of calcium phosphate ceramics. ClinMater 1993;14:65-88.

[39] Verdonschot N, van Hal CT, Schreurs BW, Buma P, Huiskes R, Slooff TJ. Time-dependent mechanical properties of HA/TCP particles in relation to morsellized bone grafts for use in impaction grafting. J Biomed Mater Res 2001;58:599-604.

[40] Jensen TB, Overgaard S, Lind M, Rahbek O, Bunger C, Soballe K. Osteogenic protein-1 increases the fixation of implants grafted with morcellised bone allograft and ProOsteon bone substitute: an experimental study in dogs. JBone Joint SurgBr 2007;89:121-6.

[41] Baas J, Elmengaard B, Bechtold J, Chen X, Soballe K. Ceramic bone graft substitute with equine bone protein extract is comparable to allograft in terms of implant fixation: a study in dogs. Acta Orthop 2008;79:841-50.

[42] Thomas KA. Hydroxyapatite coatings. Orthopedics 1994;17:267-78.

[43] Soballe K. Hydroxyapatite ceramic coating for bone implant fixation. Mechanical and histological studies in dogs. Acta OrthopScandSuppl 1993;255:1-58.

[44] Dorozhkin SV. Amorphous calcium (ortho)phosphates. Acta Biomater 2010.

[45] Soballe K, Overgaard S. The current status of hydroxyapatite coating of prostheses. J Bone Joint Surg Br 1996;78:689-91.

[46] Overgaard S, Lind M, Rahbek O, Bunger C, Soballe K. Improved fixation of porous-coated versus grit-blasted surface texture of hydroxyapatite-coated implants in dogs. Acta Orthop Scand 1997;68:337-43.

[47] Gledhill HC, Turner IG, Doyle C. Direct morphological comparison of vacuum plasma sprayed and detonation gun sprayed hydroxyapatite coatings for orthopaedic applications. Biomaterials 1999;20:315-22.

[48] Rossler S, Sewing A, Stolzel M, Born R, Scharnweber D, Dard M, et al. Electrochemically assisted deposition of thin calcium phosphate coatings at near-physiological pH and temperature. J Biomed Mater Res A 2003;64:655-63.

[49] Soballe K, Toksvig-Larsen S, Gelineck J, Fruensgaard S, Hansen ES, Ryd L, et al. Migration of hydroxyapatite coated femoral prostheses. A Roentgen Stereophotogrammetric study. J Bone Joint Surg Br 1993;75:681-7.

[50] Geesink RG, Hoefnagels NH. Six-year results of hydroxyapatite-coated total hip replacement. J Bone Joint Surg Br 1995;77:534-47.

[51] Paulsen A, Pedersen AB, Johnsen SP, Riis A, Lucht U, Overgaard S. Effect of hydroxyapatite coating on risk of revision after primary total hip arthroplasty in younger patients: findings from the Danish Hip Arthroplasty Registry. Acta Orthop 2007;78:622-8.

[52] Soballe K. Hydroxyapatite ceramic coating for bone implant fixation. Mechanical and histological

studies in dogs. Acta Orthop Scand Suppl 1993;255:1-58.

[53] Soballe K, Hansen ES, H BR, Jorgensen PH, Bunger C. Tissue ingrowth into titanium and hydroxyapatite-coated implants during stable and unstable mechanical conditions. J Orthop Res 1992;10:285-99.

[54] Daugaard H, Elmengaard B, Bechtold JE, Jensen T, Soballe K. The effect on bone growth enhancement of implant coatings with hydroxyapatite and collagen deposited electrochemically and by plasma spray. J Biomed Mater Res A 2010;92:913-21.

[55] Tian M, Chen F, Song W, Song Y, Chen Y, Wan C, et al. In vivo study of porous strontium-doped calcium polyphosphate scaffolds for bone substitute applications. JMaterSciMaterMed 2009;20:1505-12.

[56] Grynpas M. Age and disease-related changes in the mineral of bone. Calcif Tissue Int 1993;53 Suppl 1:S57-64.

[57] Li ZY, Lam WM, Yang C, Xu B, Ni GX, Abbah SA, et al. Chemical composition, crystal size and lattice structural changes after incorporation of strontium into biomimetic apatite. Biomaterials 2007;28:1452-60.

[58] Christoffersen J, Christoffersen MR, Kolthoff N, Barenholdt O. Effects of strontium ions on growth and dissolution of hydroxyapatite and on bone mineral detection. Bone 1997;20:47-54.

[59] Hench LL, Wilson J. Surface-active biomaterials. Science 1984;226:630-6.

[60] Hench LL, Xynos ID, Polak JM. Bioactive glasses for in situ tissue regeneration. JBiomaterSciPolymEd 2004;15:543-62.

[61] Oonishi H, Hench LL, Wilson J, Sugihara F, Tsuji E, Kushitani S, et al. Comparative bone growth behavior in granules of bioceramic materials of various sizes. JBiomedMaterRes 1999;44:31-43.

[62] Oonishi H, Kushitani S, Yasukawa E, Iwaki H, Hench LL, Wilson J, et al. Particulate bioglass compared with hydroxyapatite as a bone graft substitute. ClinOrthopRelat Res 1997:316-25.

[63] Thomas MV, Puleo DA, Al-Sabbagh M. Bioactive glass three decades on. JLongTermEffMedImplants 2005;15:585-97.

[64] Gao T, Aro HT, Ylanen H, Vuorio E. Silica-based bioactive glasses modulate expression of bone morphogenetic protein-2 mRNA in Saos-2 osteoblasts in vitro. Biomaterials 2001;22:1475-83.

[65] Abou Neel EA, Chrzanowski W, Pickup DM, O'Dell LA, Mordan NJ, Newport RJ, et al. Structure and properties of strontium-doped phosphate-based glasses. JRSocInterface 2009;6:435-46.

[66] Rosenberg ES, Fox GK, Cohen C. Bioactive glass granules for regeneration of human periodontal defects. JEsthetDent 2000;12:248-57.

[67] Schepers EJ, Ducheyne P, Barbier L, Schepers S. Bioactive glass particles of narrow size range: a new material for the repair of bone defects. ImplantDent 1993;2:151-6.

[68] Pazo A, Saiz E, Tomsia AP. Silicate glass coating on Ti-based implants. Acta Materialia 1998;46:2551-8.

[69] Lotfibakhshaiesh N, Brauer DS, Hill RG. Bioactive glass engineered coatings for Ti6Al4V alloys: Influence of strontium substitution for calcium on sintering behaviour. Journal of Non-Crystalline Solids; 2009.

[70] Clarkin O, Boyd D, Towler MR. Strontium-based Glass Polyalkenoate Cements for Luting Applications in the Skeleton. JBiomaterAppl 2008.

[71] Wren A, Boyd D, Towler MR. The processing, mechanical properties and bioactivity of strontium based glass polyalkenoate cements. JMaterSciMaterMed 2008;19:1737-43.

[72] Boyd D, Towler MR, Law RV, Hill RG. An investigation into the structure and reactivity of calcium-zinc-silicate ionomer glasses using MAS-NMR spectroscopy. JMaterSciMaterMed 2006;17:397-402.

[73] Hill R, Er. An alternative view of the degradation of bioglass. Journal of Material Science Letters 1996;15:1122-5.

[74] Hastings DE, Parker SM. Protrusio acetabuli in rheumatoid arthritis. Clin Orthop Relat Res 1975:76-83.

[75] Burchardt H. The biology of bone graft repair. ClinOrthopRelat Res 1983:28-42.

[76] Sherk HH, Nicholson JT. Fracture healing and the allograft reaction. Clin Orthop Relat Res 1971;76:94-9.

[77] Goldberg VM, Stevenson S. Natural history of autografts and allografts. Clin Orthop Relat Res 1987:7-16.

[78] Toms AD, Barker RL, Jones RS, Kuiper JH. Impaction bone-grafting in revision joint replacement surgery. J Bone Joint Surg Am 2004;86-A:2050-60.

[79] Aspenberg P, Astrand J. Bone allografts pretreated with a bisphosphonate are not resorbed. Acta OrthopScand 2002;73:20-3.

[80] Baas J, Elmengaard B, Jensen TB, Jakobsen T, Andersen NT, Soballe K. The effect of pretreating morselized allograft bone with rhBMP-2 and/or pamidronate on the fixation of porous Ti and HA-coated implants. Biomaterials 2008;29:2915-22.

[81] Jakobsen T, Baas J, Bechtold JE, Elmengaard B, Soballe K. Soaking morselized allograft in bisphosphonate can impair implant fixation. ClinOrthopRelat Res 2007;463:195-201.

[82] Marie PJ, Hott M, Modrowski D, De Pollak C, Guillemain J, Deloffre P, et al. An uncoupling agent containing strontium prevents bone loss by depressing bone resorption and maintaining bone formation in estrogen-deficient rats. J Bone Miner Res 1993;8:607-15.

[83] Pors Nielsen S. The Biological role of Strontium. Bone 2004;35:583-8.

[84] Bauer GC, Wendeberg B. External counting of Ca47 and Sr85 in studies of localised skeletal lesions in man. J Bone Joint Surg Br 1959;41-B:558-80.

[85] Cabrera WE, Schrooten I, De Broe ME, D'Haese PC. Strontium and bone. JBone MinerRes 1999;14:661-8.

[86] Boivin G, Deloffre P, Perrat B, Panczer G, Boudeulle M, Mauras Y, et al. Strontium distribution and interactions with bone mineral in monkey iliac bone after strontium salt (S 12911) administration. J Bone Miner Res 1996;11:1302-11.

[87] Marie PJ. Effective doses for strontium ranelate. Osteoporos Int 2008;19:1813; author reply 5-7.

[88] Leeuwenkamp OR, van der Vijgh WJ, Husken BC, Lips P, Netelenbos JC. Human pharmacokinetics of orally administered strontium. Calcif Tissue Int 1990;47:136-41.

[89] Aerssens J, Boonen S, Lowet G, Dequeker J. Interspecies differences in bone composition, density, and quality: potential implications for in vivo bone research. Endocrinology 1998;139:663-70.

[90] Raffalt AC, Andersen JE, Christgau S. Application of inductively coupled plasma-mass spectrometry (ICP-MS) and quality assurance to study the incorporation of strontium into bone, bone marrow, and teeth of dogs after one month of treatment with strontium malonate. AnalBioanalChem 2008;391:2199-207.

[91] Brennan TC, Rybchyn MS, Green W, Atwa S, Conigrave AD, Mason RS. Osteoblasts play key roles in the mechanisms of action of strontium ranelate. BrJPharmacol 2009;157:1291-300.

[92] Fromigue O, Hay E, Barbara A, Petrel C, Traiffort E, Ruat M, et al. Calcium sensing receptor-dependent and -independent activation of osteoblast replication and survival by strontium ranelate. JCell MolMed 2009.

[93] Caverzasio J. Strontium ranelate promotes osteoblastic cell replication through at least two different mechanisms. Bone 2008;42:1131-6.

[94] Atkins GJ, Welldon KJ, Halbout P, Findlay DM. Strontium ranelate treatment of human primary osteoblasts promotes an osteocyte-like phenotype while eliciting an osteoprotegerin response. OsteoporosInt 2009;20:653-64.

[95] Yamaguchi T. The calcium-sensing receptor in bone. JBone MinerMetab 2008;26:301-11.

[96] Teitelbaum SL. Bone resorption by osteoclasts. Science 2000;289:1504-8.

[97] Hurtel-Lemaire AS, Mentaverri R, Caudrillier A, Cournarie F, Wattel A, Kamel S, et al. The calcium-sensing receptor is involved in strontium ranelate-induced osteoclast apoptosis. New insights into the associated signaling pathways. JBiolChem 2009;284:575-84.

[98] Bonnelye E, Chabadel A, Saltel F, Jurdic P. Dual effect of strontium ranelate: stimulation of osteoblast differentiation and inhibition of osteoclast formation and resorption in vitro. Bone 2008;42:129-38.

[99] Buehler J, Chappuis P, Saffar JL, Tsouderos Y, Vignery A. Strontium ranelate inhibits bone resorption while maintaining bone formation in alveolar bone in monkeys (Macaca fascicularis). Bone 2001;29:176-9.

[100] Canalis E, Hott M, Deloffre P, Tsouderos Y, Marie PJ. The divalent strontium salt S12911 enhances bone cell replication and bone formation in vitro. Bone 1996;18:517-23.

[101] Takahashi N, Sasaki T, Tsouderos Y, Suda T. S 12911-2 inhibits osteoclastic bone resorption in vitro. JBone MinerRes 2003;18:1082-7.

[102] Dahl SG, Allain P, Marie PJ, Mauras Y, Boivin G, Ammann P, et al. Incorporation and distribution of strontium in bone. Bone 2001;28:446-53.

[103] Farlay D, Boivin G, Panczer G, Lalande A, Meunier PJ. Long-term strontium ranelate administration in monkeys preserves characteristics of bone mineral crystals and degree of mineralization of bone. JBone MinerRes 2005;20:1569-78.

[104] Grynpas MD, Marie PJ. Effects of low doses of strontium on bone quality and quantity in rats. Bone 1990;11:313-9.

[105] Arlot ME, Jiang Y, Genant HK, Zhao J, Burt-Pichat B, Roux JP, et al. Histomorphometric and mu-CT Analysis of Bone Biopsies from Postmenopausal Osteoporotic Women Treated with Strontium Ranelate. JBone MinerRes 2007.

[106] Grynpas MD, Hamilton E, Cheung R, Tsouderos Y, Deloffre P, Hott M, et al. Strontium increases vertebral bone volume in rats at a low dose that does not induce detectable mineralization defect. Bone 1996;18:253-9.

[107] Ammann P, Shen V, Robin B, Mauras Y, Bonjour JP, Rizzoli R. Strontium ranelate improves bone resistance by increasing bone mass and improving architecture in intact female rats. JBone MinerRes 2004;19:2012-20.

[108] Reginster JY, Seeman E, De Vernejoul MC, Adami S, Compston J, Phenekos C, et al. Strontium ranelate reduces the risk of nonvertebral fractures in postmenopausal women with osteoporosis: Treatment of Peripheral Osteoporosis (TROPOS) study. JClinEndocrinolMetab 2005;90:2816-22.

[109] Reginster JY, Felsenberg D, Boonen S, Diez-Perez A, Rizzoli R, Brandi ML, et al. Effects of long-term strontium ranelate treatment on the risk of nonvertebral and vertebral fractures in postmenopausal osteoporosis: Results of a five-year, randomized, placebo-controlled trial. Arthritis Rheum 2008;58:1687-95.

[110] O'Donnell S, Cranney A, Wells GA, Adachi JD, Reginster JY. Strontium ranelate for preventing and treating postmenopausal osteoporosis. CochraneDatabaseSystRev 2006:CD005326.

[111] Meunier PJ, Roux C, Ortolani S, Diaz-Curiel M, Compston J, Marquis P, et al. Effects of long-term strontium ranelate treatment on vertebral fracture risk in postmenopausal women with osteoporosis. Osteoporos Int 2009;20:1663-73.

[112] Park JW, Kim HK, Kim YJ, Jang JH, Song H, Hanawa T. Osteoblast response and osseointegration of a Ti-6Al-4V alloy implant incorporating strontium. Acta Biomater 2010;6:2843-51.

[113] Maimoun L, Brennan TC, Badoud I, Dubois-Ferriere V, Rizzoli R, Ammann P. Strontium ranelate improves implant osseointegration. Bone 2010;46:1436-41.

[114] Gorustovich AA, Steimetz T, Cabrini RL, Porto Lopez JM. Osteoconductivity of strontium-doped bioactive glass particles: A histomorphometric study in rats. JBiomedMaterResA 2009.

[115] Boyd D, Carroll G, Towler MR, Freeman C, Farthing P, Brook IM. Preliminary investigation of novel bone graft substitutes based on strontium-calcium-zinc-silicate glasses. JMaterSciMaterMed 2009;20:413-20.

[116] Towler MR, Boyd D, Freeman C, Brook IM, Farthing P. Comparison of in vitro and in vivo bioactivity of SrO-CaO-ZnO-SiO2 glass grafts. JBiomaterAppl 2009;23:561-72.

[117] O'Loughlin PF, Morr S, Bogunovic L, Kim AD, Park B, Lane JM. Selection and development of preclinical models in fracture-healing research. J Bone Joint Surg Am 2008;90 Suppl 1:79-84.

[118] Vestermark MT, Bechtold JE, Swider P, Soballe K. Mechanical interface conditions affect morphology and cellular activity of sclerotic bone rims forming around experimental loaded implants. JOrthopRes 2004;22:647-52.

[119] Frost HM. The biology of fracture healing. An overview for clinicians. Part I. Clin Orthop Relat Res 1989:283-93.

[120] Kirkwood. Essentials of Medical Statistics. 1st ed: Blackwell Science; 1988.

[121] Jakobsen T, Kold S, Bechtold JE, Elmengaard B, Soballe K. Local alendronate increases fixation of implants inserted with bone compaction: 12-week canine study. JOrthopRes 2007;25:432-41.

[122] Baas J, Lamberg A, Jensen TB, Elmengaard B, Soballe K. The bovine bone protein lyophilisate Colloss improves fixation of allografted implants--an experimental study in dogs. Acta Orthop 2006;77:791-8.

[123] Shaw JA, Wilson SC, Bruno A, Paul EM. Comparison of primate and canine models for bone ingrowth experimentation, with reference to the effect of ovarian function on bone ingrowth potential. J Orthop Res 1994;12:268-73.

[124] Eitel F, Klapp F, Jacobson W, Schweiberer L. Bone regeneration in animals and in man. A contribution to understanding the relative value of animal experiments to human pathophysiology. Arch Orthop Trauma Surg 1981;99:59-64.

[125] Kimmel DB, Jee WS. A quantitative histologic study of bone turnover in young adult beagles. Anat Rec 1982;203:31-45.

[126] Thomsen JS, Morukov BV, Vico L, Alexandre C, Saparin PI, Gowin W. Cancellous bone structure of iliac crest biopsies following 370 days of head-down bed rest. Aviat Space Environ Med 2005;76:915-22.

[127] van der Donk S, Buma P, Verdonschot N, Schreurs BW. Effect of load on the early incorporation of impacted morsellized allografts. Biomaterials 2002;23:297-303.

[128] Engh CA, Bobyn JD, Glassman AH. Porous-coated hip replacement. The factors governing bone ingrowth, stress shielding, and clinical results. J Bone Joint Surg Br 1987;69:45-55.

[129] Skoldenberg OG, Boden HS, Salemyr MO, Ahl TE, Adolphson PY. Periprosthetic proximal bone loss after uncemented hip arthroplasty is related to stem size: DXA measurements in 138 patients followed for 2-7 years. Acta Orthop 2006;77:386-92.

[130] Guldberg RE, Caldwell NJ, Guo XE, Goulet RW, Hollister SJ, Goldstein SA. Mechanical stimulation of tissue repair in the hydraulic bone chamber. J Bone Miner Res 1997;12:1295-302.

[131] Little DG, Ramachandran M, Schindeler A. The anabolic and catabolic responses in bone repair. JBone Joint SurgBr 2007;89-B:425-33.

[132] Lind M, Overgaard S, Soballe K, Nguyen T, Ongpipattanakul B, Bunger C. Transforming growth factor-beta 1 enhances bone healing to unloaded tricalcium phosphate coated implants: an experimental study in dogs. J Orthop Res 1996;14:343-50.

[133] Lamberg A, Schmidmaier G, Soballe K, Elmengaard B. Locally delivered TGF-beta1 and IGF-1 enhance the fixation of titanium implants: a study in dogs. Acta Orthop 2006;77:799-805.

[134] Lamberg A, Bechtold JE, Baas J, Soballe K, Elmengaard B. Effect of local TGF-beta1 and IGF-1 release on implant fixation: comparison with hydroxyapatite coating: a paired study in dogs. Acta Orthop 2009;80:499-504.

[135] Bobyn JD, Pilliar RM, Cameron HU, Weatherly GC. The optimum pore size for the fixation of porous-surfaced metal implants by the ingrowth of bone. Clin Orthop Relat Res 1980:263-70.

[136] Marie PJ. Strontium ranelate: a physiological approach for optimizing bone formation and resorption. Bone 2006;38:S10-S4.

[137] Marie PJ, Ammann P, Boivin G, Rey C. Mechanisms of action and therapeutic potential of strontium in bone. CalcifTissue Int 2001;69:121-9.

[138] Liao DP, Zhou ZY, Gu YF, Chen DM. [Experimental study of mandibular reconstruction with Sr-HAP]. Shanghai Kou QiangYiXue 2000;9:73-5.

[139] Brewster NT, Gillespie WJ, Howie CR, Madabhushi SP, Usmani AS, Fairbairn DR. Mechanical considerations in impaction bone grafting. J Bone Joint Surg Br 1999;81:118-24.

[140] Harris WH, Jackson RH, Jowsey J. The in vivo distribution of tetracyclines in canine bone. J Bone Joint Surg Am 1962;44-A:1308-20.

[141] Sun TC, Mori S, Roper J, Brown C, Hooser T, Burr DB. Do different fluorochrome labels give equivalent histomorphometric information? Bone 1992;13:443-6.

[142] Lind M. Growth factor stimulation of bone healing. Effects on osteoblasts, osteomies, and implants fixation. Acta Orthop Scand Suppl 1998;283:2-37.

[143] Fleisch H. Bisphosphonates: mechanisms of action. EndocrRev 1998;19:80-100.

[144] Pelker RR, Friedlaender GE, Markham TC, Panjabi MM, Moen CJ. Effects of freezing and freeze-drying on the biomechanical properties of rat bone. JOrthopRes 1984;1:405-11.

[145] Linde F, Sorensen HC. The effect of different storage methods on the mechanical properties of trabecular bone. JBiomech 1993;26:1249-52.

[146] Baas J. Adjuvant therapies of bone graft around non-cemented experimental orthopedic implants stereological methods and experiments in dogs. Acta OrthopSuppl 2008;79:1-43.

[147] Harrigan TP, Kareh J, Harris WH. The influence of support conditions in the loading fixture on failure mechanisms in the push-out test: a finite element study. J Orthop Res 1990;8:678-84.

[148] Dhert WJ, Verheyen CC, Braak LH, de Wijn JR, Klein CP, de GK, et al. A finite element analysis of the push-out test: influence of test conditions. JBiomedMaterRes 1992;26:119-30.

[149] Erben RG. Embedding of bone samples in methylmethacrylate: an improved method suitable for bone histomorphometry, histochemistry, and immunohistochemistry. JHistochemCytochem 1997;45:307-13.

[150] Gundersen HJ, Bendtsen TF, Korbo L, Marcussen N, Moller A, Nielsen K, et al. Some new, simple and efficient stereological methods and their use in pathological research and diagnosis. APMIS 1988;96:379-94.

[151] Howard CR, MG. Unbiased Stereology. Second ed: QTP Publications; 2005.

[152] Overgaard S, Soballe K, Jorgen H, Gundersen G. Efficiency of systematic sampling in histomorphometric bone research illustrated by hydroxyapatite-coated implants: optimizing the

stereological vertical-section design. J Orthop Res 2000;18:313-21.

[153] Gundersen HJ. Stereology: the fast lane between neuroanatomy and brain function--or still only a tightrope? Acta Neurol Scand Suppl 1992;137:8-13.

[154] Limpert ES, W Abbt, M. Log-normal Distributions across the Sciences: Keys and Clues. Bioscience 2001;51.

[155] Gruner H. Thermal Spray Coatings on Titanium. In: Brunette DT, P; Textor, M; Thomsen, Peter;, editor. Titanium in Medicine: material science, surface science, engineering, biological responses and medical application. Berlin Heidelberg: Springer-Verlag; 2001. p. 375-416.

[156] Li Y, Feng G, Gao Y, Luo E, Liu X, Hu J. Strontium ranelate treatment enhances hydroxyapatite-coated titanium screws fixation in osteoporotic rats. J Orthop Res 2010;28:578-82.

[157] Vogel W. Glass Chemistry. Springer.

[158] Gentleman E, Fredholm YC, Jell G, Lotfibakhshaiesh N, O'Donnell MD, Hill RG, et al. The effects of strontium-substituted bioactive glasses on osteoblasts and osteoclasts in vitro. Biomaterials 2010;31:3949-56.

Papers

1) Strontium-substitution of Hydroxyapatite Coating did not Improve Osseointegration and Implant Fixation

Authors
Marianne Toft **Vestermark**[1*], Ellen-Margrethe Hauge[2], Joan Elizabeth **Bechtold**[3], Thomas Jakobsen[1], Heiko Gruner[4], Kjeld Soballe[1], Jorgen Baas[1].

[1] Orthopaedic Research Lab., Department of Orthopaedic Surgery, Aarhus University Hospital, Noerrebrogade 44, Buildning 1A, DK-8000 Aarhus C, Denmark. marianne.t@vestermark.dk, thomas.jakobsen@ki.au.dk, kjeld@soballe.com, baas@ki.au.dk
[2] Research Unit for Rheumatology and Bone Biology, Aarhus University Hospital, Norrebrogade 44, Building 4A, DK-8000 Aarhus C, Denmark. ellen.hauge@ki.au.dk
[3] Orthopaedic Biomechanics Lab, Midwest Orthopaedic and Minneapolis Medical Research Foundations, 914 South 8th Street, Minneapolis, MN 55415, USA. bechtold@umn.edu
[4] Medicoat AG, Gewerbe Nord, 5506 Mägenwil, Switzerland. heiko.gruner@medicoat.ch

[*]Corresponding author: Marianne T. Vestermark, Orthopaedic Research Lab., Department of Orthopaedic Surgery, Aarhus University Hospital, Noerrebrogade 44, Buildning 1A, DK-8000 Aarhus C, Denmark, Telephone: +4551907447, Fax: +4589494150, marianne.t@vestermark.dk

Abstract
Hip replacement is on the rise but up 17% of all hip replacement surgeries are revisions. So investigations into further improvement of the longevity of the implants are needed.
The bioactivity of hydroxyapatite (HA) can be altered by chemical modification. Therefore we have investigated HA with 5% calcium substituted by strontium as coating compared to HA coating. The effect of strontium substitution was studied in a 1.3-mm gap model at 4 and 12 weeks observation in canines. The aim was to improve osseointegration of the implant by strontium substitution of the HA coating and subsequently improving implant fixation. The osseointegration and fixation of the implant was evaluated by histomorphometrical analysis and push-out test, respectively.
The histomorphometrical analysis and the push-out test showed that strontium substitution has no statistically significant effect on the osseointegration and the implant fixation.

Keywords: Strontium, HA coating, osseointegration, implant fixation, in vivo.

Introduction

Hip replacement is on the rise. By 2020, one-hundred-thousand Danes will have undergone hip replacement. Today 17% of all hip replacement surgeries are revisions, where the single most frequent indication is painful aseptic loosing of the prosthesis [1]. We believe, that the number of revisions can be reduced if early osseointegration of the implant is further improved [2].

At primary hip replacement, young patients typically receive a hydroxyapatite (HA) coated implant for cementless insertion. HA coated implants has in general good longevity and is also used for most cementless revision hip replacements [3, 4]. In experimental studies HA-coated implants have shown to be highly osseointegrated and strongly fixated in the host bone, and on both parameters the HA-coated implants were superior to uncoated titanium implants [5].

When strontium, as strontiumranelate, is used in systemic anti-osteoporotic treatment, strontiumhydroxyapatite (SrHA) is formed in bone. Overall, strontium increases the bone mass and the risk of fractures is reduced [6]. The cause of strontium's effects is that it is a dual acting agent that reduces bone resorption and increasing bone formation [7]. Furthermore synthetic SrHA has been found highly biocompatible and is believed to promote bone ingrowth [8, 9].

We have investigated the hypothesis that SrHA-coated implants will improve osseointegration and implant fixation compared to HA-coated implants after both 4 and 12 weeks. The osseointegration and fixation of the implant was evaluated by histomorphometrical analysis and push-out test, respectively.

Materials and Method

Design

With approval of our Institutional Animal Care and Use Committee, we tested the hypotheses in a four-arm paired study in 10 skeletally mature American Foxhounds (mean age 11.9 months +/- 1 month), mean weight of 29 kg (+/- 1.7 kg)). NIH guidelines for care and use of laboratory animals (NIH Publication #85-23 Rev. 1985) were observed. The number of dogs needed to be included in this study was estimated by the formula for paired studies with normal distributed data. Based on previous studies, we expected an average CV% ((sd / mean) x 100%) of 30% for three main variables Ultimate Shear Strength, gap healing by bone and implant bone ongrowth [10]. We wanted to be able to detect an increase of new bone formation and improvement in implant fixation between the groups of at least 30% (Δ). Based on these assumptions, 10 animals were included. The four arms of the study consisted of the two coatings described both at 4 weeks and 12 weeks observation time: SrHA-4, HA-4, SrHA-12, and HA-12. The implants were inserted into the cancellous bone of the metaphysis of the humerus (Fig.1). The two implants coated with strontium substituted HA of 4 and 12 weeks observation were paired within each dog. Pairing of implant was to rule out any possibility of strontium contamination of HA coated implants without strontium substitution. Positioning of the paired implants in each group was alternated systematically with a random start.

Implants

The experimental implant was a 10-mm titanium (Ti) alloy cylinder ASTM-136 (Ti6Al4V) with a diameter of 5.7 mm (+/- 0.1 mm). The implants had been coated with a commercially available structured Ti coating before SrHA or HA coating. Ti end screws, 8.0 mm in diameter, were attached to the top and bottom of the implant and ensured a concentric 1.3-mm gap around the implant. The overall height of the implant with mounted screws was 12.0 mm.

SrHA and HA powder for coating

A precipitate of white solid crystals of calcium HA with 5% calcium substituted by strontium were prepared by the method of Kumta et al. [11] with minor modifications of the synthesis. The synthesis was performed according to reaction equation:

$9.507Ca^{2+}(aq) + 0.493Sr^{2+}(aq) + 6(PO_4)^{3-}(aq) + 2OH^{-}(aq) \rightarrow Ca_{9.514}Sr_{0.493}(PO_4)_6(OH)_2\,(s)$

In a beaker, 190 g of trisodium phosphate (CAS 7601-54-9, Sigma-Aldrich 342483 Batch 03621 HE) was dissolved in 1 liter Millipore water, then 15.5 g sodium hydroxide (CAS 1310-73-2, Sigma-Aldrich 22146-5 Lot 540948-277) was added and was dissolved at 50^0C. In second beaker, 268 g of calcium chloride dihydrate (CAS 10035-04-8, Fluka Lot 1160484 Filling code 50305149) and 30.4 g of strontium chloride hexahydrate (CAS 10025-70-4, Fluka Lot 1094650 Filling code 53404170) were dissolved in 1 liter Millipore water. The content of the second beaker was slowly added to the first beaker under vigorous stirring over a time period of 6 hours. A small-grained white precipitate was then formed, the solution was centrifuged for 5 min at 2000 rpm, and flushed five times in Millipore water. The powder thus obtained was heated by increasing the temperature by 200°C/hour to 1000°C, and this temperature was maintained for 10 hours. The oven was allowed to cool to room temperature over 12 hours. The powder was grounded in a mortar. Osteologix Aps, Denmark, produced the powder.

The SrHA and HA powder then separately had to be converted into powder suitable for vacuum plasma spraying: Firstly the precipitated powder was mixed with water of high purity in a defined mass relationship. Secondly, the apatite substance was pressed to get a mechanical stable block. Thirdly, the apatite block was run through a calcination process in an oven with defined time/temperature treatment. Forthly, the now very stable apatite block was mechanically separated into the required particle range. Finally a cyclone treatment (removed all particles less 5 microns), together with sieving (upper limit -125 microns, lower limit +45 microns) the size range was adjusted for the vacuum plasma spraying. Medicoat AG, Mägenwill, Switzerland converted the powder.

This powder was characterized by x-ray powder diffraction, SEM and inductively-coupled plasma mass spectrometry by the manufactor (table 1).

A trace of Tetracalciumphosphate was found but no traces of CaO or Tricalciumphosphate. The Sr-content was uniformly distributed and morphology of the particles were visualized by SEM. The spraying conditions and specification of the powder were identical for SrHA and HA and furthermore identical with the spray powder for commercially available HA coatings of endoprosthesis for total hip replacement. The HA coating on the commercial implants has been characterized and found identical to the specifications of the spray powder of this study.

Vacuum Plasma-spray Coating

The implant cores were coated with three vacuum plasma sprayed coatings:

1. A innermost Ti-bond coating of 50 µm
2. In the middle a Ti-structured coating of 250 µm, max 300 µm
3. On top a HA or SrHA coating of 60-80 µm

Medicoat AG performed all the coatings. For the commercially available HA coating by the company, analyses have been made of both the HA spray powder and the HA after coating. The analyses confirmed that the specification of the HA powder listed

above are similar to the specification of the HA coating. Mechanical test of the tensile bond strength and shear stability was not performed.

Surgical procedure

Surgery was conducted under aseptic conditions with general anesthesia (initiated by *i.v*. thiopental 5% and maintained with isoflurane 1.5% gas). A skin incision of 7 cm was made with cautery on the lateral proximal humerus, and the deltoid muscle fascia was bluntly dissected to expose the proximal part of the humerus. A 2.5-mm guide wire was inserted anterolaterally at the level of the greater tubercle and oriented perpendicularly to the surface. Another 1.5-mm guide wire was inserted 17 mm distally and parallel to the first. The distal guide wire was cut off approximately 2 mm above the bone surface. With a cannulated drill (∅ 8.0mm) a 12-mm cavity was drilled over the proximal guide wires at a maximum speed of two rotations per second. The edge of the hole was trimmed, and the cavity irrigated with 10 ml saline for removal of periosteum and loose bone chips. One implant was inserted into the cavity, and after securing hemostasis, the soft tissue was closed in layers. This procedure was repeated for the opposite humerus.

After 8 weeks a second surgery was performed with the same surgical procedure as just described. At this second surgery an implant with the same coating as the implant in the proximal implant position was inserted at the position of the cut off 1.5 mm wire.

The dogs were given ceftriaxone (1 g, i.v) and buprenorphine hydrochloride (0.0075 mg/kg/day, i.m) administered immediately before each surgery and 3 days after each operation.

After another 4-weeks observation period, the dogs were sedated and killed with an overdose of hyper-saturated barbiturate.

The total observation period of 12 weeks was uneventful. All animals were fully mobilized within 3 days after each surgery, and there were no clinical signs of infection at any point during the observation period.

Preparation of specimens

The proximal humeri were retrieved *en bloc* and immediately frozen and stored at -20°C. Using a water-cooled Accutom-50 wheel diamond saw (Struers A/S, Roedovre, Denmark), the bone/implant specimen blocks were cut into two transverse blocks: a 3-mm thick block of the outermost part of the specimen block was cut and then refrozen for mechanical testing and a 6-mm thick block of the innermost part of the specimen block was cut for histomorphometrical analysis (Fig. 2).

Histomorphometry

The test implant was a porous coated cylinder. The estimates of the surface area density fraction was based on the stereological model for a cylinder, which is based on Buffon's needle problem for estimates of the length of the needle [12]. The observer was blinded to the coating type of the implants.

The specimens were fixated and dehydrated in graded ethanol (70-99%) prior to cold embedding in poly(methylmethacrylate) [13], and then exhaustively sectioned. This produced a total of 10 to 15 30-µm thick uniform random sampled sections per implant with a distance of 420 µm between sections (KDG-95;MeProTech, Heerhugowaard, the Netherlands). Every 2 to 3 sections were systematically sampled for the analysis, and their surfaces were stained with toluidine blue at pH 7. Tissue classification was based on morphology: new bone was a dense substance of variable organization due to age of the bone tissue, purple substance with embedded cells. Bone marrow was a cell rich conglomerate with intervening empty areas from

dissolved fat and few scattered thread-like structures. Fibrous tissue was dense, with well-organized bundles of fibers with sparsely intervening small cells.
Osseointegration, gap healing and ongrowth, was estimated in a predefined region of interest (ROI) manually drawn from an applied grid of two centralized circles: an inner circle 2.9 mm in diameter to centralize the ROI with regard to the implant and an outer circle 7.5 mm in diameter to outline the ROI at a distance of 0.75 mm out into the surrounding gap of the implant. The two components of osseointegration of the coated implant were measured by histomorphometry using a stereological system (Olympus microscope BX50 and Visiopharm Integrator system, NewCast ver. 3.0.9.0 Visiopharm, Hoersholm, Denmark). *Gap healing* was defined as volume density fraction of new bone in the ROI. For each grid point, it was counted as either hitting: new bone, fibrous tissue, or bone marrow tissue. A mean of 946 (+/- 116) points was counted for each specimen.
Ongrowth was defined as surface density fraction of new bone in contact with the coating on the implant. At interceptions between the implant coating and randomly orientated gridlines the tissue in contact with the implant coating was counted as either: new bone, fibrous tissue, or bone marrow tissue. For each implant, a mean of 443 (+/- 56) line intercepts was counted.
All estimates were counted at x287 magnification in randomly sampled fields of view in 100% of the ROI.
A single observer performed the histomorphometrical analysis. The intraobserver variation was determined as coefficients of variation (CV) on double measurements of one randomly selected implant from each treatment arm (Table 2). For the bone parameters the CV was below 10%, which verifies that the estimates are adequately precise and can be further analyzed.
Mechanical testing
Thawed specimens were tested to failure by axial push-out of the implant on a MTS Bionics Test Machine (Eden Prairie, MN, USA). The test was performed blinded and all specimens were evaluated in one session. The specimens were placed on a metal support jig with a 7.4-mm diameter central opening and under a 5.0 mm diameter cylindrical test probe. The implant was centralized over the opening, thereby assuring a distance of 0.7 mm between the implant and the support jig. The direction of loading was from the cortical surface inward. A preload of 0.5 N was applied to standardize contact conditions before initiating loading. The displacement rate was 5 mm/min with a 500 N load cell. Data points for every 10 μm of displacement were entered into an excel spreadsheet. The force-displacement curve and the mechanical parameters were calculated from the spreadsheet [14].
The means of lengths and diameters of the specimens were 3.25 (+/- 0.37) mm and 5.72 (+/- 0.06) mm, respectively. The individual specimen length was used to normalize push-out parameters. Ultimate Shear Strength (Pa) was determined from the maximal force applied until failure of the bone-implant interface. Apparent Shear Stiffness (Pa/mm) was obtained from the steepest slope of the linear section of the load-deformation curve. Total Energy Absorption (J/m^2) was calculated from the area beneath the load-deformation curve until failure [14, 15].
Scanning Electro Microscopy
In the push-out test, the mechanical strength of the interface was tested. The interface consisted of the metal implant core, Ti coating, HA coating, and bone and a failure happened in the weakest material or weakest connection between two consecutive layers. The location of the failure was inspected on SEM images of two pushed out implants. The chosen implants were one from each treatment arm after 12 weeks

observation, which Ultimate Shear Strength result was closest to the mean of the SrHA-12 and HA-12, respectively. The failure site was viewed on a Nova SEM 600 operated at 5kV.

Statistical analysis

Statistical analysis was performed using Intercooled STATA 10.0 software (StataCorp LP, College Station, TX, USA).

In this paired study, the data of the differences between treatment arms were not normally distributed for all variables. Therefore, data were transformed by natural logarithm (ln) and found normally distributed on the ln scale. An absolute difference between the ln of a pair of data equals the ln of the ratio within the pair [16]. Two tailed p-values below 0.05 were considered statistically significant. Results are presented as medians of relative differences between the paired data with 95% confidence interval. The 95% confidence intervals were obtained by back transformation of ln-transformed data.

Results

For the estimates of gap healing and ongrowth onto the implants at both 4 and 12 weeks, we could not detect an effect of strontium substituting the HA coating (Table 3 and 4, Fig. 3). Neither an improvement nor deterioration was detected. The bone ongrowth estimates were very high both at 4 and 12 weeks observation. Surface and volume fraction densities of fibrous tissue were small and often zero. The estimated fractions of fibrous tissue were of no clinical relevance and due to the many estimates of zero the statistical analysis could not be applied.

In the mechanical test, strontium substitution again showed no detectable effect on any of the mechanical parameters Ultimate Shear Strength, Apparent Shear Stiffness, or Total Energy Absorption (Table 5 and 6).

On the SEM pictures there was observed a moderate amount of bone on the surface of the HA coating but only sparsely bone was observed on the SrHA coating (Fig. 4 and 5).

Discusssion

Strontium substitution of the HA coating of titanium implants neither improve the osseointegration nor the biomechanical fixation of the implants at 4 or 12 weeks in 1.3-mm gap model.

On the other hand no deleterious effects of strontium substitution of the HA coating was detected. Ongrowth of bone onto the implant was as high as 75% for the HA coated implants and compared to previous observations made of HA coatings in this canine gap model the parameter seemed very high [17, 18]. The reason for the high fraction of ongrowth is probably due to the high purity and crystallinity of the HA coating (Table 1) [19]. No doubt that HA coatings are highly bioactive, which makes it a strong competitor for other and novel biomaterials. Since HA coatings are the gold standard and is included in the revision rate of today, then any bioactive coating to be introduced clinically must perform better than HA.

A possible deterioration of the mechanical properties of strontium substituting the HA coating was observed. Based on the results of the histomorphometrical analysis, approximately equal amounts of bone was in contact with the coatings regardless of the strontium substitution (SrHA: 74% and HA 79%) before the implants were pushed out. But on the SEM images of the implants after push-out almost no bone was on the SrHA coating but a moderate amount was left on the HA coating. Therefore, we

speculate that in the bone-implant interface of the SrHA coated implants failure happened within the coating but for the HA coated implants the failure happened in the surrounding bone. The tensile strength of the SrHA coating was not tested before implantation. The mechanical strength of the strontium-substituted coating was perhaps lower than the pure HA coating because the lattice structure had become destabilized [20, 21]. The destabilized strontium substituted HA could then more easily transformed into ß- tristrontiumcalciumphosphate (ß-TCSrP) during the vacuum plasma spraying, and was less crystalline and dissolved more easily [22, 23]. The possible ß-TCSrP or even amorphous strontium calcium phosphate compounds was likely to have formed a network of soluble material during the vacuum plasma spray coating. The soluble network would subsequently cause the coating to delaminate when loaded during the push-out test. [24].

For the stereological model for a cylinder used for the present study, two assumptions must be fulfilled: Firstly, the structure to be estimated is a geometric cylinder. Secondly, the orientation of the uniform random sampling of the histological sections is horizontal. By the first assumption of which the structure of the implant was assumed to be a perfect, smooth geometric cylinder. This was not completely the case, but the implant with rough textured coatings was considered close enough for the model to be applied. The reason was that surface of the implant still curved like a cylinder. Furthermore the implant did not approach a shape that resembles any other geometrical shape. Hence the discrepancy between the actual implant structure and a perfect cylinder is small. Any potential bias inflicted by this discrepancy is therefore considered small. The second assumption was met, which was controlled when the circle gird for drawing the ROI was applied and it was clearly noticed that the implant was a circle and not an ellipsoid. Therefore the assumption of horizontal sampling orientation was considered fulfilled.

Conclusion

HA coated Ti alloy implant can become osseointegrated and fixation in the present 1.3-mm gap model. This allowed us to investigate whether strontium substitution of the HA coating could improve osseointegration and implant fixation. Strontium substitution of HA coating of titanium implants had no effect on osseointegration or implant fixation neither after 4 weeks nor 12 weeks. But perhaps indications of deteriorated mechanical implant fixation were observed.

Acknowledgements

We thank laboratory technician Jane Pauli, Ass. Professor Jesper Skovhus Thomsen, and Professor Jens Randel Nyengaard for their excellent help with the histomorphometrical analysis.

Conflicts of interest

The strontium substituted HA powder was donated unconditionally by Osteologix Aps and produced by Ass. Prof. Jens E.T. Andersen, Institute of Chemistry, Danish Technical University, Denmark. Implant coatings were donated unconditionally by Medicoat AG, Mägenwil, Switzerland.

P. Carl Petersens Fundation, DK, Danish Rheumatism Association, and The A.P. Moeller Foundation for Advancement of Medical Science, DK supported the work unconditionally. NIH provided partial support to the study, NIH AR42051.

Contributions of authors

Marianne T. Vestermark formulated the scientific problem, planned the methodological design and the experiments, performed the experiments, interpreted the results, and wrote the manuscript.
Ellen-Margrethe Hauge planned the methodological design, performed the experiments, interpreted the results, and wrote the manuscript.
Joan E. Bechtold planned the methodological design, performed the experiments, interpreted the results, and wrote the manuscript.
Thomas Jakobsen planned the methodological design, interpreted the results, and wrote the manuscript.
Heiko Gruner planned the methodological design, performed the experiments, interpreted the results, and wrote the manuscript.
Kjeld Soballe planned the methodological design, interpreted the results, and wrote the manuscript.
Jorgen Baas formulated the scientific problem, planned the methodological design and the experiments, performed the experiments, interpreted the results, and wrote the manuscript.

References

[1] Pedersen AB, Johnsen SP, Overgaard S, Soballe K, Sorensen HT, Lucht U. Total hip arthroplasty in Denmark: incidence of primary operations and revisions during 1996-2002 and estimated future demands. Acta Orthop. 2005;76:182-9.
[2] Albrektsson T, Branemark PI, Hansson HA, Lindstrom J. Osseointegrated titanium implants. Requirements for ensuring a long-lasting, direct bone-to-implant anchorage in man. Acta Orthop Scand. 1981;52:155-70.
[3] Capello WN, D'Antonio JA, Feinberg JR, Manley MT. Hydroxyapatite coated stems in younger and older patients with hip arthritis. Clin Orthop Relat Res. 2002:92-100.
[4] Reikeras O, Gunderson RB. Excellent results with femoral revision surgery using an extensively hydroxyapatite-coated stem: 59 patients followed for 10-16 years. Acta Orthop. 2006;77:98-103.
[5] Soballe K, Hansen ES, Brockstedt-Rasmussen H, Pedersen CM, Bunger C. Hydroxyapatite coating enhances fixation of porous coated implants. A comparison in dogs between press fit and noninterference fit. Acta OrthopScand. 1990;61:299-306.
[6] O'Donnell S, Cranney A, Wells GA, Adachi JD, Reginster JY. Strontium ranelate for preventing and treating postmenopausal osteoporosis. CochraneDatabaseSystRev. 2006:CD005326.
[7] Marie PJ, Hott M, Modrowski D, De Pollak C, Guillemain J, Deloffre P, et al. An uncoupling agent containing strontium prevents bone loss by depressing bone resorption and maintaining bone formation in estrogen-deficient rats. J Bone Miner Res. 1993;8:607-15.
[8] Xue W, Hosick HL, Bandyopadhyay A, Bose S, Ding C, Luk KDK, et al. Preparation and cell-materials interactions of plasma sprayed strontium-containing hydroxyapatite coating. Surface & coatings technology. 2007;201:4685-93.
[9] Tian M, Chen F, Song W, Song Y, Chen Y, Wan C, et al. In vivo study of porous strontium-doped calcium polyphosphate scaffolds for bone substitute applications. JMaterSciMaterMed. 2009;20:1505-12.
[10] Baas J, Elmengaard B, Bechtold J, Chen X, Soballe K. Ceramic bone graft substitute with equine bone protein extract is comparable to allograft in terms of implant fixation: a study in dogs. Acta Orthop. 2008;79:841-50.

[11] Kumta PN, Sfeir C, Lee DH, Olton D, Choi D. Nanostructured calcium phosphates for biomedical applications: novel synthesis and characterization. Acta Biomater. 2005;1:65-83.
[12] Howard CR, MG. Unbiased Stereology. Second ed: QTP Publications; 2005.
[13] Erben RG. Embedding of bone samples in methylmethacrylate: an improved method suitable for bone histomorphometry, histochemistry, and immunohistochemistry. JHistochemCytochem. 1997;45:307-13.
[14] Baas J. Adjuvant therapies of bone graft around non-cemented experimental orthopedic implants stereological methods and experiments in dogs. Acta OrthopSuppl. 2008;79:1-43.
[15] Soballe K. Hydroxyapatite ceramic coating for bone implant fixation. Mechanical and histological studies in dogs. Acta OrthopScandSuppl. 1993;255:1-58.
[16] Bland JM, Altman DG. The use of transformation when comparing two means. BMJ. 1996;312:1153.
[17] Lamberg A, Bechtold JE, Baas J, Soballe K, Elmengaard B. Effect of local TGF-beta1 and IGF-1 release on implant fixation: comparison with hydroxyapatite coating: a paired study in dogs. Acta Orthop. 2009;80:499-504.
[18] Overgaard S, Lind M, Rahbek O, Bunger C, Soballe K. Improved fixation of porous-coated versus grit-blasted surface texture of hydroxyapatite-coated implants in dogs. Acta Orthop Scand. 1997;68:337-43.
[19] Soballe K, Overgaard S. The current status of hydroxyapatite coating of prostheses. J Bone Joint Surg Br. 1996;78:689-91.
[20] Grynpas M. Age and disease-related changes in the mineral of bone. Calcif Tissue Int. 1993;53 Suppl 1:S57-64.
[21] Li ZY, Lam WM, Yang C, Xu B, Ni GX, Abbah SA, et al. Chemical composition, crystal size and lattice structural changes after incorporation of strontium into biomimetic apatite. Biomaterials. 2007;28:1452-60.
[22] Bigi AM, F; Ripamonti, A; Roveri, N;. Magnisium and Strontium Interaction with Carbonate-Containing Hydroxyapatite in Aqueous Medium. Journal of Inorganic Biochemistry. 1981;15.
[23] Christoffersen J, Christoffersen MR, Kolthoff N, Barenholdt O. Effects of strontium ions on growth and dissolution of hydroxyapatite and on bone mineral detection. Bone. 1997;20:47-54.
[24] Gruner H. Thermal Spray Coatings on Titanium. In: Brunette DT, P; Textor, M; Thomsen, Peter;, editor. Titanium in Medicine: material science, surface science, engineering, biological responses and medical application. Berlin Heidelberg: Springer-Verlag; 2001. p. 375-416.

Figures and tables

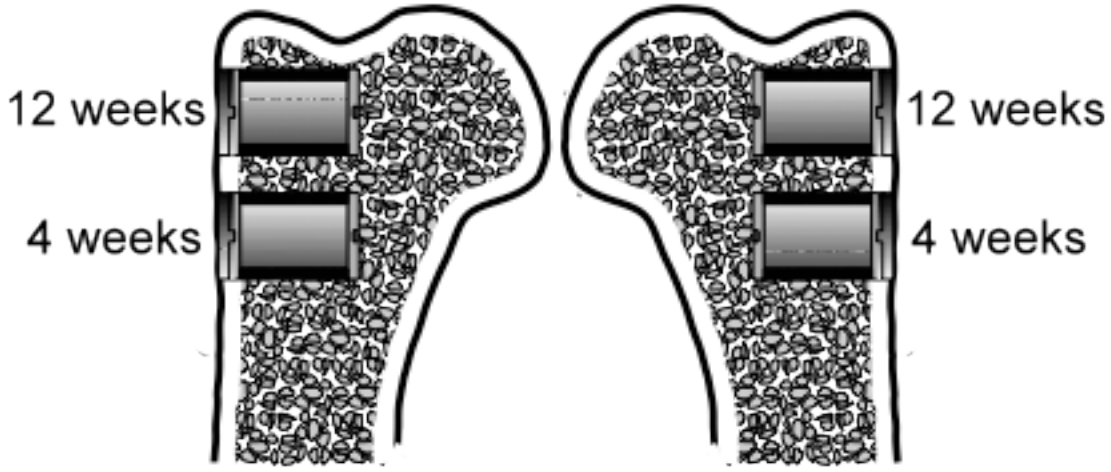

Treatment group	Chemical Formula	Observation time
SrHA-4	$Ca_{9.514}Sr_{0.486}(PO_4)_6(OH)_2$	4 weeks
HA-4	$Ca_{10}(PO_4)_6(OH)_2$	4 weeks
SrHA-12	$Ca_{9.514}Sr_{0.486}(PO_4)_6(OH)_2$	12 weeks
HA-12	$Ca_{10}(PO_4)_6(OH)_2$	12 weeks

Figure 1: Strontium-substituted HA was expected to released strontium ions. Therefore, the implants coated with SrHA were positioned next to each other as were the implants coated with HA. Positioning of the implants in each group was alternated systematically with a random start.

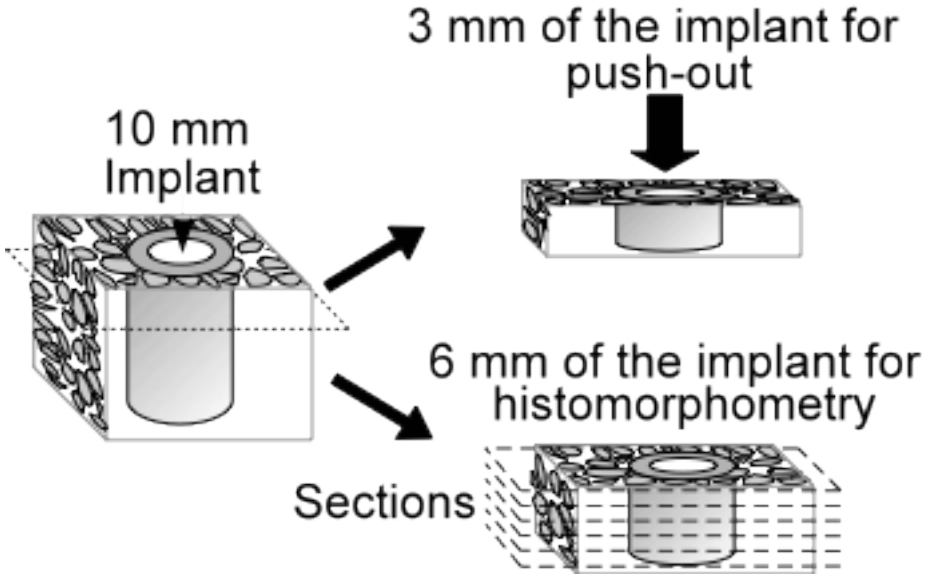

Figure 2: Preparation of the specimens and the horizontal cutting method for the histomorphometrical analysis.

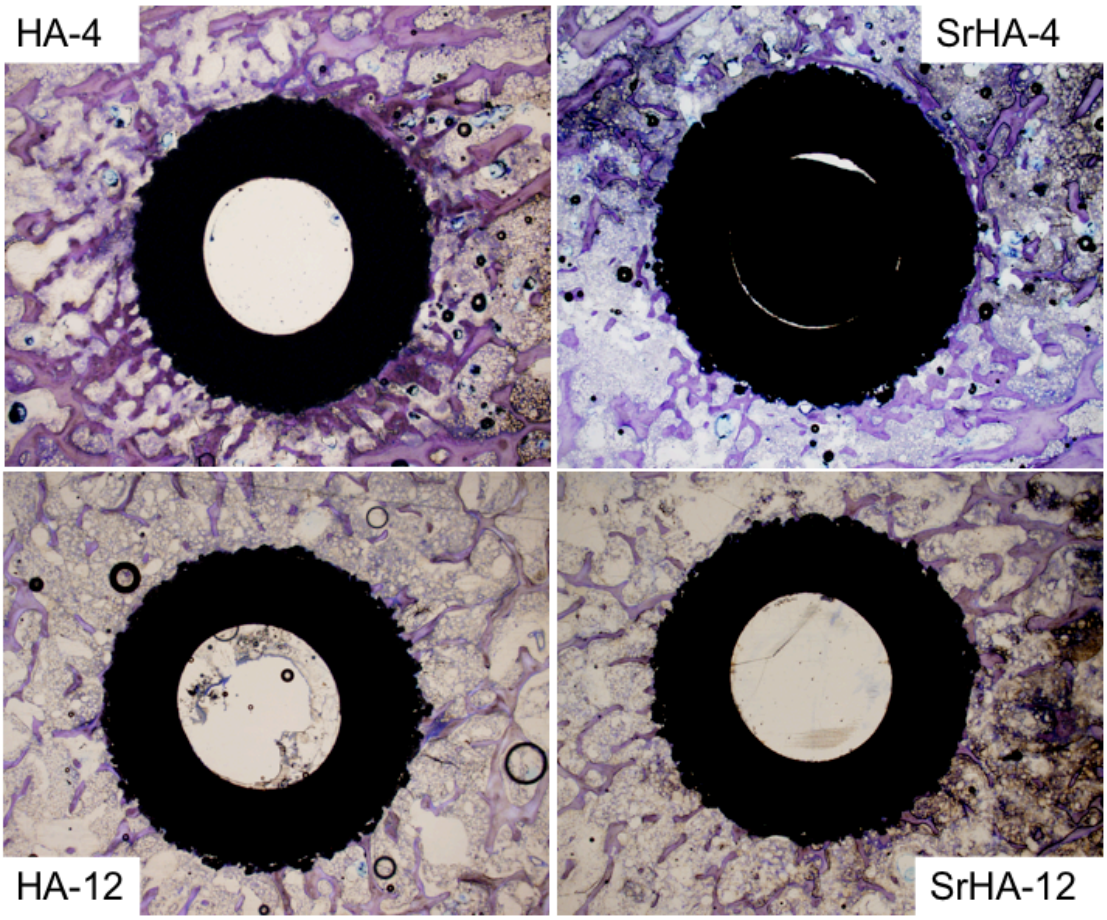

Figure 3: An overview of the gap healing and ongrowth of the SrHA and HA coated implants at 4 week, upper row, and at 12 weeks, lower row. These histological sections are medians of the specific treatment group but not from the same dog.

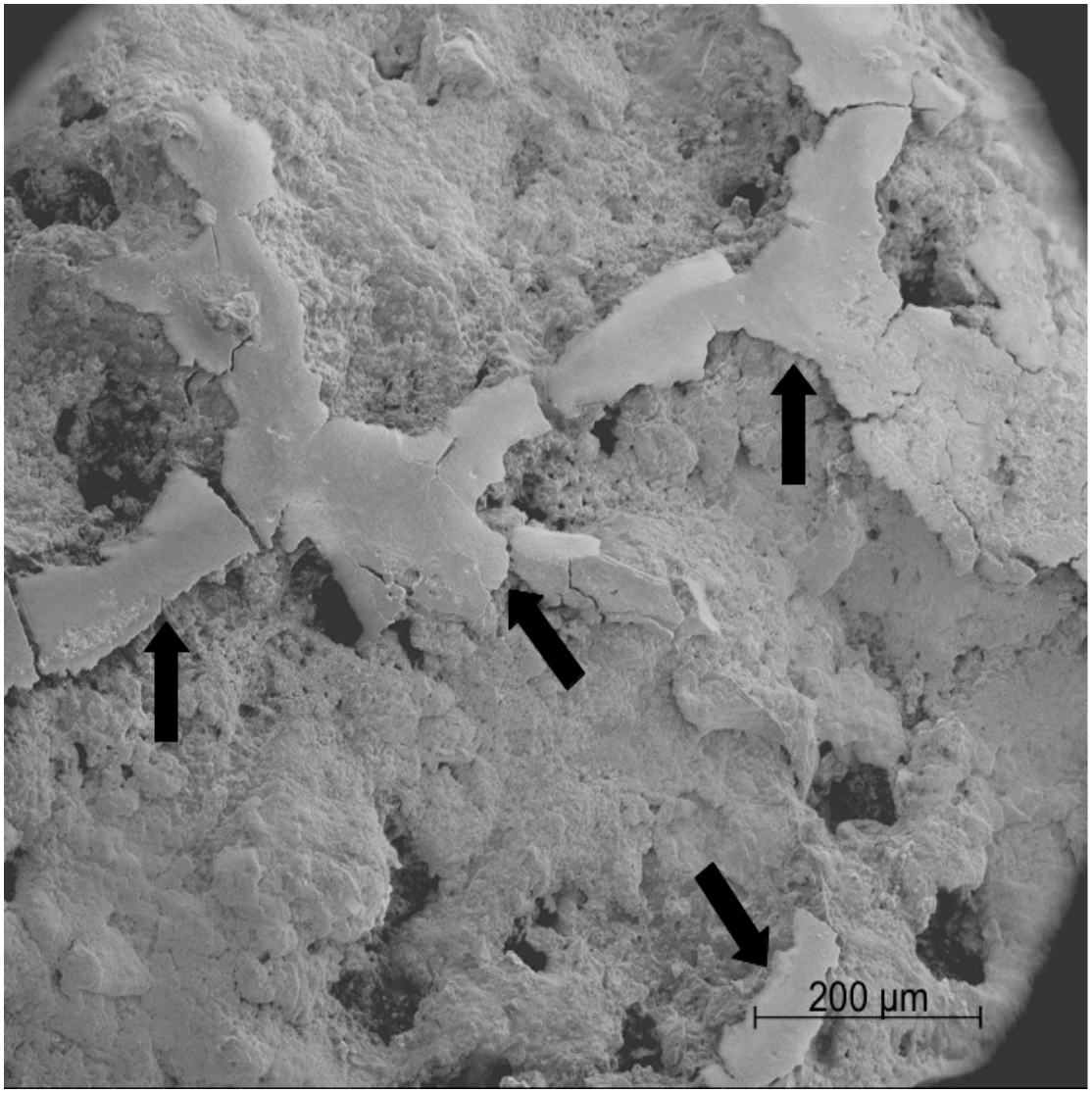

Figure 4: SEM image of the surface of a HA coated implant at 12 weeks observation time with a median Ultimate Shear Strength value. Bone can be seen on the coating (arrows).

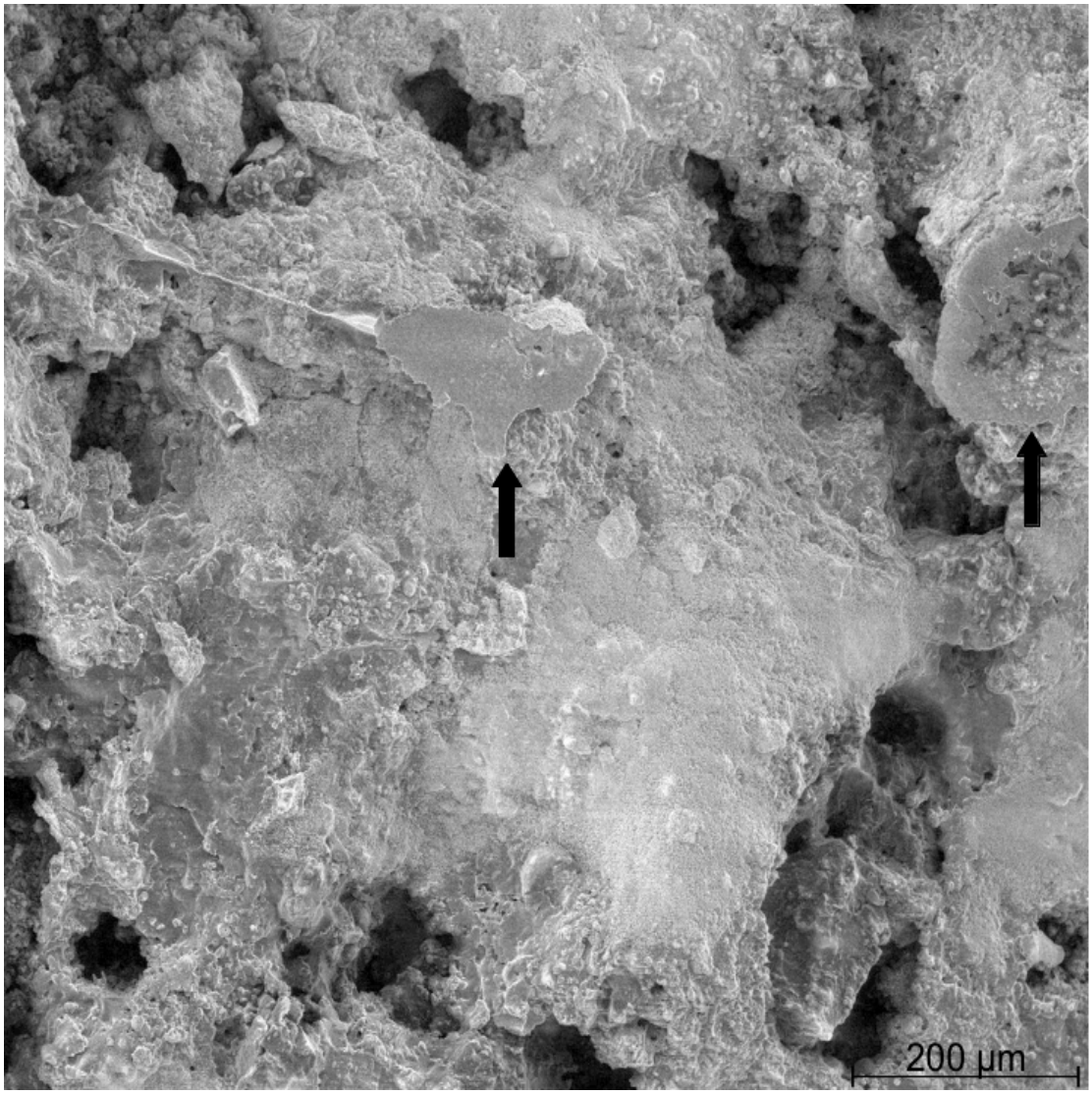

Figure 5: SEM image of the surface of a SrHA coated implant at 12 weeks observation time with a median Ultimate Shear Strength value. The flat area by the arrows have sharp edges, therefore it looks like coating broken off during the push-out test. Even if the flat areas are bone then there is considerably less bone than on the HA coating.

- HA or SrHA purity of 95%
- Ca/P or CaSr/P: 1.667 ± 0.004
- 4.86% Sr atoms in SrHA
- Particle size distribution: 75 (45-125) µm
- Bulk density: 1.16 g/cm3

Table 1: Specifications of the SrHA and HA spray powder

Coefficient of variance	New bone	Fibrous tissue
Gap healing	9.8%	0%
Ongrowth on implant	6.0%	0%

Table 2: Intra-observer variation.

Histomorphometry 4 weeks		
	Gap Healing **Bone Volume Density Fraction**	**Ongrowth** **Bone Surface Area Density Fraction**
SrHA-4	26 (23-29)	74 (66-83)
HA-4	28 (24-31)	75 (68-83)
Ratio	0.94 (0.83-1.07)	0.98 (0.83-1.16)
	p=0.31	*p*=0.79

Table 3: Presented as means (95% CI). The ratio is presented as median (95% CI).

Histomorphometry 12 weeks		
	Gap Healing **Bone Volume Density Fraction**	**Ongrowth** **Bone Surface Area Density Fraction**
SrHA-12	17 (15-19)	71 (63-78)
HA-12	19 (16-22)	75 (70-80)
Ratio	0.89 (0.73-1.09)	0.94 (0.8-1.09)
	p=0.22	*p*=0.34

Table 4: Presented as means (95% CI). The ratio is presented as median (95% CI).

Push-out test 4 weeks	Ultimate shear strength, [MPa]	Apparent shear stiffness, [MPa/mm]	Total energy absorption, [kJ/m^2]
SrHA	7.1 (5.7-8.6)	34 (27-41)	1818 (1413-2222)
HA	8.2 (6.7-9.7)	39 (31-48)	1806 (1189-2422)
Ratio SrHA/HA	0.87 (0.64-1.18)	0.87 (0.63-1.21)	1.09 (0.73-1.63)
	p=0.33	*p*=0.38	*p*=0.63

Table 5: Presented as means (95% CI). The ratio is presented as median (95% CI).

Push-out test 12 weeks	Ultimate shear strength, [MPa]	Apparent shear stiffness, [MPa/mm]	Total energy absorption, [kJ/m^2]
SrHA	3.3 (2-4.7)	16 (10-21)	794 (418-1169)
HA	4.7 (3.3-6.1)	22 (15-28)	1024 (645-1402)
Ratio SrHA/HA	0.64 (0.3-1.34)	0.69 (0.39-1.23)	0.68 (0.24-1.91)
	p=0.20	*p*=0.18	*p*=0.42

Table 6: Presented as means (95% CI). The ratio is presented as median (95% CI).

2) Title

Strontium-doped Hydroxyapatite as Bone Graft Extender Protects Allografts and Improves Ingrowth toward Implants: An Experimental Study in Dogs

Authors

[1]Marianne T. Vestermark, [2]Ellen-Margrethe Hauge, [1]Kjeld Soballe, [3]Joan E. Bechtold, [1]Thomas Jakobsen, [1]Jorgen Baas.

[1] Orthopedic Research Lab., Department of Orthopedic Surgery, Aarhus University Hospital, Denmark

[2] Research Unit for Rheumatology and Bone Biology, Aarhus University Hospital, Denmark

[3] Orthopedic Biomechanics Lab, Excelen Center for Bone and Joint Research and Education and Minneapolis Medical Research Foundations, Minneapolis, MN, USA

Corresponding author: Marianne T. Vestermark, marianne.t@vestermark.dk

Key words: strontium, allograft, bone graft extender, implants, osseointegration

Abstract

Allografts are often used during revision hip replacement surgery for stabilizing the implant. Resorption of the bone graft may exceed new bone formation, and instability of the prosthesis can develop.

We have investigated if strontium could regulate the mismatch of fast resorption of allograft and slow ingrowth of new bone. Strontium is both a bone anabolic and anticatabolic agent. Strontium was added by doping a hydroxyapatite (HA) bone graft extender. Ten dogs each received two experimental titanium implants. The implants were inserted with a 2.5 mm concentric gap into the cancellous, metaphyseal bone of the proximal humerus. The gap was filled with 50% per volume allograft mixed with 50% per volume HA with or without strontium doping. Osseointegration was evaluated by histomorphometrical evaluation of bone ingrowth and ongrowth. Mechanical implant fixation was evaluated by push-out test. Strontium-doped HA bone graft extender induced a 19% increase in new bone ingrowth and the allograft was 5% less resorbed in the gap compared to HA bone graft extender. The differences of ongrowth onto the implants and onto the bone graft extender with or without strontium doping were inconclusive in this study. In the push-out test, the difference of total energy absorption was likewise inconclusive.

In this study, the first step of the osseointegration of allografted implants was improved by strontium doping the bone graft extender. We speculate that with longer observation time or strontium released for longer, strontium doping of bone graft extender can potentially improve the full osseointegration and implant fixation.

Introduction

Total hip replacement is performed on a large number of patients of increasing younger age. Up to 17% of hip replacement surgeries currently involves revisions.

The main indication for revision surgery is painful aseptic loosening of the prosthesis (Pedersen, Johnsen 2005). In connection with aseptic loosening of the prosthesis, periprosthetic bone loss has occurred. Therefore, during revision surgery, a bone graft is often used to stabilize the prosthesis. Bone grafts are rapidly resorbed, and thus instability of the prosthesis may develop before bone ingrowth is well established and can mechanically secure the prosthesis (Aspenberg and Astrand 2002). Re-revision prevalence for uncemented acetabular components was 6.8% for allografted implants compared to 3.7% for non-allografted implants (Lie, Havelin 2004).
By decreasing the mismatch between fast resorption of a biologic graft and slower new bone formation, the outcome of grafted revision hip prostheses can perhaps be improved. Strontium is known to have both anabolic and anticatabolic effects in bone (Marie, Hott 1993). Synthetic strontium hydroxyapatite has proven highly biocompatible and is believed to promote bone ingrowth (Tian, Chen 2009, Xue, Hosick 2007).
We investigated strontium-doped hydroxyapatite (SrHA) compared to hydroxyapatite (HA) as a bone graft extender (BGE) with a two-fold purpose. First purpose is a local anabolic and anticatabolic effect of strontium. Second purpose is a slower resorption of the total graft material, because in general synthetic graft substitutes are resorbed slower (Fellah, Gauthier 2008, Hannink, Schreurs 2007). We hypothesized that strontium doping of the BGE would preserve the allograft and increase bone ingrowth and ongrowth. The improved osseointegration would then lead to improved implant fixation.

Methods and Materials

Design

We tested our hypothesis in a paired study in 10 dogs. The two treatment arms consisted of: (1) Allograft mixed with strontium-doped hydroxyapatite (SrHA) BGE, and (2) allograft mixed with hydroxyapatite (HA) BGE. The graft mixtures surrounded the implants in cancellous bone of the metaphyseal part of the proximal humerus (Fig.1).

Implants

The experimental implant was a 10-mm titanium (Ti) alloy cylinder ASTM-136 (Ti6Al4V) with a diameter of 5.7 (range 5.5-6) mm. The implants had been coated with a commercially available bead-sintered porous Ti coating, donated by DePuy Inc. (Fig.1). Ti end screws, 11.0 mm in diameter, were attached to the top and bottom of the implant and ensured a concentric 2.5-mm gap around the implant. The overall height of the implant with mounted screws was 12.0 mm.

Bone graft extender

A precipitate of calcium-strontium hydroxyapatite was used as an experimental bone graft extender for this study.

Synthesis of calcium-strontium hydroxyapatite:

White solid crystals of calcium HA with 5% (w/w) calcium substituted by strontium were prepared by the method of Kumta et al. (Kumta, Sfeir 2005) with minor modifications of the synthesis, however. The synthesis was performed according to reaction equation:

$$9.411 \cdot Ca^{2+}(aq) + 0.589 \cdot Sr^{2+}(aq) + 6PO_4^{3-}(aq)2OH^-(aq) \rightarrow Ca_{9.411}Sr_{0.589}(PO_4)_6(OH)_2(s)$$

In the first 2-liter beaker, 190 g of trisodium phosphate Na_3PO_4 (CAS 7601-54-9, Sigma-Aldrich 342483 Batch 03621 HE) was partly dissolved in 1 liter of Millipore water. After addition of 15.5 g of sodium hydroxide (CAS 1310-73-2, Sigma-Aldrich 22146-5 Lot 540948-277), the suspension was gently heated (about 50^0C) until all material was dissolved. In the second 2-liter beaker, 268 g of calcium chloride dihydrate (CAS 10035-04-8, Fluka Lot 1160484 Filling code 50305149) and 30.4 g of strontium chloride hexahydrate (CAS 10025-70-4, Fluka Lot 1094650 Filling code 53404170) were dissolved in 1 liter Millipore water. The solution in the first beaker containing trisodium phosphate and sodium hydroxide was transferred to a 5-liter beaker with a stirrer, and the content of the second beaker was slowly added under vigorous stirring over a time period of 6 hours. A small-grained white precipitate was then formed, the solution centrifuged for 5 min at 2000 rpm, and flushed five times in Millipore water. The powder thus obtained was transferred to an alumina beaker and heated by increasing the temperature by 200°C/hour to 1000°C, and this temperature was maintained for 10 hours. The oven was allowed to cool to room temperature over 12 hours. The powder was kept sterile while being ground in a mortar, weighed, and separated into batches of granules of 0.6 to 2 mm in diameter, which were packed individually in portions of 1.0 mL in double sterile containers ready for surgery. The yield was 92.6%, and by using x-ray powder diffraction (Diffractometer Huber G670, HUBER Diffraktionstechnik GmbH & Co. KG, rimsting, Germany; 1.54060 wavelength, 1 hour exposure time), the structure was confirmed and the strontium content was determined to be 6%, which was within range of the expected concentration (Fig.2). The procedure was repeated for production of HA powder without adding SrCl (Table 1).
The bone graft extender was produced and donated by Osteologix Aps, Denmark.

Allograft
Two weeks before surgery bones for bone graft were harvested under sterile conditions from two dogs not included in the study and stored at -80°C. The proximal humerus and the distal femurs were used. All soft tissue and cartilage were removed, and the bones were morselized with a Biomet bone mill, creating bone chips of 1 to 2 mm in size. The chips from the different bones were mixed together and portioned into sterile double containers and refrozen to -80°C. Immediately before surgery the bone graft was thawed, and at surgery, the allograft was divided into two portions of 1 mL in a standardized container.

Animals:
Ten female, skeletally mature American Foxhounds (mean age 11.8 (range 9.5-14) months), (mean weight 25.1 (range 23.5-26.5) kg) were included. Positioning of the implants of each treatment arm was alternated systematically with a random start in regard to right and left humerus. NIH guidelines for care and use of laboratory animals (NIH Publication #85-23 Rev. 1985) were observed, and the study was performed in our AAALAC-approved animal care facility. Minneapolis Medical Research Foundation, and the Animal Care and Use Committee had approved the protocol of the study.

Surgical procedure:
Surgery was conducted under aseptic conditions with general anesthesia (initiated by *i.v*. thiopental 5% and maintained with isoflurane 1.5% gas). A skin incision of 7 cm was made with cautery on the lateral proximal humerus, and the deltoid muscle fascia

was bluntly dissected to expose the proximal part of the humerus. A 2.5-mm guide wire was inserted anterolaterally at the level of the greater tubercle and oriented perpendicularly to the surface. Over the guide wire, a cannulated drill (∅ 11.0mm) was used to drill a 12-mm deep cylindrical cavity at a speed of maximum two rotations per second. The edge of the hole was trimmed with a scalpel to remove periosteum, and the cavity was irrigated once with 10 mL saline for removal of lose bone chips.
An implant with a mounted bottom screw was inserted into the cavity. A mixture of 1 mL allograft and 1mL SrHA or HA, was tightly packed around the implant, and the top screw was mounted. When hemostasis was secured, the soft tissue was closed in layers. The procedure was repeated for the contralateral humerus with the other bone graft mixture.
The dogs were given ceftriaxone (1 g, i.v) and buprenorphine hydrochloride (0.0075 mg/kg/day, i.m) administered immediately before surgery and 3 days after operation. The observation period of 28 days was uneventful. All animals were fully mobilized within 2 to 3 days, and there were no clinical signs of infection at any point during the observation period.
After a 4-weeks observation period, the dogs were sedated and killed with an overdose of hyper-saturated barbiturate.

Preparation of specimens
The proximal humeri were retrieved *en bloc* and, immediately after explantation, frozen and stored at -20°C. Using a water-cooled Accutom-50 wheel diamond saw (Struers A/S, Roedovre, Denmark), the bone/implant specimen blocks were cut into two transverse blocks: a 3-mm thick block of the outermost part of the specimen block was cut and then refrozen for mechanical testing and a 6-mm thick block of the innermost part of the specimen block was cut for histomorphometrical analysis. (Fig.3)

Histomorphometry
The specimens were fixated in 70% ethanol prior to cold embedding in poly(methylmethacrylate) (Erben 1997), and then completely sectioned. This produced a total of 10 to 15 30-µm thick systematic uniform random sections per implant with a distance of 420 µm between sections (KDG-95;MeProTech, Heerhugowaard, the Netherlands). Every 2 to 3 sections were sampled for the analysis, and their surfaces were stained with tolouidin blue at pH 7. Tissue classification was based on morphology: new bone was a disorganized, dense substance with embedded cells colored relatively dark purple; and allograft was a dense substance with empty cell lacunae and clear cement lines colored relatively pale purple. Bone marrow was a cell rich conglomerate with intervening empty areas from dissolved fat and few scattered thread-like structures. Fibrous tissue was dense, with well-organized bundles of fibers with sparsely intervening small cells. BGE was identified as coarsely profiled shadows.
Osseointegration, ingrowth and ongrowth, was estimated in a predefined region of interest (ROI) manually drawn from an applied grid of two centralized circles: an inner circle 2.9 mm in diameter to centralize the ROI with regard to the implant and an outer circle 10.5 mm in diameter to outline the ROI at a distance of 2.25 mm out into the surrounding gap of the implant (Fig. 4). The two components of osseointegration of the coated implant were measured by histomorphometry using a stereological system (Olympus microscope BX50 and Visiopharm Integrator system,

NewCast ver. 3.0.9.0 Visiopharm, Hoersholm, Denmark). The observer was blinded to the treatment of the specimens. *Ingrowth* was defined as volume density fraction of new bone in the ROI. The volume density was measured by counting grid points hitting the new bone. A mean of 1539 (range 1456-1803) points was counted for each specimen as either: new bone, allograft, fibrous tissue, bone marrow tissue, or BGE. *Ongrowth* was defined as surface density fraction of new bone in contact with the implant surface. At interceptions between the implant surface and randomly orientated gridlines the tissue in contact with the implant was counted as either: new bone, allograft, fibrous tissue, bone marrow tissue, or BGE. For each implant, a mean of 756 (range 655-909) line intercepts was counted.
Ongrowth onto the two types of BGE was defined as new bone in contact with the surface of BGE granules. At interceptions between the surface of granules and randomly orientated gridlines the tissue in contact with the granule was counted as either: new bone, allograft, fibrous tissue, or bone marrow tissue. A mean of 833 (range 504-1010) line intercepts was counted per implant.
All estimates were counted at x250 magnification in randomly sampled fields of view in 100% of the ROI.
The spherically coated implants and the highly irregular synthetic bone graft granules were considered to be isotropic.
A single observer performed the histomorphometrical analysis. The intraobserver variation was determined as coefficients of variation (CV) on double measurements in one randomly selected implant from each treatment arm (Table 2).

Mechanical testing
Thawed specimens were tested to failure by axial push-out of the implant on a MTS Bionics Test Machine (Eden Prairie, MN, USA). The test was performed blinded and all specimens were evaluated in one session. The specimens were placed on a metal support jig with a 7.4-mm diameter central opening and under a 5.0 mm diameter cylindrical test probe. The implant was centralized over the opening, thereby assuring a distance of 0.7 mm between the implant and the support jig. The direction of loading was from the cortical surface inward. A preload of 0.5 N was applied to standardize contact conditions before initiating loading. The displacement rate was 5 mm/min with a 500 N load cell. Data points for every 10 µm of displacement were entered into an excel spreadsheet. The force-displacement curve and the mechanical parameters were calculated from the spreadsheet (Baas 2008).
The means of lengths and diameters of the specimens were 2.62 (2.28-2.99) mm and 5.76 (5.60-6.06) mm, respectively. The individual specimen length was used to normalize push-out parameters. Ultimate shear strength (Pa) was determined from the maximal force applied until failure of the bone-implant interface. Apparent stiffness (Pa/mm) was obtained from the slope of the linear section of the load-deformation curve. Energy absorption (J/m^2) was calculated from the area beneath the load-deformation curve until failure (Baas 2008, Soballe 1993).
One pair of samples had to be excluded from the mechanical test because one of the implants had been misplaced during surgery, and therefore, the superficial part (the part used for mechanical test) did not have bone coverage on a small part of the circumference.

Statistical analysis
Based on previous studies with the same model as in this study (Jakobsen, Kold 2007), the number of dogs needed to be included in this studies was estimated by the

formula for paired studies with normal distributed data: $N = (C_{2a} + C_b)^2 \times S^2/D^2$. With a difference between groups of 50% and standard deviation of 50%, n=8 was calculated. Though, it is wise to leave room for overestimation of the expected difference between groups and underestimation of standard deviation. In addition, a dog is sometimes lost because of rarely happening complication. Therefore we estimated that 10 dogs needed to be included in this study.
Statistical analysis was performed using Intercooled STATA 10.0 software (StataCorp LP, College Station, TX, USA). In this paired study, mechanical and histological data were not normally distributed. Therefore both sets of data were analyzed by the Wilcoxon signed-rank test for statistically significant differences between two groups. The data are presented as medians with 25% and 75% interquartile ranges and *P* value less than 0.05 was considered statistically significant.

Results

Histological results

The strontium doping of the hydroxyapatite (SrHA) bone graft extender (BGE) induced two statistically significant effects: volume of new bone in the gap was increased by 19%, and 5% more allograft was left in the gap (Figs.5-8). In regard to ongrowth onto the implants and the BGE material no difference was detected between the two treatment arms. But paired plots showed that the ongrowth onto both the implants and onto the BGE was improved for six out of the ten specimens pairs. Therefore the results were found inconclusive (Table 3, figs.5-6).
There was no difference in the volume of the SrHA (24.4%) compared to the HA (24.1%) (p=0.96) in the gap.

Mechanical results

No difference was detected between the two treatment arms. But paired plots showed that the total energy absorption was improved for seven out of the nine specimens pairs (Table 4). Therefore, the results were found inconclusive. The mechanical failure occurred in the graft-implant interface for all implants.

Discussion

Strontium-doped hydroxyapatite (SrHA) as a bone graft extender (BGE) improved bone ingrowth and prolonged the presences of the small remains of allograft. This was evident in this study of allograft mixed with hydroxyapatite (HA) with or without strontium doping as a BGE when used around a Ti implant. Additionally we found inconclusive results of the ongrowth onto the implants and BGE material as well as implant fixation.
Strontium was presumably released from the strontium hydroxyapatite (Christoffersen, Christoffersen 1997). Therefore strontium induced the effects observed.
Strontium is believed to simulate a homeostatic local hypercalcemia. The reason is that both strontium and calcium are believed to stimulate the calcium-sensing receptor, CaSR. The receptor is situated in the membrane of cells of the osteoblast cell line and affects RANKL production and signaling to osteoclasts (Brennan, Rybchyn 2009). With regard to osteoclasts, strontium is known to inhibit differentiation and may even induce apoptosis of osteoclasts, which in total reduces resorption of bone (Bonnelye, Chabadel 2008, Buehler, Chappuis 2001). Strontium is also known to enhance osteoblast proliferation and differentiation, which lead to a

larger pool of active osteoblasts and thus to an increase in new bone formation (Arlot, Jiang 2007, Canalis, Hott 1996).
In this study, these effects of SrHA and presumably the released strontium had two important consequences. Firstly, SrHA increased bone ingrowth toward the implant. Secondly, the resorption of the allograft was slightly delayed when mixed with SrHA. We chose BGE granules of 0.6-2.0 mm diameter, because that is gold standard for clinical settings (Hing 2005). Then during the mechanical push-out test, we noticed that the size of the bone graft extender granules (0.6mm – 2 mm) could be close to the full thickness of the specimen block. So a large granule of up to 2 mm diameter situated in near proximity of the implant would have weakened the mechanical property of the interface wrongfully compared to clinical settings. The issue of granule size may have caused an increase in variation of the data above the expected 50% entered in the initial power calculation. The coefficient of variance of the data was calculated to be 64% for SrHA and 93% for HA for the data of the total energy absorption. The high coefficient of variance has most likely contributed to the non-significant results of the mechanical test.
The main subjects of this study were the volume of allograft and new bone in gap after 4 weeks. Therefore we chose the systematic uniform random transverse sectioning technique combined with isotropic uniform random stereological design (SUR-IUR). The SUR-IUR offers unbiased volume density estimates, whereas volume density estimates by the practically modified vertical uniform random technique would be biased (Baas 2008). The surface density estimates of bone ongrowth onto the implants and BGE granules were also unbiased since both surfaces were isotropic.
Low mechanical properties of the synthetic bone graft are one of the disadvantages of this material. The low mechanical properties were not an issue in this study because we used solid precipitates of hydroxyapatites. The implant was fixated by osseointegration. So the results of the push-out test expressed the structural and functional connection of the implant to the host bone. Therefore ingrowth, ongrowth, and presence of graft material of any origin influenced the results of the push-out test. We found more ingrowth and less resorption of the allograft when allograft was mixed with SrHA. These findings correlates well with the literature of systemic strontium induces gain in bone mass which also leads to reduced risk of fractures in osteoporotic patients (O'Donnell, Cranney 2006, Reginster, Felsenberg 2008). The inconclusive results of the ongrowth onto the implant also led to the inconclusive results of the mechanical test in this study.

Conclusion

Ti alloy implants can become osseointegrated when surrounded by this specific bone graft extender of precipitated HA mixed with allograft. This allowed us to investigate whether strontium doping of the bone graft extender had any effect on the osseointegration of the implant. The new finding of this study is that strontium significantly regulates the mismatch of rapid allograft resorption and relatively slow new bone formation. Therefore strontium doping of bone graft extender can be beneficial when an allograft is used during hip replacement surgery. In addition we speculate that the effects of strontium doping can be extended to include improved ongrowth onto the implant. Ongrowth could perhaps become evident over a longer time period, higher number of treated individuals, or by strontium released for longer time. Then the full osseointegration would be improved also leading to improved implant fixation.

Acknowledgements
We thank laboratory technician Jane Pauli and Professor Jens Randel Nyengaard for their excellent help with the histomorphometrical analysis.

Conflicts of interest
Bone graft extender was donated unconditionally by Osteologix Aps and produced by Ass. Prof. Jens E.T. Andersersen, Institute of Chemistry, Danish Technical University, Denmark. Porous implant coating was donated unconditionally by DePuy Inc, Warsaw, USA.
P. Carl Petersens Foundation, DK, Danish Rheumatism Association, NIH AR42051, and The A.P. Moeller Foundation for Advancement of Medical Science, DK supported the work unconditionally.

Contributions of authors
Marianne T. Vestermark has formulated the scientific problem, planned the methodological design and the experiments, performed the experiments, interpreted the results, and written the manuscript.
Ellen-Margrethe Hauge has planned the methodological design, performed the experiments, interpreted the results, and written the manuscript.
Kjeld Soballe has planned the methodological design, interpreted the results, and written the manuscript.
Joan E. Bechtold has planned the methodological design, performed the experiments, interpreted the results, and written the manuscript.
Thomas Jakobsen has planned the methodological design, interpreted the results, and written the manuscript.
Jorgen Baas has formulated the scientific problem, planned the methodological design and the experiments, performed the experiments, interpreted the results, and written the manuscript.

Reference List

Arlot ME, Jiang Y, Genant HK, Zhao J, Burt-Pichat B, Roux JP, et al. Histomorphometric and mu-CT Analysis of Bone Biopsies from Postmenopausal Osteoporotic Women Treated with Strontium Ranelate. JBone MinerRes. 2007.

Aspenberg P, Astrand J. Bone allografts pretreated with a bisphosphonate are not resorbed. Acta Orthop Scand. 2002 Jan;73(1):20-3.

Baas J. Adjuvant therapies of bone graft around non-cemented experimental orthopedic implants stereological methods and experiments in dogs. Acta OrthopSuppl. 2008;79(330):1-43.

Bonnelye E, Chabadel A, Saltel F, Jurdic P. Dual effect of strontium ranelate: stimulation of osteoblast differentiation and inhibition of osteoclast formation and resorption in vitro. Bone. 2008;42(1):129-38.

Brennan TC, Rybchyn MS, Green W, Atwa S, Conigrave AD, Mason RS. Osteoblasts play key roles in the mechanisms of action of strontium ranelate. BrJPharmacol. [BPH305 pii ;10.1111/j.1476-5381.2009.00305.x doi]. 2009;157(7):1291-300.

Buehler J, Chappuis P, Saffar JL, Tsouderos Y, Vignery A. Strontium ranelate inhibits bone resorption while maintaining bone formation in alveolar bone in monkeys (Macaca fascicularis). Bone. 2001;29(2):176-9.

Canalis E, Hott M, Deloffre P, Tsouderos Y, Marie PJ. The divalent strontium salt S12911 enhances bone cell replication and bone formation in vitro. Bone. 1996;18(6):517-23.

Christoffersen J, Christoffersen MR, Kolthoff N, Barenholdt O. Effects of strontium ions on growth and dissolution of hydroxyapatite and on bone mineral detection. Bone. 1997;20(1):47-54.

Erben RG. Embedding of bone samples in methylmethacrylate: an improved method suitable for bone histomorphometry, histochemistry, and immunohistochemistry. JHistochemCytochem. 1997;45(2):307-13.

Fellah BH, Gauthier O, Weiss P, Chappard D, Layrolle P. Osteogenicity of biphasic calcium phosphate ceramics and bone autograft in a goat model. Biomaterials. [S0142-9612(07)00966-0 pii ;10.1016/j.biomaterials.2007.11.034 doi]. 2008;29(9):1177-88.

Hannink G, Schreurs BW, Buma P. No positive effects of OP-1 device on the incorporation of impacted graft materials after 8 weeks: a bone chamber study in goats. Acta Orthop. [783547437 pii ;10.1080/17453670710014211 doi]. 2007;78(4):551-8.

Hennig A. [Capacity of a surface made of villi and papilli.]. Mikroskopie. 1956;11(7-8):206-13.

Hing K. Bioceramic Bone Graft Substitutes: Influence of Porosity and Chemistry. International Journal of Applied Ceramic Technology. 2005;2(3):184-99.

Jakobsen T, Kold S, Bechtold JE, Elmengaard B, Soballe K. Local alendronate increases fixation of implants inserted with bone compaction: 12-week canine study. JOrthopRes. 2007;25(4):432-41.

Kumta PN, Sfeir C, Lee DH, Olton D, Choi D. Nanostructured calcium phosphates for biomedical applications: novel synthesis and characterization. Acta Biomater. [S1742-7061(04)00013-3 pii ;10.1016/j.actbio.2004.09.008 doi]. 2005;1(1):65-83.

Lie SA, Havelin LI, Furnes ON, Engesaeter LB, Vollset SE. Failure rates for 4762 revision total hip arthroplasties in the Norwegian Arthroplasty Register. JBone Joint SurgBr. 2004;86(4):504-9.

Marie PJ, Hott M, Modrowski D, De Pollak C, Guillemain J, Deloffre P, et al. An uncoupling agent containing strontium prevents bone loss by depressing bone resorption and maintaining bone formation in estrogen-deficient rats. J Bone Miner Res. 1993 May;8(5):607-15.

O'Donnell S, Cranney A, Wells GA, Adachi JD, Reginster JY. Strontium ranelate for preventing and treating postmenopausal osteoporosis. CochraneDatabaseSystRev. [10.1002/14651858.CD005326.pub3 doi]. 2006(4):CD005326.

Pedersen AB, Johnsen SP, Overgaard S, Soballe K, Sorensen HT, Lucht U. Total hip arthroplasty in Denmark: incidence of primary operations and revisions during 1996-2002 and estimated future demands. Acta Orthop. 2005;76(2):182-9.

Reginster JY, Felsenberg D, Boonen S, Diez-Perez A, Rizzoli R, Brandi ML, et al. Effects of long-term strontium ranelate treatment on the risk of nonvertebral and vertebral fractures in postmenopausal osteoporosis: Results of a five-year, randomized, placebo-controlled trial. Arthritis Rheum. [10.1002/art.23461 doi]. 2008;58(6):1687-95.

Soballe K. Hydroxyapatite ceramic coating for bone implant fixation. Mechanical and histological studies in dogs. Acta OrthopScandSuppl. 1993;255:1-58.

Tian M, Chen F, Song W, Song Y, Chen Y, Wan C, et al. In vivo study of porous strontium-doped calcium polyphosphate scaffolds for bone substitute applications. JMaterSciMaterMed. [10.1007/s10856-009-3713-5 doi]. 2009;20(7):1505-12.

Xue W, Hosick HL, Bandyopadhyay A, Bose S, Ding C, Luk KDK, et al. Preparation and cell-materials interactions of plasma sprayed strontium-containing hydroxyapatite coating. Surface & coatings technology. 2007;201:4685-93.

Tables and figures

Table 1: Chemical formula for SrHA and HA.

	Chemical formula
SrHA	$Ca_{9.411}Sr_{0.589}(PO_4)_6(OH)_2$
HA	$Ca_{10}(PO_4)_6(OH)_2$

Table 2: Coefficient of variation for all counted parameters.

Coefficient of Variance	New Bone	Allograft	Fibrous Tissue	BGE
Ingrowth	8.7%	18%	72%	11%
Ongrowth onto implant	15%	0.0%	9%	101%
Ongrowth onto BGE	3.7%	0.0%	53%	NA

Table 3: Ongrowth onto implants and BGE. Histomorphometrical results of surface densities of the implant and BGE presented as median values in per cent with 25 % and 75 % interquartile range in parentheses.

	Surface densities fraction of tissue, %			
Ongrowth onto implant	New bone	Allograft	Fibrous Tissue	BGE
SrHA	17a (9.8-18)	0 (0-0)	26 (8.1-38)	0.5 (0.3-0.7)
HA	14a (7-17)	0 (0-0)	26 (3.3-53)	1.1 (0.4-14)
Ongrowth onto BGE				
SrHA	34b (32-36)	0 (0-0)	1.9c (0.6-2.4)	NA
HA	24b (19-37)	0 (0-0)	2.9c (0.4-4.5)	NA

a: p=0.28
b: p=0.07
c: p=0.48

Table 4: Results of the mechanical push-out test presented as median values with 25 % and 75 % interquartile range in parentheses.

	Ultimate Shear Strength, [MPa]	Apparent Shear Stiffness, [MPa/mm]	Total Energy Absorption, [kJ/m^2]
SrHA	1.7 (1.3-3.4)	9.5 (5.9-15)	350 (193-588)
HA	1.2 (0.98-3.0)	8 (7.4-18)	157 (113-413)
	P=0.68	p=0.44	p=0.09

Figure 1: Position of the cylindrical implant with mounted end screws in the proximal humerus with a surrounding 2.5-mm gap filled with allograft mixed with HA or SrHA.

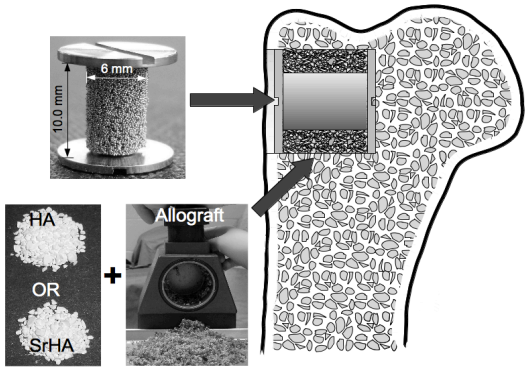

Figure 2: 6% w/w SrHA was determined by XRPD.

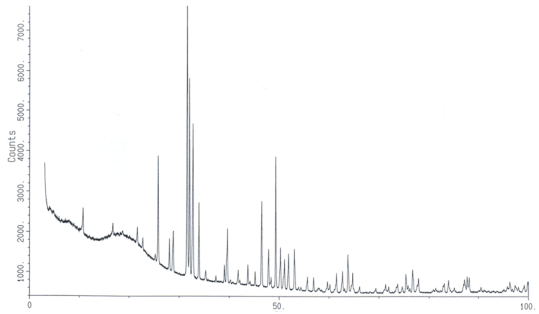

Figure 3: Preparation of the specimens and the transverse cutting method for the histomorphometrical analysis.

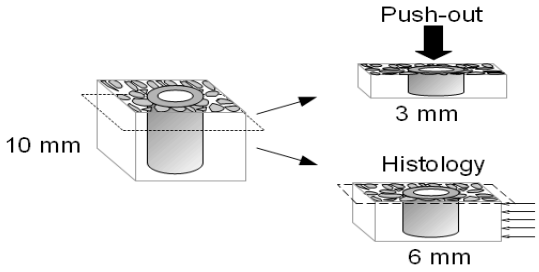

Figure 4: Manually drawn region of interest (ROI) 2.25 mm from implant surface, shown by the circle. BGE, implant with porous coating of beads. The dashed lined circle shows the approximate position of the drill hole.1.25 x objective.

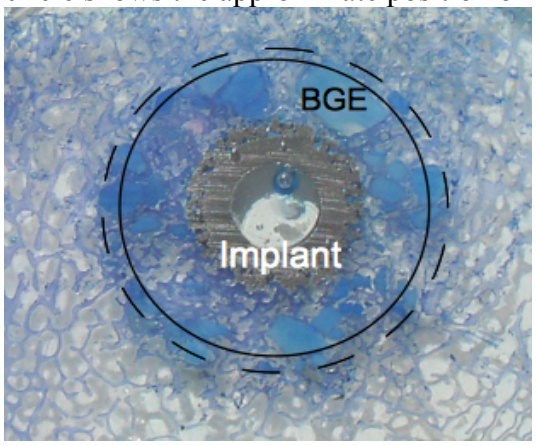

Figure 5: The implant-bone interface showing bone ingrowth and ongrowth onto the implant and SrHA. New bone (N), preserved allograft (A), ongrowth onto the implant (thin arrow), and ongrowth onto the SrHA (thick arrow). x10 objective.

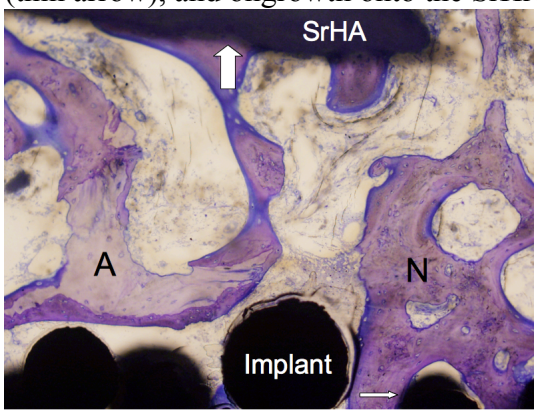

Figure 6: The implant-bone interface showing bone ingrowth and ongrowth onto the implant and HA. New bone (N), preserved allograft (A), ongrowth on implant (thin arrow), and ongrowth on HA (thick arrow). x10 objective.

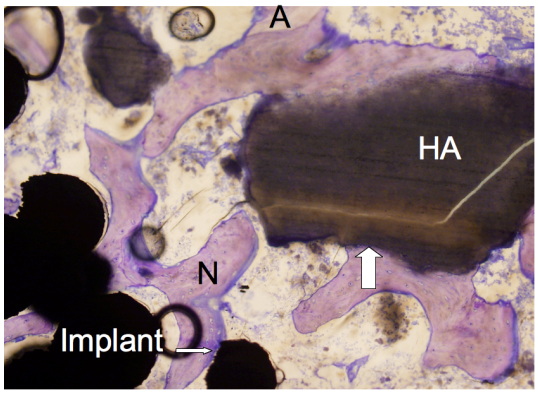

Figure 7: Paired plot of bone ingrowth.

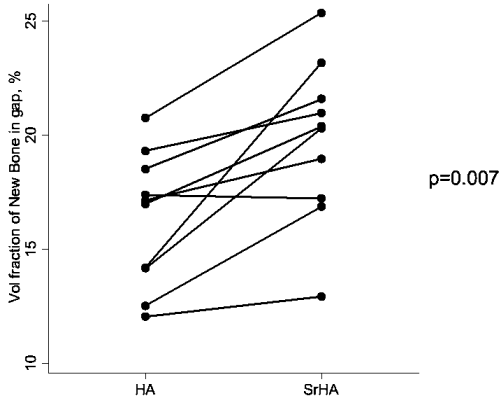

Figure 8: Paired plot of preserved allograft.

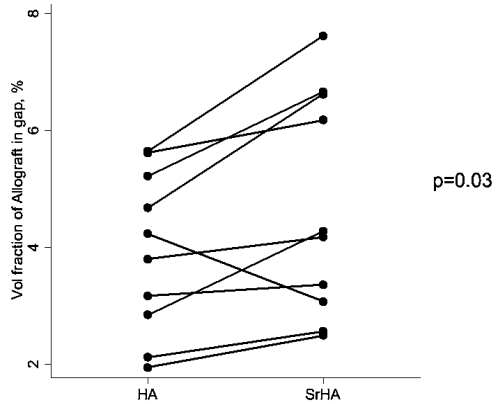

3) Grit-blasting of Titanium Implants Affects Structure and in vivo Performance of Strontium-substituted Bioactive Glass Coating

Marianne T. Vestermark[a], Delia S. Brauer[b], Kjeld Soballe[a], Thomas Jakobsen[a], Ellen-Margrethe Hauge[c], Joan E. Bechtold[d], and Jorgen Baas[a]

[a] Orthopaedic Research Lab., Department of Orthopedic Surgery, Aarhus University Hospital, Norrebrogade 44, Building 1A, DK-8000 Aarhus C, Denmark. marianne.t@vestermark.dk; kjeld@soballe.com; thomas.jakobsen@ki.au.dk; baas@ki.au.dk
[b] Department of Materials, Royal School of Mines, Imperial College London, Exhibition Road,
London SW7 2AZ, England. d.brauer@qmul.ac.uk
[c] Research Unit for Rheumatology and Bone Biology, Aarhus University Hospital, Denmark. ellen.hauge@ki.au.dk
[d] Orthopedic Biomechanics Lab, Excelen Center for Bone and Joint Research and Education, Minneapolis Medical Research Foundation, Minneapolis, MN, USA. bechtold@umn.edu

Corresponding author:
Marianne T. Vestermark
Drejovej 30, DK-8370 Hadsten, Denmark
E-mail: marianne.t@vestermark.dk
Phone: +4551907447; fax: +4589494150

Abstract:
The purpose of this experimental study was two-fold. Firstly, to improve early fixation and osseointegration of grit-blasted titanium alloy (Ti6Al4V) implants by coating them with bioactive phosphosilicate (SiO_2-Na_2O-CaO-SrO-K_2O-MgO-ZnO-P_2O_5) glass. Secondly, to further improve fixation and osseointegration by increasing the strontium content of the glass. Three bioactive glass compositions were prepared by replacing 0%, 10%, and 50% of the calcium oxide in the glass with strontium oxide.
Four experimental implants were inserted with one mm concentric gap into the humeri of 10 dogs. Implants were coated with one of the three different glass compositions or with plasma-sprayed HA (hydroxyapatite) as a control. Mechanical implant fixation was evaluated by push-out test, and osseointegration was evaluated by descriptive and quantitative histomorphometry.
Implant fixation did not improved with any of the three bioactive glass coatings compared with HA coating. This was evidenced by a lack of mechanical fixation and osseointegration of the glass-coated implants. Unexpectedly, the glass material showed reduced solubility. Raman analysis suggested the existence of aluminum contamination of the glass coatings, which most likely originated from the Al_2O_3 grit-blasting powder. We were therefore unable to evaluate whether fixation and osseointegration could be improved by increasing the strontium content of the glass.

Keywords: bioactive glass, grit-blasting, osseointegration, titanium, in vivo

1. Introduction

Primary total hip prostheses are revised by approximately 10% over 10 years mainly because of painful aseptic loosening of the implant. The rate is likely to increase because patients receive their first prosthesis at younger age and stay physically active for longer.[1] This issue therefore needs further investigation to improve prognosis of hip prostheses.

Early implant osseointegration and fixation are important for the longevity of the implants, which is shown in roentgen stereological analysis studies. [2, 3] One reason is that rapid osseointegration will stabilize the implant and seal off the bone-implant interface from wear particles in the joint fluid.

One way to improve early osseointegration could be by coating the implant with bioactive glass. Commercially, bioactive glass particles such as Biogran® are successfully used for rapid healing of odontological critical bone defects.[4] Orthopedic implants coated with bioactive glass, on the other hand, are not yet available commercially. One reason is the challenges of matching the thermal expansion coefficient (TEC) of the two implant materials, Ti6Al4V alloy implant core and the bioactive glass coating, while still maintaining the bioactive properties of the glass.[5, 6] Mismatch in TEC courses delamination of the implant-glass interface. In glass, strontium can modify the TEC, increase solubility, and increase the apatite formation induced by the bioactive glasses. Thus increasing the strontium content should increase the osteoproductive properties of glass.[6-8]

Additionally, strontium, as strontiumranelate, is known to have both anabolic and anti-catabolic effects in bone.[9, 10] These actions result in an overall gain of bone mass with improved architecture and a reduced risk of fractures in osteoporotic patients.[11]

We hypothesized that (1) the bioactive glass coating would improve implant fixation and osseointegration and (2) fixation and osseointegration would be further improved by strontium substitution of the bioactive glass coating compared with a hydroxyapatite (HA) coating in a dose-dependent manner. Implant fixation was determined by mechanical push-out and substantiated by histomorphometry of the osseointegration.

2. Method and Materials

2.1. Design

With approval of our Institutional Animal Care and Use Committee, we tested the hypotheses in a four arm paired study in 10 American Foxhounds (mean age 14.3 months, mean weight of 22.2 kg). NIH guidelines for care and use of laboratory animals (NIH Publication #85-23 Rev. 1985) were observed. The four arms of the study consisted of the coatings described below Sr0, Sr10, Sr50, and HA (control). The implants were inserted into the cancellous bone of the metaphysis of the humerus (Fig.1). Positioning of the implants in each group was alternated systematically with a random start. In one dog an adverse reaction toward HA coating was found. Mechanically the implant was not fixated and histological a dense fibrous membrane surrounded the HA-coated implant. Why the dog reacted to the HA coating this way is not clear, but no signs of infection were observed. So we decided to keep the dog in the study.

2.2. Implants

The cylindrical implant cores were made of ASTM-136 Ti6Al4V, grit-blasted (Plasma Biotal Ltd, North Derbyshire, UK), then cleaned in ethanol and acetone prior to coating with bioactive glass. The coated implant diameter was 5.98 mm (range 5.91-6.07mm) and the height 10.0 mm. To the bottom and top, a Ti6Al4V screw, 8.0 mm in diameter, was attached and ensured, on average, a 1.02-mm concentric gap around the implant

2.3. Bioactive glass

BioCeramic Therapeutics Ltd., London, UK produced the strontium substituted glass powder and performed the dip coating. The bioactive glasses in the system SiO_2-Na_2O-CaO-SrO-K_2O-MgO-ZnO-P_2O_5 were produced by a melt-quench route. In the glass 0%, 10%, and 50% of the calcium oxide was replaced by strontium oxide, and the compositions are referred to as Sr0, Sr10, and Sr50 (Table 1). The production and the technical specifications of the glass are described in the study by Lotfibakhshaiesh et al..[6]

2.4. Coatings

8.0 g poly(methylmethacrylate) (PMMA) was dissolved in 400 mL chloroform. Then 8.0 g of the glass powder (particle size of 38 µm) was dispersed in 20 mL of PMMA solution. While the dispersion was stirred, the Ti alloy implants were dipped into the glass PMMA dispersion and then kept at room temperature for the chloroform to evaporate. The dipping was repeated four times to produce a 100-µm coating, because a 100-µm thick coating was expected to degrade in 2 to 3 weeks, based on previous unpublished work in rabbits. The coated implants were heated in a dental porcelain furnace. During this sintering process, a temperature of 420°C and a 90 kPa vacuum was maintained for 30 min for the PMMA to depolymerize and the monomer to evaporate. The implants were then heated to 750°C and held at that temperature for 30 min to allow for the glass particles to sinter into one cohesive glass coating. Directly after the heating cycle in the furnace, the implants were wrapped individually under sterile conditions.

The HA vacuum plasma spray-coated control samples were comparable with commercially available HA-coated prosthesis, since coating was performed by Plasma Biotal Ltd, North Derbyshire, UK, and the HA coated implants were gamma-sterilized prior to surgery.

2.5. Surgical procedure

Surgery was conducted under sterile conditions, and under general anesthesia. A 7-cm long skin incision was made with cautery on the lateral proximal humerus. The deltoid muscle was bluntly dissected to expose the humerus. A 2.5-mm guide wire was inserted anterolaterally into the humerus at the level of the greater tubercle and oriented perpendicular to the surface. Another 2.5-mm guide wire was inserted 17 mm distally and parallel to the first. With a cannulated drill (∅ 8.0mm) a 12-mm cavity was drilled over the guide wires at a maximum speed of two rotations per second. The edge of the hole was trimmed, and the cavity irrigated with 10 ml saline for removal of periosteum and loose bone chips.

One implant was inserted into each cavity, and after securing hemostasis, the soft tissue was closed in layers. This procedure was repeated for the opposite humerus, where the implants of the other to treatment arms were inserted..

The dogs were given ceftriaxone (1 g, i.v) and buprenorphine hydrochloride (0.0075 mg/kg/day, i.m) administered immediately before surgery and 3 days postoperatively.

The observation period was uneventful. All animals were fully mobilized within 2 to 3 days, and there were no clinical signs of infection. The dogs were given 30 mg/kg tetracycline i.m. day 18 and 20 mg/kg calcein i.v. day 25, for fluorochrome labeling of the mineralization front. After 28 days, the dogs were sedated and killed with an overdose of hyper-saturated barbiturate.

2.6. Preparation of specimens

The proximal humeri were retrieved *en bloc*, immediately frozen, and stored at -20°C. Using a water-cooled wheel diamond saw, the implants with surrounding bone were cut transversely to yield a 3.5 mm thick outermost part of the implant-bone specimen, which was stored at -20°C for mechanical testing, and a 5.5 mm thick innermost part of the implant-bone specimen for histomorphometrical analysis.

2.7. Mechanical testing

Thawed specimens were tested to failure by axial push-out of the implant on an MTS Bionics Test Machine. The test was performed blinded, and all specimens were evaluated in one session. The specimens were placed on a metal support jig with a 7.4-mm diameter central opening under a cylindrical test probe of 5.0 mm in diameter. The implant was centralized over the opening thereby assuring a distance of 0.7 mm between the implant and the support jig. The direction of loading was from the cortical surface inward. A preload of 0.5 N was applied to standardize contact conditions before initiating loading. The displacement rate was 5 mm/min, with a 500 N load cell. Data points for every 10 μm of displacement were entered into a spreadsheet, and calculations of the mechanical parameters were autogenerated.[12] Push-out parameters were normalized in accordance with the estimated surface area based on length and diameter measurements of each specimen.[13] Ultimate shear strength (Pa) was determined from the maximal force applied until failure of the bone-implant interface. Apparent stiffness (Pa/mm) was obtained from the slope of the linear section of the load-deformation curve. Energy absorption (J/m^2) was calculated from the area beneath the load-deformation curve until failure.

2.8. Histomorphometry

The specimens were fixated and dehydrated in graded ethanol (70-100%) prior to cold PMMA embedding.[14] Using a vertical sectioning technique, each specimen was cut into four 30-mm thick histological sections with a microtome[15] (Fig. 2). The sections were surface stained with Toluidine blue, pH 7. Tissue classification was based on morphology, and new bone was characterized as a disorganized and dense substance with embedded cells. When these characteristics were not present, the tissue was considered non-mineralized tissue.

The implant osseointegration were divided in two: gap healing and ongrowth. Gap healing and ongrowth were estimated in a region of interest (RIO) as volume and surface area fraction densities respectively. The volume and surface area fraction densities were estimated by blinded histomorphometry using an image analysis system (NewCAST 2.0; VisioPharm, Hoersholm, Denmark). *Gap healing* was defined as the volume of new bone, so every grid point was counted as either new bone or non-mineralized tissue for a mean of 314 (range 266-398) points per implant. *Ongrowth* was defined as new bone in contact with the implant surface. Intersections between the implant surface and sine-weighted gridlines were counted as either new bone or non-mineralized tissue for a mean of 145 (114-258) line intercepts per

implant. All parameters were estimated at ×250 magnification in random sampled fields of view in 100% of the ROI.
Because the glass-coated implants were poorly osseointegration, shrinkage of the tissue occurred during the embedding process. Therefore the tissue was only differentiating into mineralized tissue (new bone) or non-mineralized tissue, and the counted at the position where it was observed. Displacement of tissue during shrinkage may have caused bone in contact with implant to be detected as bone in the gap. But even if all volume of bone in the gap were counted as ongrowth, then HA-coated implants would still show a significantly higher ongrowth ($p<0.01$). Therefore the issue of shrinkage had no influence on the results of this study.
The described techniques and preparation of specimens, together with the stereological software, made it possible to obtain highly reliable estimates with negligible bias.[12]
The ROI was manually drawn from the implant surface and 750 μm into the peri-implantary gap. At the top and bottom of the implant, 300 μm were excluded because of cutting artifacts and disruption by the screw at the end.
Double measurements on the quantitative histomorphometry were performed on one random implant from each group to determine the precision of the estimates. The intraobserver coefficients of variation (CVs) for "new bone" and "non-mineralized tissue" were 2% and 17.4% for bone volume fractions, respectively, and 0.8% for non-mineralized tissue in contact with implant, whereas CVs for bone-implant contact could not be determined because of the many zero values for the implants coated with any of the three types of bioactive glass.

2.9. Raman spectroscopy

The structure of glass as powder and coatings was investigated using Raman spectroscopy at Raman shifts between 300 and 1100 cm^{-1} (Renishaw RM 2000 connected to Leica Microscope with 50 x objective) to detect whether any crystallization had occurred during the firing process.

3. Statistical analysis

Statistical analysis was performed using Intercooled STATA 10.0 software. The histological and mechanical data in this 4 arms study were not normal distributed. Therefore they were analyzed by Friedman repeated measures analysis of variance on ranks. When a statistically significant difference within the groups was detected, then Wilcoxon-signed-rank test was used to identify the specific differences between two groups. The data are presented as medians with 25% and 75% interquartile ranges, and p values less than 0.05 were considered statistically significant.

4. Results

4.1. Mechanical testing

During mechanical testing, none of the implants in the three groups coated with bioactive glass were able to withstand the preload of 0.5 N, which initiated the data acquisition for the mechanical test. Therefore, the values for strength, total energy absorption, and stiffness were all assigned zero (See Table 2 for results).
The control group of HA-coated implants performed significantly better compared with all three intervention groups in terms of strength, total energy absorption, and stiffness ($p<0.006$, Wilcoxon-signed-rank test).

4.2. Histomorphometrical evaluation
The bioactive glass coating only induced a sparse gap healing and no ongrowth was detected. The HA coating was significantly superior on both parameters (Figs. 3 & 4).

4.3. Descriptive histomorphology
HA: The interface and gap surrounding the HA-coated implants were comparable to normal cancellous bone (i.e. connecting trabeculae from the HA and beyond the drill hole) (Fig.5). Less than 10% fibrous tissue was observed.
Bioactive glass: Unexpectedly, residue of the bioactive glass coating was observed, which typically measured 50 µm and ranged between 0 and 95µm. No variation in thickness and position on implant was observed between the three groups. For all implants, the glass material was in close contact with titanium and had not delaminated.
An unusual homogeneous substance was seen mainly between 100-400 µm from the bioactive glass coating. The substance could be divided into three types, the third type being similar to mineralized woven bone. Type 1 consisted of a homogeneous acellular substance, which in polarized light showed accumulation of disorganized collagen fibers Type 1 was present in a large amount. Type 2 was less abundantly present and quite similar to type 1 apart from the few, embedded osteoblast-like cells in the substance. Type 3 consisted of small amounts of mineralized woven bone with osteocyte-like cells embedded. This third, mineralized type was mainly observed in close proximity the cellular substance of type 2 (Fig.6). In ultraviolet light most of the areas of mineralized woven bone fluorescenced green (Fig.7). The substances were observed in loose fibrous connective tissue situated in approximately half of the extent of the bone-implant interface of every implant. In the remaining half of the interface of every implant, a very dense fibrous membrane was seen with hardly any of the homogenous substance (Fig. 8).
Neither extraordinarily wide osteoid seams nor excessive coverage of trabecular surfaces with osteoid was observed. Thus mineralization defects was not present.

4.4. Raman spectroscopy
Fig. 9 shows Raman spectra of (1) glass powder, (2) sintered glass coating on non-grit blasted Ti6Al4V alloy, and (3) sintered glass coating on a grit-blasted Ti6Al4V alloy implant. Glass powder and the sintered glass coating on non-grit blasted implant show typical amorphous patterns. On the contrary, in the spectra of the sintered glass coating on the grit-blasted implant peaks are present, which suggest the presence of crystalline phases. Comparison with reference spectra of gahnite ($ZnAl_2O_4$), geikieliete ($MgTiO_3$), magnesiocoulsonite (MgV_2O_4), and spinel suggests that the peaks were caused by a spinel-type phase of the formula MX_2O_4. Where M is a divalent cation such as zinc or magnesium and X is an ion such as vanadium or aluminum (Al).

5. Discussion
Bioactive phosphosilicate-glass coatings with strontium substitution on grit-blasted Ti6Al4V alloy implants were studied in regard to implant fixation and osseointegration. Contrary to our first hypothesis, neither osseointegration nor fixation of the implant was improved by the bioactive glass coating compared with the HA-coated implants. The bioactive glass coating failed. This was evidenced by a lack of mechanical fixation and osseointegration of the bioactive glass coated implants. We were therefore unable to test the second hypothesis whether strontium

substitution of the glass coating improved fixation and osseointegration of the implant.
The results of the study were unexpected because the bioactive glass coatings performed poorly regardless of the level of strontium substitution. The reasons for this can be many, but all are because of the chemical properties of the glass coatings. The glass coatings were not osteoproductive as intended. The chemical properties could have changed due to an unintended addition of aluminum (Al) from the Al_2O_3 particles used for grit blasting. Another reason could be that when the TEC of the glass and Ti alloy were matched then the structure of the glass changed from amorphous to crystalline. But this later theory seems unlikely because the glass coatings on smooth Ti alloy were found amorphous by XRPD.[6]
Al incorporated into a bioactive glass has two effects. Firstly, Al is an intermediate oxide because it can act either as a network modifier or a network former in the glass structure, because Al^{3+} can enter the actual silicate network.[16] In the property of network former Al induces formation of Si-O-Al bonds and forms $(AlO_4)^-$ tetrahedral. Then cations such as Na^+, K^+, or ½ Ca^{2+} are needed to achieve charge balance. This causes cross-linking of the network by reducing the number of non-bridging oxygen ions, resulting in a more polymerized glass network with reduced degradability and bioactivity. Raman spectroscopy indicated the presence of Al-containing crystal phases in the glass coatings. Which suggested that the glass coatings had undergone significant, unintended structural changes (Al-incorporation and at least partial crystallization) during the sintering process. The changes resulted in a decreased solubility and thus a decreased bioactivity of the coating. Therefore, it seems most likely that the unexpected change in chemical properties and degradability of the glass was because of Al contamination of the glass.
Secondly, Al is also known to cause mineralization defects during new bone formation.[17] Mineralization defect was not found in this study. The reason could be that only the innermost half of the glass, which had not dissolved, contained Al at deleterious amounts. But the exact same Al amount prevented the glass from dissolving. Therefore, Al was not released in amounts that could cause mineralization defects.
Remnants of Al_2O_3 from the grit blasting of the Ti6Al4V cylinders would in theory not contaminate the HA coatings. Because the HA coating was done by vacuum plasma spray rather than sintering (i.e. heat treatment at 750°C for 30 min) and therefore a reaction between HA and Al_2O_3 would only occur at the interface between the materials and not throughout the coating.
The homogenous substance observed could be the earlier and later stages of the reaction layers, a substance usually seen in connection with bioactive glass,[8, 18] The two stages being represented by the collagen-rich, non-mineralized type 1 and 2 and green fluorescing, calcein-coupled mineralization type 3, respectively. The location and amount of the homogenous substance varied. These variations could reflect an inhomogeneity of the Al-contamination and the subsequent inhomogeneous chemical composition and properties of the glass. Lopez-Sastre et al. have previously found poor osseointegration of bioactive glass-coated grit-blasted Ti alloy implants. [19, 20]

6. Conclusion

We were unable to assess whether or not strontium substitution of the glass had any effect on implant osseointegration and subsequent fixation because the glass coatings were insufficient for achieving osseointegration. The cause of this is unknown, but

aluminum contamination during processing is the most likely cause. And our results therefore suggest that pretreatment of Ti6Al4V alloy by grit-blasting with Al_2O_3 particles can have unfavorable effects on the composition, structure, and properties of sintered glass coatings. Future studies should be: firstly of this bioactive glass to investigate the in vitro and in vivo effects of avoiding grit blasting before coating, using silica or other Al-free particles rather than alumina for grit blasting, or cleaning the surface after grit blasting using *e.g*. hydrofluoric acid prior to glass coating of the implants. Secondly, to develop glasses with higher bioactivity, by increasing the phosphorous content on behalf of the silica content and keeping the network connectivity around two. Thirdly, to investigate a coating technique, which minimize substrate-glass interactions but provide a good bond, like vacuum plasma-spray.

7. Acknowledgements:
We wish to thank Dr Matthew D. O'Donnell, BioCeramic Therapeutics Ltd., for the Raman spectroscopy measurements.

8. Role of the funding source
Implant coating along with institutional research support was provided unconditionally by BioCeramics Therapeutics Ltd., UK, who had no other role in the work of this study.
P. Carl Petersens Foundation, Aarhus University, Danish Rheumatism Assn., NIH AR42051, and The A.P. Moeller Foundation for Advancement of Medical Science financially supported this work and had no role in the work of this study.

Reference List

[1] Pedersen AB, Johnsen SP, Overgaard S, Soballe K, Sorensen HT, Lucht U. Total hip arthroplasty in Denmark: incidence of primary operations and revisions during 1996-2002 and estimated future demands. Acta Orthop 2005;76:182-9.
[2] Ryd L, Albrektsson BE, Carlsson L, Dansgard F, Herberts P, Lindstrand A, et al. Roentgen stereophotogrammetric analysis as a predictor of mechanical loosening of knee prostheses. JBone Joint SurgBr 1995;77:377-83.
[3] Karrholm J, Snorrason F. Subsidence, tip, and hump micromovements of noncoated ribbed femoral prostheses. ClinOrthopRelat Res 1993:50-60.
[4] Schepers EJ, Ducheyne P, Barbier L, Schepers S. Bioactive glass particles of narrow size range: a new material for the repair of bone defects. ImplantDent 1993;2:151-6.
[5] Pazo A, Saiz E, Tomsia AP. Silicate glass coating on Ti-based implants. Acta Materialia 1998;46:2551-8.
[6] Lotfibakhshaiesh N, Brauer DS, Hill RG. Bioactive glass engineered coatings for Ti6Al4V alloys: Influence of strontium substitution for calcium on sintering behaviour. Journal of Non-Crystalline Solids; 2009.
[7] O'Donnell MD, Hill RG. Influence of strontium and the importance of glass chemistry and structure when designing bioactive glasses for bone regeneration. Acta Biomater 2010.
[8] Hench LL, Xynos ID, Polak JM. Bioactive glasses for in situ tissue regeneration. JBiomaterSciPolymEd 2004;15:543-62.
[9] Arlot ME, Jiang Y, Genant HK, Zhao J, Burt-Pichat B, Roux JP, et al. Histomorphometric and mu-CT Analysis of Bone Biopsies from Postmenopausal Osteoporotic Women Treated with Strontium Ranelate. JBone MinerRes 2007.

[10] Marie PJ, Hott M, Modrowski D, De Pollak C, Guillemain J, Deloffre P, et al. An uncoupling agent containing strontium prevents bone loss by depressing bone resorption and maintaining bone formation in estrogen-deficient rats. J Bone Miner Res 1993;8:607-15.
[11] O'Donnell S, Cranney A, Wells GA, Adachi JD, Reginster JY. Strontium ranelate for preventing and treating postmenopausal osteoporosis. CochraneDatabaseSystRev 2006:CD005326.
[12] Baas J. Adjuvant therapies of bone graft around non-cemented experimental orthopedic implants stereological methods and experiments in dogs. Acta OrthopSuppl 2008;79:1-43.
[13] Soballe K. Hydroxyapatite ceramic coating for bone implant fixation. Mechanical and histological studies in dogs. Acta OrthopScandSuppl 1993;255:1-58.
[14] Erben RG. Embedding of bone samples in methylmethacrylate: an improved method suitable for bone histomorphometry, histochemistry, and immunohistochemistry. JHistochemCytochem 1997;45:307-13.
[15] Baddeley AJ, Gundersen HJ, Cruz-Orive LM. Estimation of surface area from vertical sections. JMicrosc 1986;142:259-76.
[16] Vogel W. Glass Chemistry. Springer.
[17] Blades MC, Moore DP, Revell PA, Hill R. In vivo skeletal response and biomechanical assessment of two novel polyalkenoate cements following femoral implantation in the female New Zealand White rabbit. JMaterSciMaterMed 1998;9:701-6.
[18] Oonishi H, Hench LL, Wilson J, Sugihara F, Tsuji E, Matsuura M, et al. Quantitative comparison of bone growth behavior in granules of Bioglass, A-W glass-ceramic, and hydroxyapatite. JBiomedMaterRes 2000;51:37-46.
[19] Kitsugi T, Nakamura T, Oka M, Senaha Y, Goto T, Shibuya T. Bone-bonding behavior of plasma-sprayed coatings of BioglassR, AW-glass ceramic, and tricalcium phosphate on titanium alloy. JBiomedMaterRes 1996;30:261-9.
[20] Lopez-Sastre S, Gonzalo-Orden JM, Altonaga JA, Altonaga JR, Orden MA. Coating titanium implants with bioglass and with hydroxyapatite. A comparative study in sheep. IntOrthop 1998;22:380-3.

Figures and tables

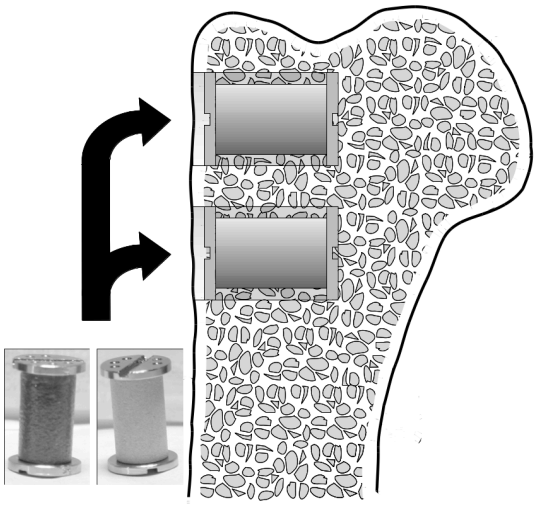

Figure 1: Strontium-substituted glass was expected to be highly soluble and large amounts of strontium would be released. Therefore, the implants coated with Sr10- and Sr50-substituted glass were positioned next to each other as were the implants coated with Sr0-substituted glass and HA. The positioning of Sr0 (left) and HA (right) is shown above.

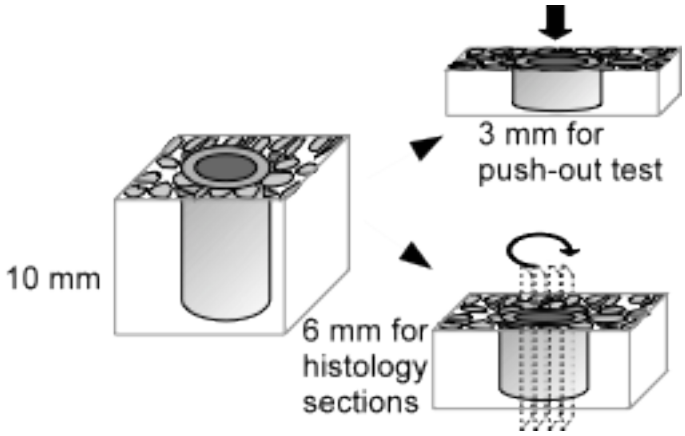

Figure 2: Preparation of the specimens into blocks for histological sectioning according to the Vertical Uniform Random method and for mechanical push-out test.

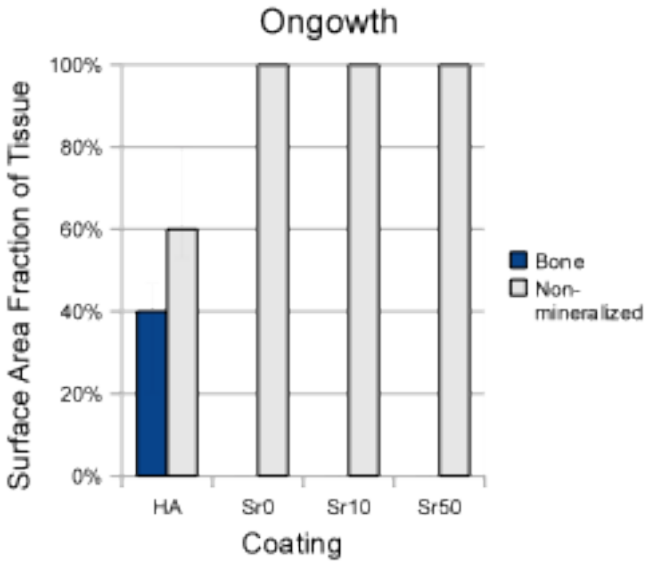

Figure 3: The relative amounts (%) of bone and non-mineralized tissue in the gap. (p<0.013 for Sr0 and Sr50, and p<0.007 for Sr10).

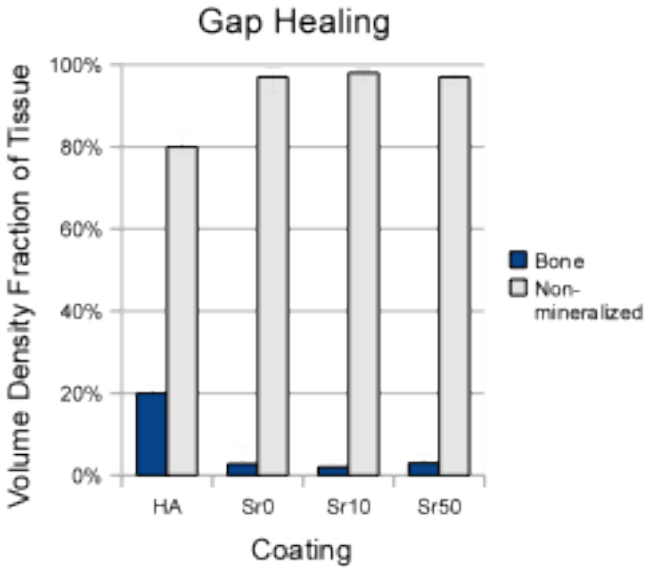

Figure 4: The relative amounts (%) of bone and non-mineralized tissue in contact with the coating (p<0.005).

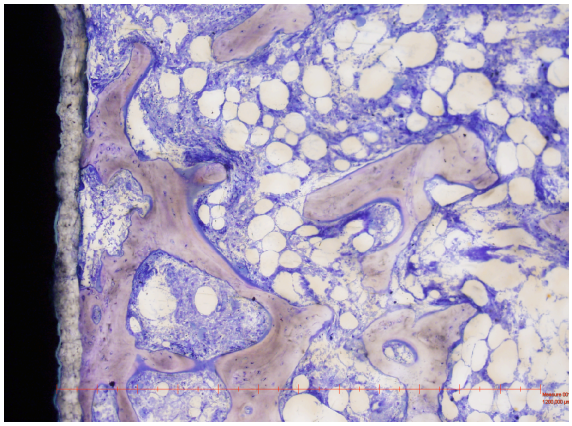

Figure 5: A HA-coated implant with a high amount of bone in the interface both as ongrowth and healing of gap. Toluidine blue, pH 7, x250 magnification.

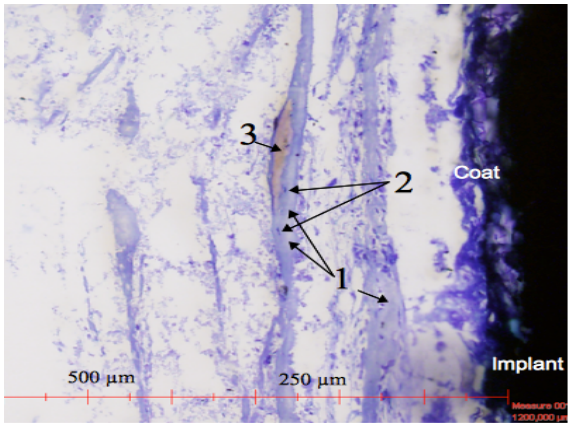

Figure 6: Sr0 bioactive glass-coated implant. In the interface, several areas of homogenous substance of types 1, 2 and 3 are seen. Toluidine blue, pH 7, 250 x magnification.

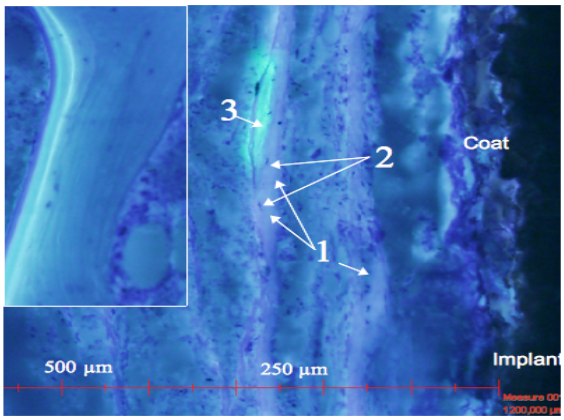

Figure 7: Fluorescence microscopy of Sr0 bioactive glass-coated implant (same view as Fig. 5). The green area (arrow 3) shows a calcein label, indication that this is an area of woven bone that mineralized 25 days after insertion of the implant. An image of the fluorochrome labels during normal remodeling is seen in the upper left corner to show the reference colors of the fluorochrome labels. Autofluorescence is seen in the other areas of the homogenous substance. U-MNV, 250 x magnifacation.

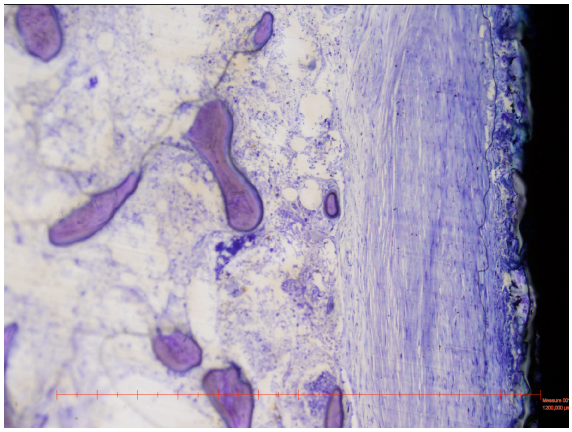

Figure 8: Sr0 bioactive glass-coated implant with a dense fibrous membrane in the interface. Toluidine blue, pH 7, x250 magnification.

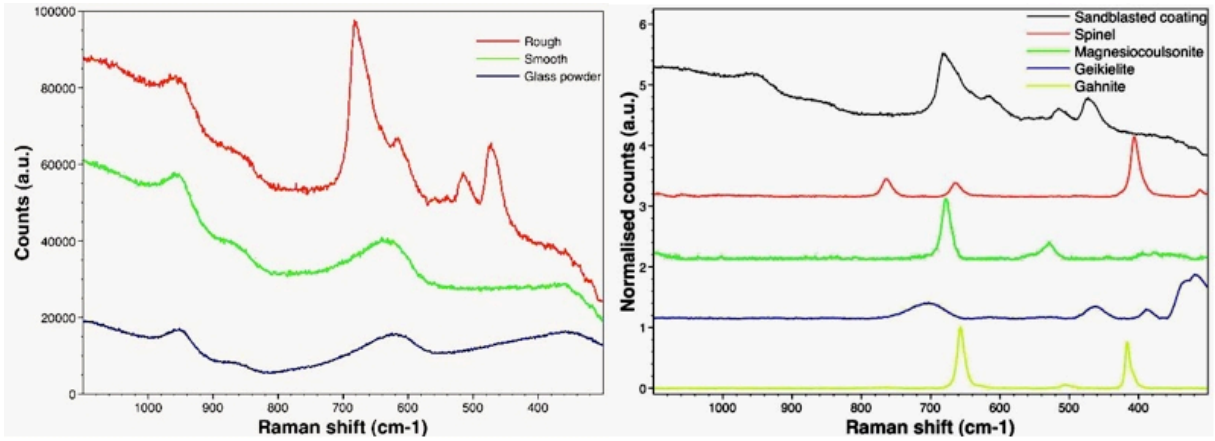

Figure 9: Results of Raman spectroscopy: (Left) Raman spectra of glass powder, glass coating on non-grit blasted Ti alloy (smooth), and glass coating on grit-blasted Ti alloy (Rough); (right) Raman spectra of glass coating on grit-blasted Ti alloy and spectra of gahnite, geikielite, magnesiocoulsonite, and spinel as controls. (Courtesy BioCeramic Therapeutics Ltd.).

Synthetic composition (mol %) of the bioactive glasses

Oxide	Sr0	Sr10	Sr50
SiO_2	49.46	49.46	49.46
Na_2O	3.30	3.30	3.30
CaO	32.62	29.36	16.31
SrO	0.0	3.26	16.31
K_2O	3.30	3.30	3.30
MgO	7.25	7.25	7.25
ZnO	3.00	3.00	3.00
P_2O_5	1.07	1.07	1.07

Table 1.

Results of the mechanical push-out test, median values (interquatile range)

	Ultimate Shear Strength (MPa)	Apparent shear stiffness (MPa/mm)	Total Energy Absorption (kJ/m^2)
HA	2.31 (0.79-4.57)	11.92 (3.95-22.26)	366.62 (92.53-634.41)
Sr0	0	0	0
Sr10	0	0	0
Sr50	0	0	0
Wilcoxon	p=0.006	p=0.006	p=0.006

Table 2